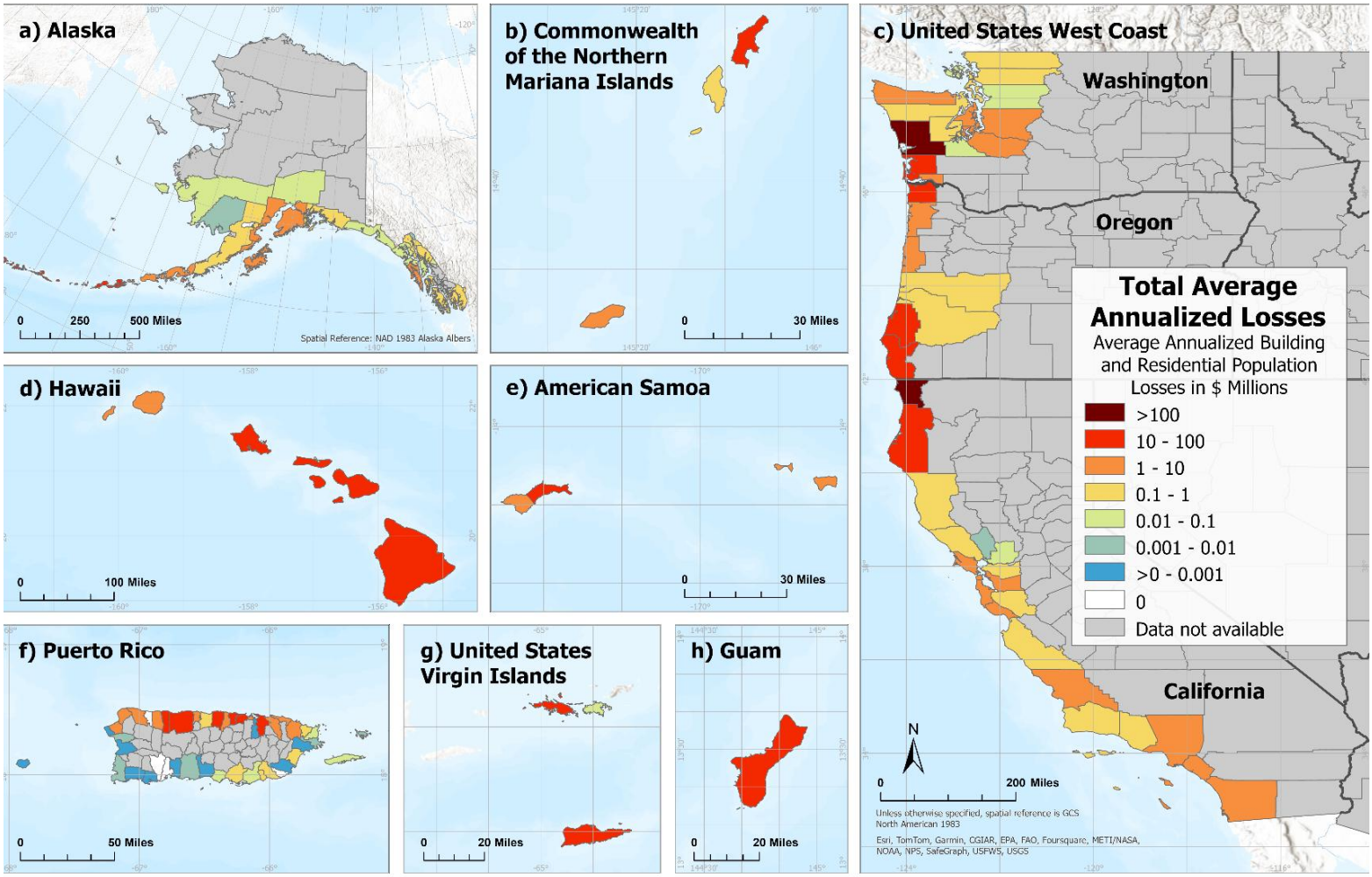

Estimated Average Annualized Tsunami Losses for the United States

FEMA P-2426 / September 2025

FEMA

USGS science for a changing world

NOAA

This page intentionally left blank

Acknowledgements

The Federal Emergency Management Agency (FEMA) acknowledges and appreciates the contributions of the following individuals and organizations who participated in the development of this report. Any use of trade, firm, or product names is for descriptive purposes only and does not imply endorsement by the U.S. Government.

Special thanks to the National Tsunami Hazard Mitigation Program for their contributions and review of this work.

Primary Contributors:

- Federal Emergency Management Agency, Washington, D.C., Natural Hazard Risk Assessment Program
  - Anne Sheehan, Geospatial Risk Analyst
  - Casey Zuzak, Senior Risk Analyst
- U.S. Geological Survey, Western Geographic Science Center
  - Nathan Wood, Supervisory Research Geographer
- Advancing Resilience in Communities, FEMA Production and Technical Services Contractor, Fairfax, Virginia
  - Doug Bausch, Niyam IT, Director of Data Science
  - Cadie Goulette Yeager, Niyam IT, GIS Analyst
- Compass, FEMA Production and Technical Services Contractor, Nashville, Tennessee
  - Alice McDougall, FACTOR Inc, Senior Consultant

Contributors and Reviewers:

- American Samoa Department of Homeland Security
  - Mulivanu Aiumu, Emergency Manager
  - Vinnie Atofau, Deputy Director
- California Geological Survey
  - Jason Patton, Engineering Geologist
  - Nicholas Graehl, Engineering Geologist
  - Rick Wilson, Senior Engineering Geologist
- California Office of Emergency Services

- Todd Becker, Senior Emergency Services Coordinator
- Yvette LaDuke, Program Manager

- Federal Emergency Management Agency
  - Hannah Rabinowitz, FEMA Region 10, Earthquake Program Manager
  - Kara Jacobacci, FEMA Region 10, Risk Analyst
  - Katherine Landers, Natural Hazard Risk Assessment Program, Geospatial Risk Analyst

- National Oceanic and Atmospheric Administration
  - Chip McCreery, Pacific Tsunami Warning Center, Director of Pacific Tsunami Warning Center
  - Christa von Hillebrandt-Andrade, International Tsunami Information Center Caribbean Office, Manager
  - Christopher Moore, Pacific Marine Environmental Laboratory, Principal Investigator
  - David Snider, National Tsunami Warning Center (Alaska), Tsunami Warning Coordinator
  - Elinor Lutu-McMoore, National Weather Service, Meteorologist in Charge
  - Gregory Schoor, National Weather Service, Branch Chief
  - Kara Langkilde, National Weather Service, Administrative Support Assistant
  - Nicolas Arcos, National Centers for Environmental Information, Physical Scientist
  - Raymond Tanabe, National Weather Service, Director for the Pacific Region
  - Sarah Rogowski, National Weather Service, Emergency Response Specialist/Meteorologist
  - Summer Ohlendorf, National Tsunami Warning Center, Science Officer

- Oregon Department of Mining and Geology Industry
  - Fletcher O'Brien, Geospatial Analyst
  - Jonathan Allen, Coastal Geomorphologist

- U.S. Geological Survey
  - William Barnhart, Assistant Coordinator, Earthquake Hazards Program
  - Rich Briggs, Research Geologist
  - Stephanie Ross, Geophysicist and Tsunami Scenarios Coordinator

- University of Alaska Fairbanks
  - Dmitry Nicolsky, Research Associate Professor
  - Elena Suleimani, Tsunami Modeler
  - Mike West, Alaska State Seismologist

- University of Puerto Rico
  - Elizabeth Vanacore, Associate Research Professor
  - Hernan Porras, Principal Investigator
  - Victor Huerfano, Research Professor

- Virgin Islands Territorial Emergency Management Agency
  - Graciela Rivera, Territorial Hazard Mitigation Officer
  - Regina Browne, Deputy Director of Planning and Preparedness

- Washington Emergency Management Department

- Dante DiSabatino, Tsunami Vertical Evacuation Structure Project Manager
- Elyssa Tappero, Tsunami Program Manager
- Ethan Weller, Tsunami Program Coordinator
- Maximilian Dixon, Hazards and Outreach Program Supervisor
- Corina Allen, Chief Hazards Geologist

- Washington Geological Survey
  - Alex Dolcimascolo, Tsunami Geologist
  - Daniel Eungard, Tsunami Geologist

- Althea Rizzo, Oregon Emergency Management, Geologic Hazards Program Coordinator
- Anthony Picasso, Alaska Division of Homeland Security and Emergency Management, Earthquake, Tsunami, Volcano Program Manager
- Barrett Salisbury, Alaska Seismic Hazards Safety Commission, Earthquake and Tsunami Hazards Program Manager
- Chip Guard, Tropical Weather Sciences, Meteorological Consultant
- Edward Fratto, Northeast States Emergency Consortium, Executive Director
- Kwok Fai Cheung, University of Hawai'i at Manoa, Professor of Ocean and Resources Engineering
- Jennifer Sims, Niyam IT, Director of GIS
- Juan Horrillo, Texas A&M University, Associate Professor of Ocean Engineering
- Kristen Gelino, Nodi Solutions
- Mario Kaipat, Commonwealth of the Northern Mariana Islands Homeland Security & Emergency Management, Program Coordinator
- Roy Watlington, University of Virgin Islands
- Skylar Suiso, Hawai'i Emergency Management Agency, Project Specialist
- Stephan Grilli, University of Rhode Island, Distinguished Professor and Chair
- Stephen Cahill, Guam Homeland Security, Tsunami Specialist
- Wildaomaris González Ruiz, Puerto Rico Emergency Management Agency, Tsunami Program Manager Preparedness

This page intentionally left blank.

Table of Contents

Acronym List

AAL	Average Annualized Loss
ABL	Agent Based Model
AGL	Above Ground Level
AKDGG	Alaska Division of Geological & Geophysical Surveys
ARP	Annual Return Period
ASCE	American Society of Civil Engineers
ASCII	American Standard Code for Information Interchange
CalOES	California Governor's Office of Emergency Services
CGS	California Geological Survey
CNMI	Commonwealth of the Northern Mariana Islands
CSZ	Cascadia Subduction Zone
CUDEM	Continuously Updated Digital Elevation Model
DEM	Digital Elevation Model
DHS	Department of Homeland Security
DOGAMI	Oregon Department of Geology and Mineral Industries
EAL	Expected Annual Loss
EPSZ	East Philippines Subduction Zone
FEMA	Federal Emergency Management Agency
FSCDB	Full South Caribbean Deformed Belt
GAT	Great Aleutian Tsunami
GBS	General Building Stock
GEM	Global Earthquake Model
GIS	Geographic Information Systems

HARN	High Accuracy Reference Network
HIEMA	Hawaii Emergency Management Agency
HIFLD	Homeland Infrastructure Foundation-Level Data
IDW	Inverse Distance Weighted Interpolation
IMG	"Imagine" grid file format, originally from ERDAS (Earth Resources Data Analysis System).
KMZ	A zipped Keyhole Markup Language file GIS format.
LA	Lesser Antilles
LiDAR	Light Detection and Ranging
MHHW	Mean Higher High Water is the average level of the highest tide for each day computed over a 19-year period. This 19-year period is the National Tidal Datum Epoch that accounts for cyclical changes in the moon's orbit.
MOST	Method of Splitting Tsunami
MSL	Mean Sea Level
MTJ	Mendocino Triple Junction
NCEI	NOAA's National Centers for Environmental Information
NED	National Elevation Data
NEOWAVE	Non-hydrostatic Evolution of Ocean WAVE
NetCDF	Network Common Data Form
NOAA	National Oceanic and Atmospheric Administration
NSI	USACE's National Structure Inventory
NTHMP	National Tsunami Hazard Mitigation Program
PMEL	NOAA's Pacific Marine Environmental Laboratory
PMT	Predicted Maximum Tsunami
PTHA	Probabilistic Tsunami Hazard Analysis

RNSZ	Ruykuy-Kuyshu-Nankai Subduction Zone
RES3A	Residential Multi-Family Dwelling– Duplex
RES3B	Residential Multi-Family Dwelling – 3-4 Units
RES3C	Residential Multi-Family Dwelling – 5-9 Units
RES3D	Residential Multi-Family Dwelling – 10-19 Units
RES3E	Residential Multi-Family Dwelling – 20-49 Units
RES3F	Residential Multi-Family Dwelling – 50+ Units
SELFE	Semi-implicit Eulerian Lagrangian Finite Element Model
SIFT	Short-term Inundation Forecasting for Tsunamis
SOEST	School of Ocean and Earth Science and Technology, University of Hawai‘i at Mānoa
SRTM	Shuttle Radar Topography Mission
TB	Terabyte
TIF	Tagged Image File Format
TIN	Triangular Irregular Network
UBC	Uniform Building Code
UDF	User-Defined Facility
USACE	United States Army Corps of Engineers
USGS	United States Geological Survey
UTM	Universal Transverse Mercator
VITEMA	Virgin Islands Territorial Emergency Management Agency
VSL	Value of a Statistical Life ($12.5 million, 2022)
WEMD	Washington Emergency Management Division
WGS	Washington Geological Survey
WGSC	Western Geographic Science Center

Executive Summary

Tsunami hazards are substantial threats to coastal communities across the United States (U.S.) and its territories. U.S. states and territories collaborate through the National Tsunami Hazard Mitigation Program (NTHMP) to develop their own tsunami-hazard information for outreach and evacuation planning. An effort to curate this tsunami-hazard information to support comprehensive risk analysis at the national level has not yet been completed. In support of this effort, the Federal Emergency Management Agency (FEMA) collaborated with the NTHMP, the National Oceanic and Atmospheric Administration (NOAA) and the U.S. Geological Survey (USGS) starting in 2023. This collaboration included the collection and analysis of existing tsunami hazard data and methods in the U.S. Tsunami subject matter experts identified and selected scientifically defensible methods for estimating the risks to buildings and populations in coastal communities. These efforts may support decision making regarding resilience policies, priorities, strategies and funding levels.

Tsunamis can be triggered by earthquakes, subaerial or submarine landslides, volcanic eruptions, glacial calving, near-earth objects, weather or other events. These events can cause severe destruction, injuries, and loss of life due to powerful currents and flooding. Tsunamis pose a substantial threat to the western United States and all U.S. territories, as described below.

- Hawaii is threatened by distant tsunamis due to its central location in the Pacific Ocean basin and has a history of local events.
- Alaska, particularly the Aleutian Islands, faces local tsunami threats due to proximity to the Alaska-Aleutian Subduction Zone, as well as distant tsunamis from around the Pacific Ocean basin.
- The western coast of the U.S. is threatened by distant tsunamis from around the Pacific Ocean basin and local source tsunamis from earthquakes generated within the Cascadia Subduction Zone in the Pacific Northwest.
- American Samoa faces local tsunami threats from earthquakes generated in the nearby Tonga Trench, as well as distant tsunami threats.
- Guam and the Commonwealth of the Northern Mariana Islands are threatened by local tsunamis from the nearby Mariana Subduction Zone, as well as distant sources from around the Pacific Ocean Basin.
- Puerto Rico and the United States Virgin Islands are threatened by multiple local and distant tsunami sources, such as the Puerto Rico Trench (PRT), given their location in the complex seismic region of the Caribbean Sea.

Several historical events stand out because of their catastrophic impacts.

- In the Pacific Northwest, the 1700 Cascadia earthquake caused a tsunami that affected coastal Native American communities, though the extent of the damage is not fully documented (Ludwin, et al., 2005).

- In Puerto Rico, the 1918 earthquake triggered a tsunami that caused $77 million in damage in 2022 dollars and 116 fatalities, primarily along the western coast (Coffman et al., 1982).

- The 1946 Aleutian Islands earthquake triggered a massive tsunami that devastated Hilo, Hawaii, killing 158 people and resulting in approximately $375 million in damage (adjusted to 2022 dollars) (Fisher et al., 2023).

- The 1964 Alaska earthquake (M 9.2) generated tsunamis that caused severe destruction in some communities across Alaska, Oregon, and California. This disaster led to a total of 124 fatalities and approximately $2.9 billion in property damage (adjusted to 2022 dollars) (Brocher et al., 2014) (Alaska Science Center, 2024).

- In American Samoa, a tsunami generated by the 2009 Samoa earthquake (M_w 8.1) caused widespread devastation, resulting in 34 confirmed fatalities (Apatu et al., 2013) and economic losses exceeding $160 million (adjusted to 2022 dollars) (DHS, 2011).

More recent events, including the 2010 Chile earthquake, the 2011 Japan earthquake, and the 2022 Tonga volcanic eruption, resulted in millions of dollars in damage to numerous ports and harbors in the U.S. South Pacific territories, Hawaii, and along the west coast of the U.S. (Lynett, et al., 2022) (Wilson, et al., 2013). Since these events, the expansion of the built environment in low-lying areas along the coast has increased the exposure of buildings and people, thereby further escalating community risk from tsunamis.

This report provides a comprehensive national assessment of earthquake-generated tsunami risk. It does not include impacts from tsunamis generated by landslides, volcanic eruptions, glacial calving, near-earth objects, weather, or other events. This study is based on the best available hazard data from the U.S. Pacific Coast (California, Oregon and Washington), Alaska, Hawaii, U.S. Pacific Territories (American Samoa, Guam and Commonwealth of the Northern Mariana Islands) and Caribbean Territories (Puerto Rico and United States Virgin Islands). Tsunami risks associated with states along the East Coast, Gulf Coast, and Great Lakes are not included in this study because Hazus 6.1 software (FEMA 2024a) does not currently include the ability to analyze tsunami risk in those states. Once modeling capabilities and tsunami hazard data become available for additional states, FEMA may incorporate these data into future editions of this study.

This study used state- and territory-level tsunami hazard data, an enhanced version of the National Structure Inventory for Hazus 6.1 and population analysis, and pedestrian-evacuation analyses conducted by the USGS and NTHMP state partners as part of a comprehensive approach to estimate potential losses. This represents a first step toward establishing a national baseline of relative tsunami risk across the U.S. The tsunami hazard data provided by California were multi-return period probabilistic data, while other states and territories provided deterministic scenarios. FEMA

estimated return periods for the deterministic scenarios to enable the calculation of potential annualized losses for both buildings and populations.

Loss estimation methods used in this study leverage the same base exposure data that were used across all analyses. Tsunami hazard and estimated return period data were collected for each state and territory and these same hazard data were used to estimate Average Annualized Loss (AAL) for both building and residential population of each state and territory. Different methodologies were used to estimate building loss and population loss.

- Building losses were estimated using Hazus 6.1, an economic loss modeling software created by FEMA. Building losses, as referred to in this study, measure the Capital Stock Loss, or the replacement value of structural, non-structural, contents and inventory damage (2022 dollars) (FEMA, 2024b).

- Population losses were estimated based on evacuation modeling summarized in Wood et al. (2025a). This study assessed the number of residents that may have insufficient time to evacuate modeled tsunami hazard zones before the estimated wave arrival time, assuming they began walking to high ground 10 minutes after ground shaking began for local scenarios and 65 minutes after for distant scenarios. To calculate the population equivalence loss in dollars, the Value of a Statistical Life (VSL) of $12.5 million (2022) was used to convert population loss estimates into a monetary population equivalence value (FEMA, 2023b).

FEMA annualized the building and residential population losses at the Census block level using the Riemann sums equation (Appendix D) and aggregated these losses to Census tract and county-equivalent geographies. Average annualized losses are the estimated long-term value of tsunami losses to the general building stock and population in any single year in a specified geographic area (e.g., state, county, Census tract). This study also uses an average annualized tsunami loss ratio, which expresses estimated average annualized tsunami loss as a fraction of the building inventory replacement value. These interrelated risk indicators help compare relative tsunami risk.

This study estimates that annualized building and residential population-equivalent losses from earthquake-generated tsunamis exceed $1 billion (2022 U.S. Dollars) (Figure E-1). The majority (79%) of the potential losses are driven by impacts on residential population, with potential population losses exceeding $790 million. Because of data and methodology limitations, this study only evaluates population loss for residential populations and does not account for non-residential populations.

Based on evacuation modeling summarized in Wood et al. (2025a) and a related database (Wood et al., 2025b), FEMA estimates that tsunami-related fatalities of residents across all analyzed states and territories are estimated at an average annualized rate of 64, 35 and 22 people per year for departure delays of 10-, 5- and 0- minutes, respectively, from the start of earthquake ground shaking for local tsunamis. Most of these fatalities would result from a local Cascadia Subduction Zone event in the Pacific Northwest or a local PRT event in Puerto Rico. In the local Cascadia Subduction Zone-affected states, improving reducing departure delay alone does not eliminate the potential for

fatalities; therefore, other approaches to reduce potential loss of life may be warranted. For the purposes of this study, each resident who is unable to evacuate in time before a wave arrives at the building is considered a fatality. A county, state or territory can use the statistical relationship between departure delays and estimated average annualized fatalities to determine the most effective and resilient strategies for investment.

The Hazus 6.1 analysis indicates that the average annualized loss for buildings is approximately $209 million. The total estimated economic exposure (building and contents value) for Census blocks expected to have inundation from modeled scenarios is approximately $750 billion. Hawaii accounts for almost half of these building losses, roughly $92 million per year, with $160 billion in exposure in Census blocks with potential for inundation.

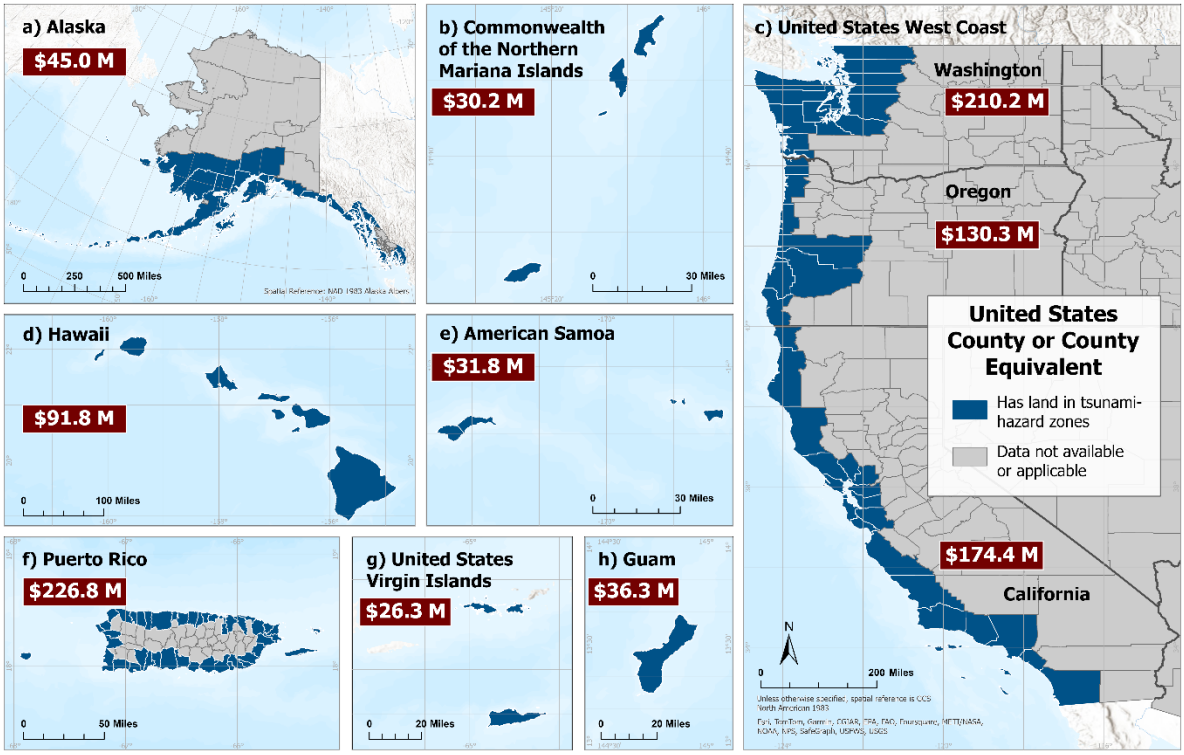

Figure E-1: Total State and Territory Average Annualized Losses and County or County Equivalents with land in tsunami-hazard zones

This study marks a milestone in efforts to quantify and compare national tsunami risk. By integrating the National Structure Inventory dataset with Hazus 6.1 earthquake building attributes, state and territory tsunami hazard data, Hazus 6.1 analysis, and evacuation modeling, FEMA was able to estimate average annualized loss for buildings and residential populations. Although this study is comprehensive, several data gaps were identified, and future improvements can be made as additional data become available. These improvements include the addition of more hazard data to fill existing gaps, such as probabilistic hazard data; improved tsunami source information for seismic events with limited probability data; and the incorporation of casualty parameters beyond the scope

of this analysis. Further research areas include the potential impacts to infrastructure, large commercial ports, other maritime and harbor facilities, and non-residential populations, such as tourists. Additionally, subsequent studies may be expanded to include tsunamigenic events beyond earthquakes and tsunami risk assessments, such as subaerial and submarine landslides, for the Great Lakes and East and Gulf Coasts.

Through FEMA's collaboration with NTHMP, NOAA and the USGS, this study incorporated the best available hazard data and methods to date, allowing the relative comparison of risk across the country. Results from this initiative may be used to:

1. Improve our understanding of tsunami risk in the United States;
2. Provide baseline loss estimates for tsunami risk and promote state and local risk awareness;
3. Compare tsunami risk with that of other natural hazards with the caveat that the identified gaps in tsunami hazard data will result in higher tsunami risk; and
4. Build community resilience through comprehensive pre-disaster planning for tsunami response and recovery, ensuring preparedness, swift action and sustainable rebuilding.

This page intentionally left blank.

1. Introduction

1.1. Background

Tsunamis are massive, long-period waves generated by gravitational displacements of bodies of water. These displacements can be caused by earthquakes, subaerial or submarine landslides, volcanic eruptions, glacial calving, near-earth objects, weather, or other events and pose a constant threat to coastal communities in the United States (U.S.), its territories, and around the world.

This report outlines the data and methods used by the Federal Emergency Management Agency (FEMA) to conduct the first-ever Average Annualized Loss (AAL) study based on tsunami hazard data provided by individual states and territories. The study estimates building and economic losses for the U.S. Pacific Coast (California, Oregon, and Washington), Alaska, Hawaii, U.S. Pacific Territories (American Samoa, Guam, and the Commonwealth of the Northern Mariana Islands), and Caribbean Territories (Puerto Rico and the United States Virgin Islands). Average annualized loss studies like this one can be used to inform natural hazard risk assessments (Ward et al., 2020). To conduct this study, FEMA collaborated with multiple federal and state agencies, stakeholder organizations, and groups such as the USGS, NOAA, and the National Tsunami Hazard Mitigation Program (NTHMP) to incorporate the best available data and methods. NTHMP is administered by the National Weather Service's Tsunami Program and includes representatives from many national, state, and territory organizations (National Weather Service 2025). The NTHMP mission is to mitigate the impact of tsunamis through mapping and modeling, public education, community response planning, hazard assessment, and warning coordination.

Natural hazard risk assessments for building and economic loss estimation traditionally use probabilistic data to estimate average annualized loss. For tsunami risk assessments specifically, these probabilistic data are referred to as a Probabilistic Tsunami Hazard Analysis (PTHA). Probabilistic Tsunami Hazard Analysis integrates geological, geophysical and statistical data to model various factors like the frequency of seismic events, the propagation of tsunami waves, and the estimated inundation and flood depth of coastal areas. A robust Probabilistic Tsunami Hazard Analysis includes both frequent, lower impact scenarios and rarer, catastrophic scenarios. This analysis also incorporates methods that explicitly account for uncertainties in earthquake occurrence and other tsunami generation processes. At the time of this study, Probabilistic Tsunami Hazard Analysis data are available only in California (California Geological Survey 2025).

In the U.S., tsunami-hazard assessments have primarily involved deterministic scenario data at the state or territory level for use in outreach and evacuation planning in support of emergency management. Deterministic scenarios each represent one specific scenario, often focusing on rare and catastrophic events (often referred to as a maximum considered event) to support outreach and evacuation planning. Many states now have a broad range of deterministic scenarios that include both high frequency and longer return period events (Wood et al. 2025a). Although Probabilistic Tsunami Hazard Analysis data are preferred when conducting risk assessments focused on infrastructure loss, deterministic data coupled with return periods can also be used to estimate

average annualized loss. In these instances, data for multiple return periods and sources may improve average annualized loss estimates (FEMA 2024a).

For the assessment of building losses, this study uses Hazus Version 6.1, a standardized engineering-based tool, to estimate building losses from natural disasters such as floods, earthquakes, hurricanes, and tsunamis nationwide (FEMA, 2024b). Population loss estimates for this study leverages Wood et al. (2025a), which estimates the number of residents in each scenario who may have insufficient time to evacuate from a tsunami. For the purposes of this study, each resident who is unable to evacuate in time before the wave arrives at the building is considered a fatality.

This technical report is organized into five chapters. Chapter 1 is an introduction that lays out the scope of the project. Chapter 2 summarizes the identification of risk parameters and describes the methods used to develop the building loss estimates and fatality loss estimates. Chapter 3 outlines the results of the study. Chapter 4 identifies study limitations. Chapter 5 concludes the study and outlines next steps. The Appendices contain a glossary of terms and provide more detailed technical information on the methodology, data, and supplemental analyses conducted. The study results are published as a USGS data release (Sheehan et al., 2025), and the Hazus 6.1 results and study regions are available on FEMA's Hazus Loss Library (FEMA, 2025b).

1.2. Scope of Project

The scope of this project includes estimates of average annualized loss for buildings and residential population to tsunamis for Alaska, American Samoa, California, the Commonwealth of the Northern Mariana Islands, Guam, Oregon, Puerto Rico, the United States Virgin Islands and Washington using building data from the National Structure Inventory (USACE, 2022), enhanced with Hazus 6.1 earthquake building attribution, evacuation-modeling for tsunami scenarios (Wood et al. 2025a), and state-specific tsunami hazard and return period data (FEMA, 2024c). Any mention of Washington in this report refers explicitly to the state of Washington. Only earthquake-generated tsunami losses are captured in this study due to limited return period and hazard data availability for other tsunami types. In addition, only losses from the tsunami waves themselves were estimated, meaning that any potential earthquake losses from a modeled event have not been captured. Please refer to FEMA P-366 (FEMA, 2023a) for Hazus Estimated Annualized Earthquake Losses for the United States. This study does not combine earthquake and tsunami losses.

This study evaluates two metrics: Average Annualized Building Loss and Average Annualized Population Loss. Average Annualized Building Loss was estimated using Hazus 2022 building replacement valuations to generate building losses for each state and territory. These results are annualized. The Average Annualized Population Loss analysis leverages the results of Wood et al. (2025a), as well as the Value of a Statistical Life at $12.5 million (2022) to estimate a population loss equivalent (FEMA, 2023b). Wood et al. (2025a) incorporates local, regional, and distant tsunami events to estimate the residential population that may have insufficient time to evacuate prior to the wave arrival.

This study is the first to include and standardize tsunami average annualized loss data across the U.S. Pacific Coast, Alaska, Hawaii, Caribbean Territories and Pacific Territories. Tsunami risk associated with states along the Great Lakes and East and Gulf coasts of the United States are not included due to software limitations. Hazus 6.1 software does not currently include the ability to analyze tsunami risk in those states. Once modeling capabilities and tsunami hazard data become available for additional states, FEMA may incorporate these data into future editions of this study.

This study does not explicitly account for marine and harbor facilities or infrastructure, such as gas, water, and sewer pipelines, roads, and bridges. Additionally, some populations—including liveaboard residents, visitors, tourists, employees, and other non-residential populations—are not included due to the lack of readily available national exposure data. These missing assets and populations at risk to tsunamis would increase tsunami loss estimates. FEMA will continue to work with other federal, state, tribal, and local partners to develop these capabilities in the future.

Wood et al. (2025a) suggests that residential populations have sufficient time to evacuate from distant tsunami scenarios considered in this assessment. However, the factors that increase losses for both local and distant tsunamis, including mobility issues, potential for traffic congestion, unfamiliarity with evacuation routes (particularly for tourists), or living conditions (e.g., liveaboards or cruise ship passengers), may pose substantial barriers to successful evacuation. FEMA will continue to work with partners to develop the methods and data required to improve the analysis.

1.3. Building and Population Risk Analysis Data Sources

To estimate average annualized loss for buildings and the residential population from tsunamis, the same base exposure data were used across all analyses. Tsunami hazard and return period data were collected for each state and territory and these same hazard data were used to estimate both building and residential population average annualized loss for each state.

1.3.1 EXPOSURE DATA

National Structure Inventory data with attribution updated for Hazus 6.1 (FEMA, 2024b) were leveraged to estimate the average annualized building and residential population losses that Alaska, American Samoa, California, Guam, Hawaii, Commonwealth of the Northern Mariana Islands, Oregon, Puerto Rico, United States Virgin Islands and Washington experience from tsunamis (FEMA, 2024c). The building valuations used are based on 2022 building and content replacement valuations by occupancy type and region as described in FEMA (2024b). The National Structure Inventory database (U.S. Army Corps of Engineers [USACE], 2022), from which this study derives its point-on-structure latitude and longitude coordinates, uses Homeland Infrastructure Foundation-Level Data (HIFLD) (HIFLD, 2020) LightBox parcel data (LightBox, 2020) to derive attributes such as occupancy type for residential structures, and Esri's business layer for many non-residential structures as described in USACE (2022). For building locations, this inventory uses footprints from the publicly available Microsoft Bing (Microsoft, 2018) and FEMA's USA Structures (FEMA, 2025a), which includes both Oak Ridge National Laboratory footprints from imagery extraction and the National Geospatial-Intelligence Agency footprint polygons generated by Light Detection and Ranging

(lidar) technology to improve structure location and other attributes (Yang et al., 2024). FEMA's building loss analysis incorporates the structure location and valuation attributes to estimate economic loss. Wood et al. (2025a) used the structure location, occupancy type and estimated number of residential units to distribute polygonal data of 2020 Census Bureau block counts that estimate residential populations (U.S. Census Bureau 2020). Using this information, pedestrian evacuation models estimate the number of residents unable to evacuate from a tsunami in time.

1.3.2 TSUNAMI HAZARD DATA

FEMA and the USGS engaged with state and territory organizations (refer to Table 1-1) to collect the best available hazard data for scenarios that have been selected and modeled by those organizations to conduct analysis. Estimates of average annualized losses and discussions of tsunami threats in each state and territory are based on state-by-state interpretations of best available data for modeled scenarios and not on a complete understanding of all possible tsunami sources. For example, some states and territories have modeled tsunami inundation from both local and distant earthquakes (e.g., Oregon and Guam), some have only modeled local sources (e.g., American Samoa), and others have only modeled distant sources (e.g., Hawaii). The lack of discussion of certain tsunamigenic sources is based on the availability of geospatial hazard data and should not be construed as the absence of a threat. Additional tsunami hazard modeling information was also documented (refer to Table 1-2) due to states/territories using different bathymetric-topographic data sources including Continuously Updated Digital Elevation Model (CUDEM) and Shuttle Radar Topography Mission (SRTM) data to inform the differing numerical models used to produce the tsunami hazard data.

Table 1-1: Tsunami Hazard Dataset Sources

State or Territory	Dataset Source
Alaska	Alaska Division of Geological & Geophysical Surveys
American Samoa	University of Hawai'i at Mānoa
California	California Geological Survey
Guam	University of Hawai'i at Mānoa, NOAA Pacific Marine Environmental Laboratory (PMEL)
Hawai'i	University of Hawai'i at Mānoa
Commonwealth of the Northern Mariana Islands	Commonwealth of the Northern Mariana Islands Office of Homeland Security and Management, PMEL
Oregon	Oregon Department of Geology and Mineral Industries (DOGAMI)
Puerto Rico	University of Puerto Rico
United States Virgin Islands	University of Puerto Rico, PMEL
Washington	Washington Geological Survey (WGS), DOGAMI

Table 1-2: Tsunami Hazard Dataset Numerical Modeling Information

State or Territory	Data Format	Bathymetric-Topographic Data Used	Numerical Model Used
Alaska	TIF, vector (refer to Section 2.3.1)	NGDC/NCEI/NOAA CUDEM	Alaska Model (Horrillo et al., 2014)
American Samoa	KMZ	NGDC/NCEI/NOAA CUDEM	Non-hydrostatic Evolution of Ocean WAVE (NEOWAVE) (Yamazaki et al., 2009, 2011)
California	TIF	SRTM30+ model, NOAA Tsunami Gridding Program	Modified GeoClaw (Thio, 2019)
Guam	Refer to Section 2.6.1	Refer to Section 2.6.1	Refer to Section 2.6.1
Hawaii	KMZ, TIF	NGDC/NCEI/NOAA CUDEM	NEOWAVE (Yamazaki et al., 2009, 2011) and Method of Splitting Tsunami (MOST) (Horrillo et al., 2014)
Commonwealth of the Northern Mariana Islands	TIF	NGDC/NCEI/NOAA CUDEM	MOST (Horrillo et al., 2014)
Oregon	TIF	DOGAMI LiDAR supplemented with USGS 10m and NCEI bathymetric data	Semi-implicit Eulerian Lagrangian Finite Element Model (SELFE) (Horrillo et al., 2014)
Puerto Rico	NetCDF	National Geophysical Data Center DEM for Puerto Rico	MOST and Short-term Inundation Forecasting for Tsunamis (SIFT) (Horrillo et al., 2014)
United States Virgin Islands	NetCDF	USGS NED 1/3rd arcsecond	HySEA (González Vida et al., 2016)
Washington	TIF	NGDC/NCEI/NOAA CUDEM	GeoClaw, MOST, SELFE

1.3.3 RETURN PERIOD DATA

Return period data are necessary for calculating average annualized loss for tsunamis because they indicate the average time interval, measured in number of years, between tsunami event occurrences. This interval is used in the average annualized loss estimation to convert return period losses into an annualized format, representing the loss per year. However, because geologic and

historical records suggest wide ranges of recurrences for certain tectonic sources, determining return periods for tsunami sources can be subjective.

There is currently no nationally consistent set of tsunami scenarios with associated hazard zones and return periods in the U.S. that are used by states or territories with similar threats. In this absence, the development of tsunami scenarios and related hazard zones has occurred over the past several decades, based on decisions made by and carried out by individual states and territories. As a result, source parameters for some tsunami sources have been characterized differently by different states or territories. For example, an Aleutian-Alaska Subduction Zone earthquake scenario may generate a local tsunami that impacts Alaskan coastal communities and a distant tsunami that affects coastal communities in Hawaii, Oregon, Washington, and California (Wood et al. 2025c). As noted in this report, the seismic parameters vary in the scenarios for each of the four states, resulting in different estimates of recurrence periods. Please note the estimated return period and the methods to determine them in the "Return Period Data" sections for each of the states and territories included in this analysis.

Table 1-3 contains source information for state/territory return period data, which are a foundational part of generating results in an average annualized loss study. Only California's probabilistic tsunami-hazard analyses and Hawaii's American Society of Civil Engineers (ASCE) probabilistic tsunami-hazard analysis explicitly recognize recurrence periods. For the remaining U.S. states and territories, FEMA worked with respective state/territory tsunami subject matter experts to determine scientifically defensible methodologies to estimate return periods for every scenario. Additional information on the methods FEMA used to estimate return periods can be found in the respective sections for each state and territory.

Regardless of approach, estimated return periods for each state and territory do not consider the time since the last tsunami. This time-independent analysis approach assumes that the probability of a tsunami occurring is constant over time. Time-dependent analysis, on the other hand, considers the changes in probability of a tsunami occurring over time (Goda and De Risi, 2024). This approach can acknowledge the tectonic stress accumulation, historical patterns, and/or recent seismic activity, causing the likelihood of a tsunami event to increase or decrease accordingly. The data to support a robust method to incorporate time-dependence are not uniformly available. However, time dependence, especially when considering seismogenic tsunami risk that requires the accumulation of stress on a fault, may be important to consider in future updates as new methods are being developed (Goda and De Risi, 2024).

Table 1-3: Tsunami Return Period Source

State or Territory	Return Period Source
Alaska	FEMA; refer to Section 2.3.2 for more information
American Samoa	University of Hawai'i at Mānoa
California	California Geological Survey

State or Territory	Return Period Source
Guam	University of Hawai‘i at Mānoa, NOAA PMEL
Hawaii	University of Hawai‘i at Mānoa
Commonwealth of the Northern Mariana Islands	University of Hawai‘i at Mānoa, NOAA PMEL
Oregon	Oregon Department of Geology and Mineral Industries
Puerto Rico	FEMA; refer to Section 2.10.2 for more information
United States Virgin Islands	FEMA; refer to Section 2.11.2 for more information
Washington	Washington Geological Survey, FEMA; refer to Section 2.12.2 for more information

2. Analyzing Tsunami Risk

To analyze earthquake-generated tsunami risk across the U.S. Pacific Coast, Alaska, Hawaii, the Pacific Territories, and Caribbean Territories, FEMA worked in close collaboration with tsunami subject matter experts from agencies such as the USGS and NOAA, as well as members of the NTHMP.

2.1. Building Loss Methodology

FEMA analyzed tsunami risk for buildings by combining national building exposure data with available state/territory-supplied tsunami hazard data (including flow depth grids, maximum runup grids, digital elevation models [DEMs], velocity data, and/or momentum flux data) and converting to GIS grid formats as needed using Microsoft (Redmond, Washington) Excel and ArcGIS Pro (ESRI, Redlands, California) and combined with national building exposure data. The building loss components of the study used Hazus 6.1, an economic loss modeling software for natural hazards developed by FEMA and released in 2023. This information helped inform the study of how many exposed buildings could be lost. The tsunami model fragility functions use the same building and design-level classifications as the Hazus earthquake model. Appendix B contains an overview of Hazus 6.1. For this study, the team leveraged site-specific National Structure Inventory data with Hazus earthquake building types and design levels appended. Building valuation data used 2022 U.S. dollar values for replacement. This addition to the inventory dataset increases the accuracy of the losses because the dataset contains building-specific location data, recent valuations and updated estimates of building attribution.

To compare relative building losses across counties, states and territories, Census block building exposure values are used to communicate potential exposure and to create loss ratios. However, using Census block exposure values to compare loss rates does not indicate that each structure in every Census block with inundation could be affected. The intent of the loss ratios is to highlight regions and communities with a high severity or rate of losses compared to total exposure. This may create cases where a very small portion of a Census block in a dense urban area (e.g., Honolulu or Seattle) is given a low ratio. However, Census blocks are relatively small geographic areas, and due to the uncertainty in inundation modeling, it is reasonable to consider Census blocks with inundation as high risk. Therefore, FEMA chose to use the exposure of each inundated Census block to compare relative loss ratios among states and territories.

In Hazus 6.1, all structural damage in a tsunami is driven by the estimation of momentum flux that can be output directly from numerical models, estimated by combining velocity and flow depth data or an empirical ASCE energy grade equation when no velocity data are available. All building, non-structural and content losses are estimated using flow depth relative to the foundation height of the structures. For more information on Hazus 6.1, please refer to Appendix B. After losses for each scenario were estimated using Hazus 6.1, an average annualized loss estimation was conducted using the Riemann sums method. For more information on the Riemann sums method, please refer to Appendix D. The average annualized loss produced an estimation of how much structural and non-

structural loss a building may experience on an annual basis. These losses were exported at the Census block level and then aggregated to the Census tract and county geographies.

The Hazus 6.1 tsunami model can produce a Level 1, Level 2 or Level 3 analysis based upon available hazard data types. Refer to Table 2-1 for the input data and files each Hazus Level can use. Refer to Table 2-2 for the Hazus level used for each state and territory analysis. Because Level 3 data are directly output from the numerical model, they are considered the most accurate in terms of estimating losses. Results based on Level 2 inputs can be higher because those data assume the maximum velocity and flow depth are occurring at the same place and time. The accuracy of Level 1 results is affected by the fact that the energy grade line empirical relationship is significantly influenced by flow depth, resulting in the highest velocities where flow depth is greatest. However, tsunami velocities can be very large in shallow and constricted settings and if there are buildings exposed in those areas, structural losses will be underestimated using the Level 1 approach. A supplemental study FEMA conducted using the California Probabilistic Tsunami Hazard Analysis data provided the opportunity for a comparison of Level 1, Level 2, and Level 3 average annualized loss results in Crescent City, California. Crescent City was selected due to its high risk, so that the relative differences in potential losses can be characterized. Refer to Appendix F, Section F.1.

Table 2-1: Hazus Tsunami Model Level Overview

Level	Hazard Data Required	Input Data Files and Formats
Level 1	Runup Only – Mean Sea Level (MSL)	Maximum Runup height grid ---AND--- DEM grid
Level 1 – Quick Look	Single Maximum Runup	DEM grid and single maximum runup value (MSL)
Level 2	Flow Depth Above Ground Level (AGL) and Velocity	Maximum Flow Depth grid and Velocity grid ---OR--- Maximum Depth and Velocity NetCDF NOAA SIFT (.nc) files
Level 3	Median Depth AGL (ft) and Median Momentum Flux (ft^3/s^2)	Median Depth grid ---AND--- Median Momentum Flux grid

Table 2-2: State or Territory Hazus Level Used

State or Territory	Input Hazus Analysis Level
Alaska	Level 1; refer to Section 2.3.1 for more information.
American Samoa	Level 1
California	Level 3
Guam	Level 1
Hawaii	Level 1 and Level 3; refer to Section 2.7.1 and Appendix C, Section C.5 for more information.
Commonwealth of the Northern Mariana Islands	Level 1 and Level 2; refer to Section 2.8.1 and Appendix C, Section C.6 for more information.
Oregon	Level 3
Puerto Rico	Level 2
United States Virgin Islands	Level 3
Washington	Level 3 and Level 2; refer to Section 2.12.1 for more information.

2.1.1 TSUNAMI HAZARD DATA PREPROCESSING FOR HAZUS 6.1

Please refer to Appendix C for additional information regarding the state- and territory-specific processes and GIS methods employed.

2.1.2 LEVEL 1 INPUTS AND PREPROCESSING

A Hazus Level 1 analysis requires a runup grid and a DEM to run. Runup grid data can be created from runup vector data by extracting DEM values to points along the inundation boundary to estimate runup. Runup grid data can also be obtained from a depth grid by adding the DEM values to the depth grid values.

2.1.3 LEVEL 2 INPUTS AND PREPROCESSING

The Hazus Level 2 analysis required inputs are a depth grid (maximum depth in feet AGL) and a velocity grid (maximum velocity in ft/sec). Additionally, in some cases, the data were converted from Hazus levels manually outside of Hazus which both speeds up analysis and helps make the inputs consistent where multiple levels of hazard data are provided. Maximum flow depth is estimated by subtracting the best available DEM from the runup grid data. The empirical ASCE function (Equation 2- 1) (FEMA, 2024a) is used to estimate maximum velocity:

$$\text{Maximum Velocity} = 0.85 \times \sqrt{\left(9.81 \times \text{Max\_Flowdepth} \times \left(1 - \left(\frac{\text{DEM}}{R}\right)\right)\right)}$$

Equation 2-1

Where 9.81 is the value for acceleration of gravity in meters per second squared, "Max_Flowdepth" represents the maximum flow depth grid, "DEM" is the digital elevation model, and R is the maximum runup height with units in meters.

2.1.4 LEVEL 3 INPUTS AND PREPROCESSING

Hazus Level 3 analysis requires median depth in feet and median momentum flux in ft^3/s^2. Using the conversion factors in Table 2-3, input data are converted from meters to feet, m^3/s^2 to ft^3/s^2, and maximum values to median values.

Table 2-3: Hazus Level 3 Analysis Conversion Factors

Conversion	Factor
Conversion from Maximum to Median Values	0.6667
Conversion of Flow Depth meters to feet	3.28084
Conversion of Momentum Flux m^3/s^2 to ft^3/s^2	35.3147

2.2. Population Loss Methodology

To estimate tsunami risk to residents, FEMA leveraged Wood et al. (2025a) that is based on various pedestrian-evacuation modeling efforts performed by the USGS and State partners (refer to Appendix H for a summary of these efforts). The tsunami-evacuation study summarized in Wood et al. (2025a) was used to estimate the number of residents in each Census block that may or may not have sufficient time to evacuate from a modeled tsunami-inundation zone based on distances to safety and estimated wave arrival times for local, regional, and distant tsunami scenarios. For the purposes of this study, wave arrival is defined as the first instance when a location on land experiences inundation. FEMA considered each person who was unable to evacuate an inundation zone prior to wave arrival to be a fatality and assigned the Value of a Statistical Life (VSL) using $12.5 million for the base year of 2022 (FEMA, 2023b).

2.2.1 POPULATION EXPOSURE METHODOLOGY

Wood et al. (2025a) leveraged the National Structure Inventory building points and additional Hazus attribution along with the 2020 Census block-level residential population. The residential population was distributed to the building points classified as residential, including single family of various configurations, manufactured homes, multi-family of various configurations, institutional dormitories, and nursing homes (Table 2-4; refer to Wood et al., 2025c for more information). Non-residential populations were not considered in this analysis. The multi-family residential classes (RES3A through

RES3F) were assigned a weight based on the lower end of a range for a Hazus-specific occupancy types (e.g., RES3C = 5 units). Weights for institutional dormitories and nursing homes were assigned by dividing national population totals for each category by the number of building points with that specific code, resulting in an average population of 35.83 for institutional dormitories and 14.28 for nursing homes. These numbers were then divided by the average persons per household (2.57) based on the five-year 2018-2022 American Community Survey (U.S. Census Bureau, 2023). This resulted in weights of 14 for institutional dormitories and 6 for nursing homes, which is interpreted not as absolute counts but instead as relative weights, i.e., we assume there are 6 times the number of people in a nursing home than there are in a single-family residence in the same census block. The residential Census block population was distributed to the points based on this unit weight (Table 2-4: Residential Population Weighting Table 2-4).

Table 2-4: Residential Population Weighting

Residential Code	Description	Unit Weight
RES1-1SNB	Single Family Residential, 1 story, no basement	1
RES1-1SWB	Single Family Residential, 1 story, with basement	1
RES1-2SNB	Single Family Residential, 2 story, no basement	1
RES1-2SWB	Single Family Residential, 2 story, with basement	1
RES1-3SNB	Single Family Residential, 3 story, no basement	1
RES1-3SWB	Single Family Residential, 3 story, with basement	1
RES1-SLNB	Single Family Residential, split-level, no basement	1
RES1-SLWB	Single Family Residential, split-level, with basement	1
RES2	Manufactured Home	1
RES3A	Multi-family housing 2 units	2
RES3B	Multi-family housing 3-4 units	3
RES3C	Multi-family housing 5-10 units	5
RES3D	Multi-family housing 10-19 units	10
RES3E	Multi-family housing 20-50 units	20
RES3F	Multi-family housing 50 plus units	50
RES4	Average Hotel	EXCLUDE
RES5	Institutional Dormitory	14
RES6	Nursing Home	6

2.2.2 EVACUATION STUDIES

Travel times to safety were assigned to each residential building point based on pedestrian-evacuation modeling and various assumptions of departure delays, which have been documented in past tsunami disasters (Yun and Hamada 2012; Lindell et al. 2015; Reese et al. 2011; Apatu et al. 2016; EERI 2010).

For tsunami scenarios considered to be local events, three sets of travel times for each point based on departure delays of 0, 5 and 10 minutes from the start of the earthquake ground shaking are analyzed. A 0-minute departure delay assumes individuals begin to evacuate immediately after an earthquake begins, though this is purely for modeling purposes because immediate evacuation may not be feasible in the case of strong ground shaking. A 5-minute delay assumes individuals "drop, cover, and hold on" during earthquake ground shaking (believed to be 3-5 minutes for many subduction zone earthquake sources) and then proceed to evacuate once shaking has stopped. A 10-minute delay assumes individuals wait for ground shaking to end and then take additional time to orient themselves, leave buildings, and evacuate to high ground. Ultimately, tsunami subject matter experts of the NTHMP recommended using a 10-minute departure delay to estimate the number of residents who cannot evacuate from local tsunami events, providing a consistent standard for comparisons.

For regional and distant events, departure delays of 65, 75, and 90 minutes were used based on recommendations from NTHMP subject matter experts. A 65-minute delay represents the estimated time required to issue an official tsunami alert, and the longer delays are considered reasonable given that wave-arrival times for regional or distant events typically occur hours after the triggering event.

The evacuation behavior of at-risk individuals is unlikely to be consistent; therefore, the various departure delays allowed this study to demonstrate how shorter departure delays, even at the scale of just 5 minutes, can significantly reduce fatalities from a tsunami event where safety is nearby. In many areas, especially the island areas with nearby high ground, reducing departure delays may substantially reduce the potential for tsunami fatalities. For the U.S. states in the Cascadia region (Washington, Oregon, and California), while improving reaction times provides some reduction in potential fatalities, a high number of potential fatalities remain at a 0-minute departure delay given the far distances to high ground. This suggests that additional and alternative solutions, such as safe havens located above or outside of inundation zones, may be necessary to minimize the significant potential loss of life.

Wood et al. (2025a) couples National Structure Inventory residential points, Census block counts, and pedestrian-evacuation modeling that leverages various modeling studies (Appendix H) based on geospatial path-distance modeling algorithms as described in Wood and Schmidtlein (2012) and implemented in geospatial software packaged as the USGS Pedestrian Evacuation Analyst (Jones 2024). Data summarized in Wood et al. (2025a) include:

1. Assigning wave-arrival times to each residential building point for each tsunami scenario.

2. Assigning pedestrian travel times to safety for each residential building point from pedestrian-evacuation modeling that integrates slope and land cover characteristics and assumes a base pedestrian travel speed of 1.2 m/s (Federal Highway Administration, 2006).
3. Estimating residential population exposure to tsunamis as a function of the time (in minutes) when flow depth is greater than 0 meters, minus the evacuation travel time to safety (including the departure delay, e.g., 10 minutes for local events and 65 minutes for distant events).

Pedestrian-evacuation modeling used in this analysis primarily assumes travel only along existing road networks for at-risk residents. Evacuation modeling for the State of Washington assumes all bridges would be damaged by a Cascadia Subduction Zone earthquake and therefore unavailable during a tsunami evacuation; similarly, Oregon applies this assumption to bridges constructed before the year 2000. More detailed studies for Guam (Wood et al., 2023) and American Samoa (Wood et al., 2019) included evacuations across roads and undeveloped areas as determined by land cover data and visual interpretation of satellite imagery.

For residential building points where the estimated travel times are greater than modeled wave-arrival times, the residential population at these points are summed and assumed by FEMA to be fatalities. The results for each state and territory are summarized in each state and territory section. For a list of the tsunami-inundation modeling sources by scenario, please refer to Appendix H.

FEMA estimates of fatalities are intended to provide a relative risk comparison across jurisdictions. Because some states have previously conducted evacuation studies for other purposes, including planning and assessing requirements for structural (e.g., vertical evacuation) and non-structural (e.g., warning, education, and outreach) mitigation measures, a brief review of these studies is included in a sub-section for each applicable state or territory.

2.3. Alaska

Alaskan coastal communities along the northern Pacific Ocean are susceptible to tsunamis generated by local and distant earthquakes, subaerial and submarine landslides, and volcanic eruptions. The Aleutian Trench is a major local source of seismically generated tsunamis in Alaska, with the 1964 Alaska earthquake (M 9.2) being a historical example. The Alaska-Aleutian Subduction Zone is composed of multiple segments that can rupture and generate large tsunamigenic earthquakes, affecting the Gulf of Alaska, Cook Inlet and the nearby Aleutian Islands. Alaska is also at risk to tsunamis from distant sources surrounding the Pacific Rim. Submarine landslides can arrive within minutes after generation, either independently or by an earthquake, and therefore pose significant threats in several Alaskan coastal communities. Subaerial landslides in Alaska can be caused by glacial calving, which, in the United States, is unique to Alaska. Finally, there are numerous active volcanoes in Alaska along the Aleutian Arc, whose eruptions can generate dangerous tsunamis. This study considered only tsunamis generated by local earthquakes for Alaska. In addition, the distant source from a Cascadia scenario was reviewed; however, the overland inundation was determined to be minimal in all the communities evaluated. Although the Cascadia scenario would likely result in damage in the ports and harbors due to increased currents, impacts to buildings and populations are likely minimal.

2.3.1 TSUNAMI HAZARD DATA

Tsunami scenarios in Alaska were created for individual coastal communities or clusters of neighboring communities. Therefore, there is not one unifying scenario for tsunamis generated by earthquakes within the Alaska-Aleutian Subduction Zone. In addition, the data and metrics needed to determine average annualized loss for each of these scenarios, e.g., estimated return periods, did not exist for each Alaskan tsunami scenario. Alaskan tsunami hazard data were collected from the Alaska Division of Geological & Geophysical Surveys website and the data server of the Geophysical Institute at the University of Alaska Fairbanks. The focus of these scenarios was to assess the potential of large tsunamis through an analysis of deterministic sources as described in Suleimani, et al., 2019 and 2023.

The Alaska studies included many potential tsunami scenarios for each individual community. The sources for each community consider variations in seismic parameters. For example, in Adak, there are eight different scenarios for a tsunamigenic earthquake in the Andreanof Islands region (Suleimani et al. 2019). Among the scenarios in the same community, the scenarios with the largest inundation areas were selected. In some cases, where scenarios inundated more land in undeveloped areas (e.g., nearby estuaries), the scenarios that inundated the greatest amount of land in the developed areas were selected for analysis for each community.

Hazard data for each scenario were received at the community level for each of the 56 communities included in this study (Table 2-5). Additional details on each Alaskan tsunami scenario, including citations for the original hazard-modeling reports can be found in Wood et al. (2025b). Data formats shared include maximum runup values and scenario-based data, in both vector and grid forms. For several scenarios, the post-earthquake event ground surface elevation changes were estimated based on Okada (1985) and added to the DEM data in grid form. This is critical because large subduction zone earthquakes can extensively deform and often lower the landward elevation in an earthquake. As such, the use of the post-event, deformed DEM data results in a more accurate analysis of potential impacts. Appendix E identifies the Alaskan scenarios where deformed DEM data were available. The hazard data were pre-processed to generate the final inputs required for Hazus; for further details, refer to Appendix C, Section C.1. Although processed through the Hazus Tsunami Model Level 2 interface, the original hazard data for Alaska are classified as Level 1 because they lack velocity data from the original numerical model.

Table 2-5: Alaska Tsunami Hazard Data Attribution by Community

Community	Tsunami Source(s) (Segment of Aleutian Arc)	Data Format	Return Period	Earthquake Magnitude M_w)
Adak	Andreanof	Grid	113	8.8
Akhiok	Kodiak, Kenai, Barren Islands	Grid	379	9.3
Akutan	Andreanof, Fox Islands, Sanak	Grid	210	9.2
Anchor Point	Kodiak, Barren Islands, Kenai, Prince William Sound	Vector	379	9.0
Anchorage	Prince William Sound, Kenai, Kodiak	Grid	379	9.2
Atka	Andreanof	Grid	113	8.8
Chenega Bay	Prince William Sound	Grid	594	9.0
Chignik	Shumagin, Semidi	Grid	222	9.0
Chiniak	Kodiak, Kenai, Barren Islands	Grid	379	9.3
Cold Bay	Sanak, Shumagin	Grid	169	8.9
Cordova	Prince William Sound, Kenai	Vector	441	8.8
Craig	Kodiak, Barren Islands, Kenai, Prince William Sound	Vector	379	9.0
Dillingham	Andreanof, Fox Islands, Sanak	Vector	210	9.2
Elfin Cove	Prince William Sound, Kenai	Grid	441	9.0
False Pass	Sanak, Shumagin	Vector	169	9.0
Gustavus	Prince William Sound, Kenai	Grid	441	9.0
Haines	Barren Islands, Kenai, Prince William Sound, Yakataga	Grid	441	9.2
Homer	Kodiak, Barren Islands, Kenai, Prince William Sound	Grid	379	9.3
Hoonah	Prince William Sound, Kenai	Grid	441	9.0
Hydaburg	Barren Islands, Kenai, Prince William Sound	Vector	441	9.2
Juneau	Barren Islands, Kenai, Prince William Sound, Yakataga	Grid	441	9.2

Community	Tsunami Source(s) (Segment of Aleutian Arc)	Data Format	Return Period	Earthquake Magnitude M_w)
Karluk	Kodiak, Semidi	Grid	169	9.3
Kasaan	Barren Islands, Kenai, Prince William Sound	Vector	441	9.3
Ketchikan	Kodiak, Barren Islands, Kenai, Prince William Sound	Vector	379	9.0
King Cove	Sanak, Shumagin	Grid	169	8.9
Klawock	Barren Islands, Kenai, Prince William Sound	Vector	441	9.3
Kodiak	Kodiak, Barren Islands	Grid	379	9.1
Larsen Bay	Kodiak, Semidi	Grid	169	9.3
Metlakatla	Barren Islands, Kenai, Prince William Sound	Vector	441	9.2
Nanwalek	Kodiak, Barren Islands, Kenai, Prince William Sound	Vector	379	9.3
Nelson Lagoon	Andreanof, Fox Islands, Sanak	Vector	210	9.2
Nikolski	Andreanof, Fox Islands, Sanak	Grid	210	9.25
Old Harbor	Kodiak, Kenai, Barren Islands	Grid	379	9.3
Ouzinkie	Kodiak, Kenai, Barren Islands	Grid	379	9.3
Pasagshak Bay	Kodiak, Semidi	Vector	169	9.3
Pelican	Barren Islands, Kenai, Prince William Sound	Vector	441	9.2
Perryville	Sanak, Shumagin	Vector	169	9.0
Platinum	Andreanof, Fox Islands, Sanak	Vector	210	9.2
Point Baker	Barren Islands, Kenai, Prince William Sound	Vector	441	9.2
Port Alexander	Kodiak, Barren Islands, Kenai, Prince William Sound	Vector	379	9.0
Port Graham	Kodiak, Barren Islands, Kenai, Prince William Sound	Vector	379	9.3

Community	Tsunami Source(s) (Segment of Aleutian Arc)	Data Format	Return Period	Earthquake Magnitude M_w)
Port Lions	Kodiak, Kenai, Barren Islands	Grid	379	9.3
Port Protection	Barren Islands, Kenai, Prince William Sound	Vector	441	9.2
Saint George	Andreanof, Fox Islands, Sanak	Vector	210	9.2
Saint Paul	Andreanof, Fox Islands, Sanak	Vector	210	9.2
Sand Point	Sanak, Shumagin, Semidi	Grid	169	8.9
Seldovia	Kodiak, Kenai	Grid	379	9.3
Seward	Prince William Sound, Yakataga	Grid	594	9.0
Shemya	Attu, Amchitka	Vector	295	9.0
Sitka	Kodiak, Barren Islands, Kenai, Prince William Sound	Grid	379	9.2
Skagway	Barren Islands, Kenai, Prince William Sound, Yakataga	Grid	441	9.2
Tatitlek	Prince William Sound	Grid	594	9.0
Unalaska	Andreanof, Fox Islands, Sanak	Grid	210	9.1
Valdez	Prince William Sound, Kenai	Grid	441	8.8
Whittier	Barren Islands, Kenai, Prince William Sound	Grid	441	9.2
Yakutat	Prince William Sound, Kenai	Vector	441	9.0

2.3.2 RETURN PERIOD DATA

The estimation of return periods for the Alaska tsunami source scenarios was primarily based on a Briggs et al. (2024) and conversations with subject matter experts from the USGS and the Alaska Earthquake Center as shown in Table 2-5. There are unique challenges in assigning return periods for Alaska earthquake sources to the completed tsunami modeling. Most of the modeled tsunami events result from multi-segment ruptures of the Alaska-Aleutian Subduction Zone. Based on geologic and tsunami deposit evidence, multiple return periods are often available for each segment, and these return periods do not necessarily represent the frequency with which multiple segments break at the same time. In addition, return periods may be available from multiple methods, including paleoseismic data, paleotsunami data or geodesy-based estimates. Because there are large uncertainties in the available hazard data and gaps in the potential tsunami sources (e.g.,

landslides), FEMA used a cautious approach based on the shortest recurrence time from either the paleoseismic, paleotsunami or geodetic study.

For each of the 56 communities in Alaska, FEMA used the following logic to choose a return period for multi-segment scenarios because many of the scenarios were not the result of an earthquake rupturing only a single segment:

- If the scenario had a primary segment, the shortest return period was used.
- If there was no clear primary segment for the scenario, the shortest return period of the segment was used.
- If there were multiple primary segments for the scenario, the shortest return period of the segments was used.

Other states, including Hawaii, Washington, and Oregon, have distant tsunami scenarios that relate to earthquakes generated within the Alaska-Aleutian Subduction Zone. As noted in their respective sections, these scenarios have different seismic parameters, such as magnitude, and therefore have different estimated return periods. For example, a local tsunami scenario that impacts King Cove, Alaska is based on a Mw 8.9 Alaska-Aleutian Subduction Zone earthquake, whereas a distant tsunami scenario impacting Hawaiian coastlines is based on Mw 9.3 and Mw 9.6 earthquakes from the same Alaskan region. Differences in earthquake assumptions lead to different estimates of return periods.

2.3.3 AVERAGE ANNUALIZED BUILDING LOSS

The losses are based on each of the nine return periods available for the communities (Table 2-5) which they affect. Because each community is modeled based on the impacts of a single scenario with the shortest return period, the average annualized rate is based on 1 over the return period (e.g., 1/113 = 0.00884956). The results produced a total estimated loss of about $28 million in building loss on an average annualized basis with the top five boroughs listed in Table 2-6.

Table 2-6: Top Five Boroughs and Total Statewide Average Annualized Building Loss and Exposure

Rank	Borough	Average Annualized Building Losses	Building Exposure to Tsunami	Building Loss Ratio (USD per $1 million)
1	Kodiak Island	$8,429,522	$5,054,630,925	$1,667.68
2	Aleutians West	$6,369,037	$2,361,502,931	$2,697.03
3	Kenai Peninsula	$5,069,101	$4,676,961,432	$1,083.84
4	Anchorage	$2,201,798	$4,170,012,181	$528.01

Rank	Borough	Average Annualized Building Losses	Building Exposure to Tsunami	Building Loss Ratio (USD per $1 million)
5	Aleutians East	$2,091,693	$606,285,023	$3,450.01
	State Total	$27,974,572	$26,530,081,448	$1,054

In the Aleutians West Borough, over 80% of the residential population and building value are exposed to the tsunami hazard. On a per capita level, Alaska's annualized per capita projected loss based on the residential population exposed in all affected census blocks is one of the highest in the country ($609 per person per year). The annualized building loss ratio is over $1,000 per $1 million in exposure. The seismic design levels used in Hazus for Alaska are based on the FEMA Building Code Adoption Tracker (FEMA, 2024a), which indicates that despite Alaska's high earthquake risk, fewer than 3% of Alaska jurisdictions adopt and enforce seismic resistant residential codes. The lack of local building codes may contribute to the increased impacts observed in the results.

2.3.4 AVERAGE ANNUALIZED RESIDENTIAL POPULATION LOSS

In 1964, Alaska suffered the largest local tsunami fatality event in U.S. history when 106 people perished in the 1964 Alaska earthquake (M 9.2) (Brocher, et al., 2014). Including local landslide generated tsunamis, Alaska has an observed historical annualized fatality rate of 1.63 since 1845.

Wood and Peters (2025a) summarizes pedestrian-evacuation modeling based on Alaska Division of Geological & Geophysical Surveys (AKDGG) tsunami hazard zones for the community scenarios listed in Table 2-5. AKDGG tsunami-hazard reports contain many earthquake-generated tsunami scenarios in each community. For Wood and Peters (2025a), the AKDGG tsunami scenario that generated the maximum extent of inundation in the developed areas of a community was selected. Although high ground may be nearby for many communities, a road-only pedestrian evacuation approach is implemented due to the prevalence of heavy vegetation and the potential for overland areas to be impassable during wintertime tsunami events. The shoreline wave arrival times for tectonic scenarios used in the analysis ranged from 15 to 120 minutes. Although available in some communities, tsunami-hazard zones for landslide-related scenarios were not included in this study due to limitations with assigning return periods to landslides and for consistency with other states and territories.

According to AKDGG hazard zones, National Structure Inventory residential points, evacuation modeling (Wood and Peters 2025a), and population-exposure results (Wood et al, 2025a), the largest number of residents that may have insufficient time to evacuate before wave arrival based on the selected scenarios occur in the following communities:

- Adak based on a M_w 8.0 Alaska-Aleutian Subduction Zone, Andreanof fault segment;
- Anchor Point based on a M_w 9.0 Alaska-Aleutian Subduction Zone, Kodiak fault segment;

- Seward based on a M_w 9.0 Alaska-Aleutian Subduction Zone, Prince William Sound fault segment; and
- Pasagshak on Kodiak Island based on a M_w 9.3 Alaska-Aleutian Subduction Zone, Kodiak fault segment.

After applying the recurrence rates, total average annualized fatalities for Alaska are an estimated 1.37 fatalities per year (Table 2-7). This fatality rate based on tectonic events aligns well with the historical fatality rate that includes landslide sources. The average annualized residential population loss rates are significantly influenced by the 113-year return period for the Aleutians West tsunami sources (0.93 annualized fatalities), and the largest exposed residential population is in Seward, which is within the Kenai Peninsula Borough.

Table 2-7: Average Annualized Fatalities Based on Residential Population Unable to Evacuate Inundation Zone Using a 10 Minute Departure Delay

Rank	Boroughs	Average Annualized Fatalities	Scenario Fatalities	Exposed Population
1	Aleutians West	0.93	128	2,444
2	Kenai Peninsula	0.33	160	3,862
3	Kodiak Island	0.10	17	3,797
4	Lake and Peninsula	0.00	1	224
	State Total	1.37	306	17,541

2.3.5 STUDY LIMITATIONS

Hazard Data

Although Cascadia scenarios could impact Alaska's maritime areas, they are not expected to significantly inundate inland areas, especially when compared to the number and frequent return periods of local Alaska sources.

The hazard data for Alaska consisted of runup grids and vector products only, with no velocity or momentum flux data. As a result, Hazus estimates those values using the method shown in Equation 2-1. Deformed DEM data were not available for all scenarios, and in some scenarios, the runup was estimated from the inundation vector data. Refer to Appendix C, Section C.1 for additional details and methods. The uncertainty this may produce in building loss results may be limited in Alaska coastal communities because much of the building exposure is light-frame construction that reaches complete damage states at lower depths and velocities.

Unique to Alaska is the occurrence of 10 Universal Transverse Mercator (UTM) Zones across the study area. This adds uncertainty to the geographic projection of the intersection of the building and underlying inundation grids since only one zone could be defined for each scenario in Hazus. Buildings on the margins of these zones could have additional uncertainty due to the projection. Although this uncertainty was not quantified, we observed that losses based on Hazus study regions that spanned several zones were 5-10% different than when scenarios were confined to a single UTM Zone. Therefore, the analysis areas were broken up to ensure they did not cross multiple zones to minimize impacts.

Missing Exposure Data

Industrial fishing and shipping facilities with high replacement values are in at-risk Alaska ports. These structures are likely underrepresented in the National Structure Inventory building data and valuation methods. Additionally, Alaska has some location-poor National Structure Inventory exposure points in areas such as St George Island, Alaska, where building points are mislocated in the Pacific Ocean.

Missing Hazard Data on Exposed Structures

Appendix F, Section F.3.1 presents an analysis for National Structure Inventory building points in Alaska located along the coast at elevations of less than 5 meters and less than 10 meters that are not included within the areas covered by available tsunami hazard data. The analysis identifies slightly over 2,000 buildings with an estimated replacement cost valuation of $2.5 billion, located along the coast outside hazard data coverage with an elevation of 5 meters or less. If we further exclude the low tsunami risk North Slope and Northwest Artic boroughs, the exposure without hazard coverage drops to slightly over 1,100 buildings with a replacement cost valuation of $1.0 billion. When compared to the building exposure that is covered by hazard data (Table 2-6, $26.6 billion), this indicates that the available tsunami hazard data coverage gap as it relates to building exposure in Alaska may be about 4%.

Population Loss

A significant limitation of this risk analysis is the inability to evaluate the impacts on Alaska's temporary populations, including coastal workforce and tourist populations. Each summer, approximately 1.3 to 1.5 million passengers travel on cruise ships through Alaska's Inside Passage (Cruise Lines International Association, 2025), introducing large populations that may be unfamiliar with tsunami threats. Given Alaska's extensive coastline, robust tourism sector, and maritime industries (e.g., fishing and canning), the actual number of exposed individuals is likely considerably higher than the estimates in this study, which are based solely on the residential population.

2.4. American Samoa

American Samoa, which is in the South Pacific Ocean, faces threats from earthquake-generated tsunamis, submarine landslides, and volcanic eruptions. On Tuesday, September 29, 2009, a M_w 8.1 earthquake occurred 120 miles south-southwest of American Samoa, about 13 kilometers below the

seabed at 6:48 a.m. Samoa Standard Time. On American Samoa, the tsunami resulted in 34 confirmed fatalities, more than a hundred injuries and the destruction of approximately 200 homes (Dominey-Howes and Thaman, 2009) (Apatu et al., 2013) where FEMA assistance program operating expenses exceeded $160 million in 2022 dollars (DHS, 2011).

2.4.1 TSUNAMI HAZARD DATA

Modeling performed by Dr. Kwok Fai Cheung from the University of Hawai'i at Mānoa provides the American Samoa probable maximum tsunami (PMT) inundation based on a M_W 9.05 earthquake within the Tonga Trench Subduction Zone. Inundation is based on an initial sea level at mean higher high water plus ~15 cm to represent projected shifts in total water levels. The data were provided in ranges of flow depth in meters in a KMZ format and are further described in Wood et al. (2019).

The University of Hawai'i at Mānoa also provided inundation maps for American Samoa based on the historical 2009 tsunami resulting from a M_W 8.1 earthquake on the Tonga Trench Subduction Zone including an initial sea level at the mean higher high water plus 15 cm in ranges of flow depth in meters in a KMZ format (Table 2-8).

The hazard data provided supports a Hazus Level 1 analysis. Please refer to Appendix C, Section C.2 for preprocessing steps.

Table 2-8: American Samoa University of Hawai'i at Mānoa Hazard Data

Scenario	Tsunami Source	Return Period
Tonga Trench Subduction Zone - M_W 9.05, probable maximum tsunami + 15 cm of total water level increase	Tonga Trench	1,000 years
Historical Tonga Trench Subduction Zone - M_W 8.1, Modeled 2009 Tsunami + 15 cm of total water level increase	Tonga Trench	100 years

2.4.2 RETURN PERIOD DATA

Dr. Kwok Fai Cheung used characteristic magnitude-frequency distributions based on the amount of slip for a certain earthquake magnitude (Uslu et al. 2010; Uslu et al. 2013; Wood et al. 2019; Wood et al. 2023) using a scaling relationship summarized in Kanamori (1977) and slip rates and preferred coupling coefficients in Berryman et al. (2015) to estimate the time needed to accumulate sufficient strain for 1,000-year return period. For the return period of the modeled 2009 tsunami scenario, Dr. Cheung estimated a 100-year return period (Table 2-8). This estimation is grounded in the observation that the 2009 event likely originated from a similar Tonga Trench source as the 1915 tsunami, which resulted in three fatalities.

2.4.3 AVERAGE ANNUALIZED BUILDING LOSS

The losses are based on the 1,000- and 100-year return period inundation resulting in an estimated loss of about $15 million in building loss on an average annualized basis. Total economic losses to buildings are modeled at $266 million based on the 2009 tsunami hazard data (100-year), aligning well with observed 2009 losses. The observed losses as measured by FEMA's disaster funding costs were over $160 million in 2022 dollars. The difference between the total modeled losses and FEMA payouts is expected because FEMA assistance does not cover all damages; there are caps to the grants and Federal shares provided for both individual and public assistance programs.

Table 2-9: Top Three Counties and Total Territory-wide Average Annualized Building Loss and Exposure

Rank	County Equivalent	Average Annualized Building Losses	Building Exposure to Tsunami	Building Loss Ratio (USD per $1 million)
1	Eastern District	$10,995,684	$3,376,193,999	$3,257.02
2	Manu'a District	$1,193,952	$235,105,814	$5,080.65
3	Western District	$2,800,046	$1,374,046,762	$2,037.89
	Territory Total	$14,989,682	$4,985,346,575	$ 3,006.96

Almost $15 million building capital tsunami average annualized loss is estimated for American Samoa (Table 2-9). American Samoa faces one of the highest annualized per capita projected losses in the nation, estimated at $641 per person, based on the residential population exposed across all affected Census blocks. The annualized building loss ratio is also high, exceeding $3,000 per $1 million in exposure—nearly double that of the next highest U.S. jurisdiction. This may be due to the prevalence of more at-risk building types and the use of outdated seismic design standards in Hazus for American Samoa. According to FEMA's Building Code Adoption Tracker (FEMA, 2024a), American Samoa has adopted the outdated 1964 UBC, which is not resistant to seismic hazards based on current standards. American Samoa also lacks a reported residential building code.

2.4.4 AVERAGE ANNUALIZED RESIDENTIAL POPULATION LOSS

Residential population losses for the 1,000- and 100-year return period inundation are based on evacuation modeling (Jones et al. 2018a) and population-exposure analyses (Wood et al. 2019), resulting in an average annualized rate of 1.34 fatalities (Table 2-10). Almost 11,000 residents are exposed to potential tsunami inundation. Comparing the modeled 100-year fatalities to the 34 observed fatalities in 2009 indicates that the residential population unable to reach safety based on the 10- and 5-minute departure delays are 86 and 8, respectively. The results appear to indicate that the average departure delay in 2009 was within the range of the analysis.

Table 2-10: Average Annualized Fatalities Based on Residential Population Unable to Evacuate Inundation Zone Using a 10 Minute Departure Delay

Rank	County Equivalent	Average Annualized Fatalities	Scenario Fatalities*	Exposed Population*
1	Eastern District	1.05	120	7,893
2	Western District	0.27	50	2,547
3	Manu'a District	0.02	4	515
	Territory Total	1.34	174	10,955

*Note: The scenario fatalities and exposed population are based on the 1,000-year probable maximum tsunami event, while the average annualized fatalities are across all available return periods (1,000 and 100 year).

2.4.5 STUDY LIMITATIONS

Hazard Data

There were two flow depth grids available for American Samoa, which represented the probable maximum tsunami scenario modeled based on mean higher high water (1,000-year return period) and the 2009 American Samoa Tsunami event (100-year return period), which both included the initial sea level at mean higher high water plus 15 cm of projected increases in total water levels to inform losses. The American Samoa tsunami data lacked momentum flux and velocity data, which, in addition to depth grids, more accurately represents potential building losses. Data availability led the study to use tsunami Hazus Level 1 analyses, which is generally considered to produce results with the lowest accuracy among the three levels of Hazus analyses. For more information about the tsunami Hazus analyses, please refer to Appendix F, Section F.1.

To generate average annualized loss using the Riemann sums method (Appendix D), losses are best represented when study areas have hazard data from multiple return periods and within those return periods, hazard data from all sources affecting the study area. Although the scenarios available covered a span of 900 years, from 100 years to 1,000 years, studies that include additional scenarios and data types may aid in the refinement of losses and create a more complete hazard curve. Uncertainty in the estimated return period is also introduced using the scaling relationship and available slip rates for the Tonga Trench Subduction Zone.

Missing Hazard Data on Exposed Structures

The building inventory coverage analysis (Appendix F, Section F.3) indicates that all sections of the coast in American Samoa are covered by available hazard data.

Population Loss

Please refer to Section 4.4 for additional information regarding limitations across all study areas.

2.5. California

Tsunamis that affect California can originate from earthquakes generated by local, regional, and distant sources, as well as from submarine landslides in offshore canyons. Earthquake sources around the Pacific Ocean are considered, including the Cascadia Subduction Zone, the Alaska-Aleutian Subduction Zone, the Japan Trench, and the Kamchatka Subduction Zone. The primary local tsunami threat stems from earthquakes in the Cascadia Subduction Zone, primarily affecting Del Norte and Humboldt Counties in northern California, with estimated wave-arrival times as short as 10 minutes due to the proximity of the Mendocino Triple Junction (MTJ)—the convergence point of the Gorda, North American, and Pacific plates. For the Cascadia source, co-seismic uplift or subsidence is also factored into inundation modeling.

2.5.1 TSUNAMI HAZARD DATA

The California Geological Survey (CGS) provided seven Probabilistic Tsunami Hazard Analysis momentum flux, flow depth, velocity and runup return period grids across seven return periods (Table 2-11) (California Geological Survey, 2025). These data are optimal for risk assessment and average annualized loss estimations to buildings because they incorporate a comprehensive range of frequent, low loss events as well as the rarer, more catastrophic events. As of 2024, California is the only state to have multiple-return period, and state-wide Probabilistic Tsunami Hazard Analysis data (California Geological Survey, 2025). The California hazard data allowed for testing the sensitivity of average annualized loss results when the number of return periods was reduced. It also enabled comparisons across different Hazus analysis levels, including Level 1 (runup only), Level 2 (maximum flow depth and velocity), and Level 3 (median flow depth and momentum flux) as detailed in Appendix F, Section F.1. These comparisons are useful in characterizing the uncertainties that may arise in areas where data are more focused on catastrophic evacuation scenarios than on risk assessment.

These data were modeled using a modified version of GeoClaw and downloaded from the California Geological Survey website (California Geological Survey, 2025). More information can be found in their technical documentation (Thio, 2019). The documentation provides a comprehensive list of sources that were considered, and the return periods that were used. A logic tree (Thio, 2019; Figure C-2) developed for the Cascadia Subduction Zone indicates that both partial ruptures and entire zone ruptures were considered and weighted by return period. For the northern Del Norte and Humboldt Counties, the maximum inundation and velocity in the probabilistic tsunami products were assumed to be primarily influenced by the Cascadia Subduction Zone-related earthquakes for return periods of 975 years and larger. For the remainder of the state, the primary influences on maximum inundation and velocity for all return periods are distant tsunamis generated by earthquakes in the Alaska-Aleutian Subduction Zone based on input provided by California subject matter experts. Thio (2019) provides additional detail on seismic parameters for the various Alaska-Aleutian Subduction Zone scenarios that contributed to the probabilistic products.

The hazard data provided support a Hazus Level 3 analysis. Please refer to Appendix C, Section C.3 for preprocessing steps.

Table 2-11: California Geological Survey Tsunami Hazard Data

Annual Return Period (ARP)	Tsunami Source	Return Period
Probabilistic Tsunami Hazard Analysis –ARP 72 year	Distant – Multiple Sources	72 years
Probabilistic Tsunami Hazard Analysis – ARP 100 year	Distant – Multiple Sources	100 years
Probabilistic Tsunami Hazard Analysis – ARP 200 year	Distant – Multiple Sources	200 years
Probabilistic Tsunami Hazard Analysis – ARP 475 year	Distant – Multiple Sources	475 years
Probabilistic Tsunami Hazard Analysis – ARP 975 year	Local – Cascadia Subduction Zone Distant – Multiple Sources	975 years
Probabilistic Tsunami Hazard Analysis – ARP 2,475 year	Local – Cascadia Subduction Zone Distant – Multiple Sources	2,475 years
Probabilistic Tsunami Hazard Analysis – ARP 3,000 year	Local – Cascadia Subduction Zone Distant – Multiple Sources	3,000 years

2.5.2 RETURN PERIOD DATA

According to Thio (2019) the 72-, 475-, 975- and 2,475-, year recurrences were chosen by the California Geological Survey because they corresponded with the 50%, 10%, 5%, and 2% probabilities of exceedance within the next 50 years, which are probabilities often used in engineering applications. The 100-, 200- and 3,000- year recurrences were chosen by CGS due to the probabilities' significance in measuring flood risk (Thio, 2019). As a result, the California data provided the most complete representation of the average annualized losses for buildings as outlined in Appendix D.

Oregon and Washington have tsunami scenarios based on Cascadia Subduction Zone earthquakes that are different but comparable to California products. In Washington, there is one Cascadia Subduction Zone-related scenario based on a Mw 9.0 earthquake and an estimated return period of 2,500 years, which is comparable to the 2,475-year product for California. In Oregon, there are five Cascadia Subduction Zone-related scenarios with varying earthquake magnitudes and related return periods. The Oregon "L" scenario is based on a Mw 9.0 earthquake with an estimated return period of 3,333 years, which is comparable to the 2,475-year CA product. The Oregon "M" scenario is based on a Mw 8.9 earthquake with an estimated return period of 1,000 years, which is comparable to the 975-year CA product.

2.5.3 AVERAGE ANNUALIZED BUILDING LOSS

Table 2-12: Top Five Counties and Total Statewide Average Annualized Building Loss and Exposure

Rank	County	Average Annualized Building Losses	Building Exposure to Tsunami	Building Loss Ratio (USD per $1 million)
1	Santa Cruz	$6,728,356	$16,200,123,419	$415.33
2	San Mateo	$6,422,488	$53,706,726,310	$119.59
3	Marin	$5,678,206	$32,884,535,884	$172.67
4	San Francisco	$5,354,637	$36,456,972,856	$146.88
5	Del Norte	$3,879,434	$8,451,627,451	$459.05
	State Total	$44,464,801	$348,610,274,427	$127.55

Most of the statewide average annualized building losses ($44 million) occurs in the northern California counties with the top five loss counties led by Santa Cruz and San Mateo (Table 2-12). Del Norte County has the highest building loss ratio of about $460 per year per $1 million in building exposure. San Mateo and Alameda counties each have over $50 billion in building stock exposure within the tsunami-affected census blocks.

2.5.4 AVERAGE ANNUALIZED RESIDENTIAL POPULATION LOSS

Residential population losses are based on pedestrian evacuation modeling (Peters et al., 2020) and population-exposure analyses (Wood et al., 2025a) performed for the 975- and 2,475-year return period inundation resulting in an average annualized rate of 10.39 fatalities (Table 2-13). The initial study from which the results were derived used a walking speed of 0.89 m/s, which is the impaired walking speed from the DOT, in order to incorporate residents who may be in the evacuation area (Peters et al., 2020). The results were updated in Wood et al. (2025a) to a 1.2 m/s travel speed to be consistent with other states and territories. These return periods were selected since the inundation maximums in Del Norte and Humboldt Counties are driven by the local Cascadia Subduction Zone scenario that provides the wave arrival times used in the analysis. More frequent return period events were excluded because the maximum inundations for those are more influenced by distant sources with larger arrival times.

All potential fatalities occur in the northernmost counties, Del Norte and Humboldt, which are geographically near the Cascadia Subduction Zone where wave arrival times are much shorter (Wood et al., 2025a). With an estimated wave-arrival time of 10 minutes in these counties, assuming a 10-minute departure delay yields an almost 99% fatality rate for the exposed residential population. This drops to 62% and 34% at 5 and 0-minute departure delays, respectively.

Evacuation modeling for distant source tsunamis indicates sufficient time to evacuate for the remaining California counties. Peters et al. (2020) and Wood et al. (2020) indicate that outside of

Del Norte and Humboldt Counties, the fastest estimated tsunami arrival time is 252 minutes, while the longest walk time based on a slow-walk scenario is 190 minutes. However, the inability to account for infrastructure, non-residential populations, and human behavior likely limits the analysis. Statewide, 486,209 residents are exposed to the 2,475-year scenario—more than in any other state. However, the majority (473,264) face distant scenarios, likely allowing sufficient time to evacuate.

Table 2-13: Average Annualized Fatalities Based on Residential Population Unable to Evacuate Inundation Zone Using a 10 Minute Departure Delay

Rank	County	Average Annualized Fatalities	Scenario Fatalities*	Exposed Population*
1	Del Norte	8.02	9,761	9,856
2	Humboldt	2.38	3,064	3,088
	State Total	10.39	12,825	12,944

*Note: Residential population exposed is based on the sum of the population distributed to all inundated building points in tsunami hazard zones and fatalities represent the population unable to reach safety given a 10-minute departure delay (Wood et al., 2025a).

2.5.5 CALIFORNIA TSUNAMI EVACUATION STUDIES

Wood et al. (2013) evaluated potential population challenges from a distant-tsunami scenario associated with a magnitude 9.1 megathrust earthquake east of the Alaska Peninsula. The study discusses how fatalities could result from this distant scenario, such as from secondary fatalities from vehicular accidents or heart attacks. However, there was no quantification or method proposed to estimate fatalities from distant events.

Peters et al. (2020) and Wood et al. (2020) provided data and a publication, respectively, that evaluated pedestrian evacuation time for three statewide probabilistic scenarios (475, 975 and 2,475) for California. The data provided pedestrian travel time along the inundated road networks throughout the state for various walk speeds.

2.5.6 STUDY LIMITATIONS

Hazard Data

California provided seven probabilistic hazard grids for the 72-, 100-, 200-, 475-, 975-, 2,475- and 3,000-year return periods (California Geological Survey, 2025), all of which were used in analyzing building losses. For the return periods where fatalities were expected, only the 975-year and 2,475-year return periods were incorporated into the Wood et al. (2025a) evacuation study, which informed average annualized loss for fatalities. This is because the Cascadia event, which is a local event for northern California, begins to heavily influence the depth grids at the 975-year and greater return periods. The 475-year return period inundation is primarily influenced by the distant Alaska scenario, which would not be appropriate to inform an evacuation study using Cascadia arrival times and the

local-source departure delay of 10 minutes. As a result of having only two return periods to represent the loss curve compared to the five Cascadia return periods leveraged for Oregon, average annualized population losses in California were disproportionately lower when compared to the comparable 2,475 losses alone. Please refer to Appendix F, Section F.2 for additional information.

Missing Hazard Data on Exposed Structures

Appendix F, Section F.3.2 presents an analysis for California of the National Structure Inventory building points along the coast at elevations of less than 5 meters and less than 10 meters that are not included in current tsunami hazard coverage for California. The majority of the buildings missing hazard data are in areas between analysis grids where small slivers, several hundred feet wide, that can be addressed by slightly extending the analysis areas in future model runs. The only significant exposure with no hazard data was Avalon on Catalina Island where slightly over 160 buildings with a replacement cost of $180 million are exposed at elevations of 5 meters or less. The analysis indicates a gap in coverage of slightly over 950 buildings with a $1.2 billion valuation along the coast with an elevation of 5 meters or less. Based on the building exposure that is covered by hazard data (Table 2-12, $348.6 billion), these results indicate that the available hazard data covers 99.6% of the building exposure in California. For more information on the limitations of California's hazard data, please refer to the California Department of Conservation AECOM Probabilistic Tsunami Hazard Maps for California Phase 2 technical documentation (Thio, 2019).

An additional building loss gap occurs because of the lack of Hazus 6.1 analysis coverage for Sacramento County where Wood et al. (2025a) estimates a potential residential population exposure of 118 persons.

Population Loss

When estimating residential population losses, California encounters limitations due to only having data for two Probabilistic Tsunami Hazard Analysis return periods, compared to the five Cascadia Subduction Zone return periods that were available for Oregon. Although Cascadia Subduction Zone-related, 2,475-year population losses in California are larger, the average annualized population losses are disproportionately lower (refer to Appendix F for additional information). Additional Probabilistic Tsunami Hazard Analysis modeling work may better depict the entire loss curve for annualizing loss (Appendix D). Please refer to Section 4.4 for additional information on limitations.

Maritime Impacts

A limitation of this risk analysis is the inability to evaluate the impacts on the nine commercial ports and over 70 harbors and marinas along the California coast that are exposed to tsunamis. Recent events, such as the 2010 Chile tsunami, the 2011 Japan tsunami, and the 2020 Tonga tsunami, caused over $100 million in damages, highlighting that ports and harbors are among the most prone areas to tsunami hazards (Wilson et al., 2013; Lynett et al., 2022). Ports, such as the Port of Los Angeles and Port of Long Beach, are critical hubs for Pacific commerce, with the USGS Science Application for Risk Reduction (SAFRR) study estimating over $1 billion in lost commerce for the U.S. for each day these ports are inoperable (Ross et al., 2013). Additionally, many harbors and marinas

serve as vital economic centers for their communities, supporting fishing fleets and tourism industries.

2.6. Guam

Locally generated tsunamis in Guam are caused by large earthquakes in the Mariana Subduction Zone with more distant sources generated by several subduction zones around the Pacific Ocean basin including the East Philippine Subduction Zone (EPSZ), Nankai, Ryukyu, New Guinea, Manus, and Kuril Subduction Zones (KSZ) (Wood et al., 2023). Based on the tsunami history of Guam from 1849 to 1993 (Lander et al., 2002a), Guam has had three tsunamis large enough to cause damage. Based on a review of historical accounts, Lander et al. (2002a) determined that Guam had damaging tsunamis in 1849, 1892, and 1993. Another two to six events were described but were not verifiable as true tsunamis. The M_w 7.8 tsunamigenic earthquake of August 8, 1993, about 50 km to the east of Guam, helped renew interest in potential Guam tsunamis. A small segment of the Marianas Trench near Guam was the location of the 1993 event; however, a quiet area south of this may be the site of a similar future tsunamigenic earthquake. According to Lander et al. (2002a) most of the damage from a local tsunami is thought to primarily affect the more relatively unpopulated east coast, and the likelihood of a local tsunami from the west is minimal. However, the 1849 tsunami that had 6.1 meters of runup at Agat and evidence of a submarine landslide in Apra Harbor based on a southern source may affect both the east and west coasts of Guam.

2.6.1 TSUNAMI HAZARD DATA

Tsunami runup and depth grid data were available for two scenarios total, one local, and one distant, from two different sources. NOAA Pacific Marine Environmental Laboratory (PMEL) (Uslu et al., 2010) provided mapping for the northwest and northeast coast, including the harbor area, and University of Hawai‘i at Mānoa (Wood et al., 2023) provided modeling for the southern coast (Table 2-14). It is important to note that the northern coast is generally comprised of steep topography with few buildings exposed to tsunami hazards (Appendix F, Section F.3.3).

The local source consists of a modeled M_w 8.5 scenario of the Mariana Subduction Zone provided by PMEL (Uslu et al., 2010, Segment 57-60) for the northwest and northeast coast and the Local Preferred Maximum (M_w 8.3 Mariana Subduction Zone) for the southern coast provided by the University of Hawai‘i (Wood et al., 2023). Two additional flow depth grids were available for the distant scenario, each covering a different part of the Guam coast: East Philippine Subduction Zone M_w 8.5 (Uslu et al., 2010, Segment 8-12) for the northwest and northeast coast and the Distant Preferred Maximum (M_w 8.3, East Philippine Subduction Zone) for the southern coast provided by the University of Hawai‘i (Wood et al., 2023). As momentum flux and velocity data were not available from either source, the hazard data provided support a Hazus Level 1 analysis. Please refer to Appendix C, Section C.4 for preprocessing steps.

Table 2-14: Guam Tsunami Hazard Data Formats and Numerical Models

Scenario	Data Format	Bathymetric-Topographic Data Source	Numerical Modeling Source
Marianas Subduction Zone - M_W -8.5, Segment 57-60 for northwest and northeast coast	IMG	USACE Joint Airborne LiDAR Bathymetry Technical Center of Expertise, NOAA's National Geophysical Data Center	MOST
Marianas Subduction Zone - M_W 8.3, Local Preferred Maximum for southern coast	IMG	Pacific Fisheries Science Center, Pacific Islands Benthic Habitat Mapping Center, NOAA CUDEM	NEOWAVE
East Philippines Subduction Zone - M_W 8.5, Segment 8-12 (EPSZ) for northwest and northeast coast	IMG	USACE Joint Airborne LiDAR Bathymetry Technical Center of Expertise, NOAA's National Geophysical Data Center	MOST
East Philippines Subduction Zone - M_W 8.3, Distant Preferred Maximum (M_w 8.3 Philippine) for southern coast	IMG	Pacific Fisheries Science Center, Pacific Islands Benthic Habitat Mapping Center, NOAA CUDEM	NEOWAVE

2.6.2 RETURN PERIOD DATA

Characteristic magnitude-frequency distributions were developed for Guam using a scaling relationship from Kanamori (1977) and slip rates with preferred coupling coefficients from Berryman et al. (2015), following approaches in Uslu et al. (2010, 2013) and Wood et al. (2019, 2023). These inputs define the time required to accumulate strain and thus the recurrence intervals for the modeled earthquakes. Based on GEM slip-rate data (Berryman et al., 2015), the estimated return periods are approximately 500 years for a local Mw 8.3 Mariana Subduction Zone event and 2,200 years for a M_w 8.3 East Philippine Subduction Zone distant event (Table 2-15).

Table 2-15: Guam Tsunami Hazard Data Sources and Return Periods

Scenario	Tsunami Source	Return Period
Mariana Subduction Zone M_w 8.5, Segment 57-60 for northwest and northeast Coast – NOAA PMEL	Local – Mariana Subduction Zone	500 years
Local Preferred Maximum (M_w 8.3 Mariana Subduction Zone) for southern coast – University of Hawai'i at Mānoa	Local – Local Preferred Maximum (Mariana Subduction Zone)	500 years
EPSZ M_w 8.5, Segment 8-12 (EPSZ) for northwest and northeast Coast – NOAA PMEL	Distant – EPSZ	2,200 years

Scenario	Tsunami Source	Return Period
Distant Preferred Maximum (M_w 8.3 EPSZ) for southern coast – University of Hawai'i at Mānoa	Distant – Distant Preferred Maximum (EPSZ)	2,200 years

2.6.3 AVERAGE ANNUALIZED BUILDING LOSS

The Guam hazard data input is considered a Level 1 Hazus assessment; however, because the velocity grid was created outside of Hazus using Equation 2-1, the Hazus Tsunami Model Level 2 interface was used to analyze building losses on Guam for both scenarios. The average annualized loss was computed for each Census block based on building losses for the 2,200- and 500-year scenarios. Guam is divided into 19 municipalities called villages and has no county equivalents. The territory-wide results are summarized in Table 2-16.

Table 2-16: Total Territory-Wide Average Annualized Building Loss and Exposure

Rank	Territory	Average Annualized Building Losses	Building Exposure to Tsunami	Building Loss Ratio (USD per $1 million)
	Territory Total	$368,602	$3,455,696,131	$106.69

Almost $3.5 billion in building value is exposed in Census blocks with tsunami impacts, resulting in an estimated average annualized loss of about $370,000 per year and $107 per year for every $1 million in building exposure.

Although both Guam and Commonwealth of the Northern Mariana Islands currently both use a local and distant source for scenario modeling, the smaller magnitude of the local source for Guam results in a more frequent return period (500-year for Guam versus 1,587-year for Commonwealth of the Northern Mariana Islands). This more frequent return period provides Guam with a more complete range of losses for estimation of average annualized loss than Commonwealth of the Northern Mariana Islands.

2.6.4 AVERAGE ANNUALIZED RESIDENTIAL POPULATION LOSS

Residential population losses are based on modeled pedestrian evacuations out of the 500-year return period local scenario, resulting in an average annualized rate of 2.87 fatalities (Table 2-17) (Peters et al., 2023; Wood et al., 2023). There are 1,436 persons affected by the local tsunami scenario with insufficient travel time to safety based on a 10-minute departure delay. This affected population decreases to 378 with a 5-minute departure delay and to 147 with no departure delay (Wood et al., 2025a).

Table 2-17: Average Annualized Fatalities Based on Residential Population Unable to Evacuate Inundation Zone Using a 10 Minute Departure Delay

Rank	Territory	Average Annualized Fatalities	Scenario Fatalities	Exposed Population
	Territory Total	2.87	1,436	1,833

2.6.5 STUDY LIMITATIONS

Hazard Data

Only four flow depth grids were available for Guam to assess potential losses, covering the east, west and south sides of the island for a local and a distant scenario. The north side of the island, characterized by steep topography, has no tsunami exposure to buildings. Due to limited data, the study used two Hazus Level 1 analyses, the least accurate of the three Hazus analysis levels. For more information about the tsunami Hazus analyses levels, please refer to Section 2.1.1. When generating average annualized losses using the Riemann sums method (Appendix D), loss estimates may be more accurate when study areas have hazard data from multiple return periods and representation from all sources affecting the study area. Uncertainty in the estimated return periods are also introduced using the scaling relationship and available slip rates for the Marianas Trench and East Philippines Subduction Zones.

Missing Hazard Data on Exposed Structures

There was a data gap that affected approximately 300 exposed coastal structure points with elevations <5 meters along the southwest coast, as well as 44 exposed structures along the northern coast (Appendix F, Section F.3.3).

Population Loss

Please refer to Section 4.4 for additional information regarding limitations across all study areas.

2.7. Hawaii

Since 1813, Hawaii has experienced a tsunami on average every two years, with a damaging tsunami occurring on average every five years (Dudley and Lee, 1998). Tsunamis affecting Hawaii can be locally generated or originate from distant sources throughout the Pacific Ocean basin (Wood et al., 2007). Hawaii is also home to Kīlauea, the world's most active volcano, and rare catastrophic tsunamis have been generated with flank failure collapses with inland runups of several hundred meters (McMurtry et al., 2004). Hawaii was struck by the second deadliest local tsunami (1868) and deadliest distant tsunami (1946) in the United States. Runups of more than 15 meters were measured for the 1946 and 1957 distant tsunamis, as well as the 1868 and 1975 locally generated tsunamis on the island of Hawai'i.

2.7.1 TSUNAMI HAZARD DATA

Hazard data for Hawaii were collected for three major source scenarios (Table 2-18 and Table 2-19):

University of Hawai'i, School of Ocean and Earth Science and Technology (SOEST) Standard Evacuation Scenario: The first source was based on the modeling done by SOEST at the University of Hawai'i at Mānoa to establish the standard tsunami evacuation area in Hawaii (Hawaii Emergency Management Agency (HIEMA), 2021). This scenario was based on the five largest tsunamis in the last 200 years. The maximum flow depths (depth of tsunami flooding on land) of the 1946 Aleutian (M 8.6), 1952 Kamchatka (M 9.0), 1957 Aleutian (M 8.6), 1960 Chile (M 9.5) and 1964 Alaska (M 9.2) earthquakes were simulated at both mean-sea-level (MSL) and high tide conditions for the Hawai'i Tsunami Mapping Project, 2009. For this scenario study, the maximum high tide condition values were used.

Great Aleutian Tsunami (GAT): Initially begun in 2010 based on the lessons from the 2004 M_w 9.3 Sumatra-Andaman earthquake and accelerated after the lessons learned from the larger than expected 2011 Tohoku earthquake (M_w 9.1) and tsunami, scientists began investigating plausible worst-case tsunami inundation modeling scenarios along the Aleutian Trench. A tsunami generated in this eastern Aleutians source region based on probable maximum tsunamis from M_W 9.3 and 9.6 Aleutian earthquakes (Bai et al., 2023) would provide the shortest evacuation time, approximately 4-5 hours, for Hawaii residents, making it the most dangerous far-field tsunami source for Hawaii. However, based on the distant scenario modeling assumptions, no fatalities are projected. Every county in Hawaii now uses both the standard (tier 1) and extreme (tier 2) evacuation zones in their evacuation planning (HIEMA, 2021).

Dr. Kwok Fai Cheung with SOEST performed the modeling for the GAT scenarios (Bai et al., 2023). Dr. Cheung provided the GIS databases containing a ~10m grid of inundation depth in meters for each county. Because these data do not include velocity, the ASCE empirical equation (Equation 2-1) was used to estimate the velocity from runup rather than from the numerical model. As a result, the GAT scenario is considered by Hazus methodologies to be a Level 1 hazard input, despite being run through the Hazus Tsunami Model Level 2 interface.

ASCE Design Scenario: The Tsunami Loads and Effects Subcommittee of ASCE, provides the requirements and building codes for comprehensively designing tsunami-resilient buildings for the United States since the adoption of this standard in the International Building Code 2018 edition. To support the implementation of these codes, ASCE has provided Probabilistic Tsunami Hazard Analysis data and online tools that provide the 2,500-year offshore maximum tsunami amplitude, as well as maximum runup points inland. Because the 2,500-year offshore amplitudes include events that are likely very rare, a return period of ~3,500 years is used for the purpose of annualizing losses for the Hawaii scenarios. In Hawaii, these data are further enhanced by the state's coastal zone mapping program to provide high resolution tsunami data. High resolution data, including momentum flux and flow depth based on NEOWAVE (Yamazaki et al., 2009, 2011) were completed for O'ahu in 2019, Kaua'i in 2023 and the developed areas of the island of Maui in 2023. These

data are available for application along with ASCE 7-28 when performing tsunami design of buildings or other structures in Hawaii.

Table 2-18: Hawaii Tsunami Hazard Data Formats and Numerical Models

Scenario	Data Format	Bathymetric-Topographic Data Source	Numerical Modeling Source
SOEST Standard Evacuation Zone Scenario	KMZ	10-meter NED	NEOWAVE
Great Aleutian Tsunami - M_W 9.3 and 9.6	TIF	10-meter NED	NEOWAVE
ASCE Design Scenario	High Resolution were ASCII grids and low resolution are runup points	CUDEM bathytopo for High Res, 10-meter NED for Low Res	High Resolution is based on NEOWAVE, Low Resolution MOST

Table 2-19: Hawaii Hazard Data and Level of Hazus Analysis

Return Period	Hazus Data Input	Hazus Analysis
400 years	Maximum Runup Height and DEM Grid	Level 1
1,500 years	Maximum Runup Height and DEM Grid	Level 1
3,500 years	Maximum Runup Height and DEM Grid Median Flow Depth Grid and Median Momentum Flux Data	Level 1 for Hawai‘i and Kalawao counties, Level 3 for O‘ahu, Kaua‘i, and Maui

2.7.2 RETURN PERIOD DATA

Return periods (Table 2-20) are estimated for each of the three modeled scenarios as follows:

SOEST Standard Evacuation Scenario: This scenario was based on the five most severe events in the last 200 years occurred between 1946 and 1964, including the historical distant tsunami events affecting Hawaii from the 1946 Aleutian (M 8.6), 1952 Kamchatka (M 9.0), 1957 Aleutian (M 8.6), 1960 Chile (M 9.5) and 1964 Alaska (M 9.2) earthquakes. However, the USGS (La Selle et al., 2020) studied sediment cores collected in Hawaii and could only identify the aforementioned historical events between 1946 and 1964, as well as a major event around 1350 with much more severe inundation than the historical records. The USGS study found no evidence of tsunami deposits before ~1350 and between ~1350 and 1946. La Selle et al. (2020) was unable to find good correlation between paleotsunami evidence in the Aleutians with the Hawaii data, although only

three cores were studied in Hawaii. As a result of these time gaps, although the SOEST scenario represents a 200-year record, a 400-year return period is assigned.

Great Aleutian Tsunami (GAT): Although a rare occurrence, inundation from probable maximum tsunamis from M_w 9.3 and 9.6 earthquakes in the eastern Aleutians Islands would far exceed the flooding observed in Hawaii from past historical tsunamis (Bai et al., 2018 and Bai et al., 2023). Butler et al. (2014) proposed that a giant earthquake in the eastern Aleutian Islands between 1425–1665 was located between the source regions of the 1946 Aleutian (M 8.6) and 1957 Aleutian (M 8.6) earthquakes. Based on the studies of the USGS (La Selle et al., 2020) and Butler et al. (2014), we have estimated a return period of ~1,500 years for the GAT scenario. The return period for this distant tsunami scenario created in the eastern Aleutian Islands is higher than local scenarios generated for Alaskan communities (e.g., 169 years for the King Cove, AK, local tsunami scenario) primarily due to differences in estimated scenario magnitudes (e.g., Mw 9.3 and 9.6 for the Hawaii scenario and Mw 8.9 for the King Cove scenario).

ASCE Design Scenario: ASCE provides data and online tools that identify the 2,500-year offshore maximum tsunami amplitude, as well as maximum runup points inland. The development of the 2,500-year design maps is described in Thio et al. (2017) and Wei et al. (2017). Because the 2,500-year offshore wave heights include large uncertainties, a return period of ~3,500 years is used for the purpose of annualizing losses for the Hawaii scenarios.

Table 2-20: Tsunami Hazard Data and Return Periods

Scenario	Tsunami Source	Return Period
SOEST Standard Evacuation Zone Scenario	Distant – Combined Maximums of 5 Historical Events	400 years
Great Aleutian Tsunami	Distant – Eastern Aleutian Islands	1,500 years
ASCE Design Scenario	Distant – Probabilistic	3,500 years

2.7.3 AVERAGE ANNUALIZED BUILDING LOSS

Table 2-21: Top Five Counties and Total Statewide Average Annualized Building Loss and Exposure

Rank	County	Average Annualized Building Losses	Building Exposure to Tsunami	Building Loss Ratio (USD per $1 million)
1	Honolulu	$42,806,143	$102,890,337,490	$416.04
2	Maui	$27,969,760	$28,528,747,008	$980.43
3	Hawaii	$13,259,960	$16,681,030,029	$794.91
4	Kauai	$7,685,554	$11,432,461,535	$672.28

Rank	County	Average Annualized Building Losses	Building Exposure to Tsunami	Building Loss Ratio (USD per $1 million)
5	Kalawao	$49,699	$101,681,006	$492.07
	State Total	$91,771,117	$159,634,257,068	$574.88

The Hawaii average annualized building stock losses are about $92 million per year (Table 2-21), and are the highest in the nation, almost double the second highest state (California), demonstrating its significant tsunami risk. Honolulu County comprises almost half the total losses, however, Maui and Hawaii Counties have the highest potential losses based on exposure indicative of higher loss severities.

2.7.4 AVERAGE ANNUALIZED RESIDENTIAL POPULATION LOSS

A pedestrian evacuation modeling study summarized in Jones et al. (2018b) and Wood et al. (2018) for Oʻahu Island, Hawaii, suggests that residents in tsunami-hazard zones associated with distant Alaskan sources have sufficient time to evacuate before wave arrival. At the time of this study, no local-source tsunami scenarios provided the necessary wave runup, arrival times, and recurrence data to annualize population loss, leading the study to apply a 0-fatality rate for Hawaii. This limitation is further discussed below.

2.7.5 HAWAII TSUNAMI EVACUATION STUDIES

Wood et al. (2007) provided the first evaluation of population exposure based on the standard tsunami evacuation zone using the SOEST 400-year scenario for 65 coastal communities. Their results indicate that the population exposure in that zone consisted of over 80,000 residents, 67,000 employees, and 50,000 daily visitors. In addition, the zone contains 5,779 businesses and numerous dependent-population facilities including 49% of all hotels, 242 outpatient care facilities, 41 schools, 19 child-day-care facilities, as well as public venues and critical facilities. This study predates the mapping of the larger extreme evacuations zone and ASCE inundation areas that includes over 400,000 individuals. The study was used to help outline the types of dependent and tourist populations exposed.

Wood et al. (2018) and Jones et al. (2018b) summarize pedestrian evacuation modeling for both standard and extreme tsunami hazard zones on Oʻahu Island to assess where individuals may be more likely to use vehicles rather than walking to safety. The use of the extreme zone tripled the number of residents, employees, and facilities serving at-risk populations that would be encouraged to evacuate. Additionally, the use of the extreme zone reduced the percentage of pedestrians able to reach safety within 15 minutes from 98% to 76%. The study also indicated that evacuations for distant tsunami events are likely to be successful, given wave arrival times on the order of hours, the existence of the U.S. tsunami warning system, and the distance to safety.

Based on historical occurrence and geologic observations, the Big Island of Hawaiʻi (Hawaii County) is the most likely location for local tsunami impacts in Hawaii. However, these scenarios may affect

the small islands including large beach communities with little or no warning. Local tsunami scenario inundation in Waikīkī, although not currently mapped, is expected to expose smaller populations and occur less frequently.

2.7.6 STUDY LIMITATIONS

Hazard Data

Most of the hazard data sources (Bai et al., 2018; Bai et al., 2023; HIEMA, 2021; and Wei et al., 2017) for Hawaii lack the velocity and/or momentum flux data needed to more accurately quantify building structural impacts. Some of the hazard products, especially the older 400-year modeling, are available only at coarse (e.g., 30 meter) resolutions and with ranges of potential flow depths. Additional Probabilistic Tsunami Hazard Analysis data, supported by paleotsunami recurrence information, would enhance the risk data for Hawaii, which is threatened by a broad range of potential tsunami sources. Incorporating harbor facility losses, including the extensive military and aviation infrastructure exposed, may be expected to significantly increase losses and improve the potential tsunami risk data for Hawaii.

Missing Hazard Data on Exposed Structures

The building inventory coverage analysis (Appendix F, Section F.3) indicates that all sections of the coast in Hawaii are covered by available hazard data.

Population Loss

This analysis does not indicate potential population losses in Hawaii from distant sources because there may be sufficient time to evacuate to safety (Wood et al., 2018). Local scenario losses are also excluded due to data gaps. Historically, Hawaii has experienced the largest loss of life in the U.S. from distant tsunamis; however, these losses occurred before the establishment of the modern U.S. tsunami warning system. Fatalities for distant tsunamis are possible given uncertainties in human behavior. A particular concern for Hawaii is the potential for extreme distant scenarios, which may expose over 400,000 residents and over 250,000 daily visitors (Hawai‘i Tourism Authority, 2024), as well as exposed populations aboard cruise ships and on beaches year-round. No event of this magnitude has occurred since the warning system was established, and the potential exposed population far exceeds that of past events within this system's operational period. As data and methods are developed that can improve estimates of potential fatalities from distant and local tsunamis in Hawaii, additional losses may be included. Please refer to Section 4.4 for additional information regarding limitations across all study areas.

2.8. Commonwealth of the Northern Mariana Islands

The Commonwealth of the Northern Mariana Islands comprises 14 islands, with most development and population centers in the Municipalities of Saipan, Tinian, and Rota. While the Commonwealth of the Northern Mariana Islands receives frequent tsunami waves from events in the region, historically, they have not been destructive. The largest and most recent wave event was a 3.5-foot

wave that hit at low tide from the 2011 Tohoku tsunami. A NOAA PMEL tsunami hazard assessment for the Commonwealth of the Northern Mariana Islands (Uslu et al., 2013) indicated that the greatest tsunami threats to the Commonwealth of the Northern Mariana Islands are from tsunamis triggered by earthquakes along the western Aleutian Islands, the Cascadia Subduction Zone, the Philippines Trench, the Japan Trench, the Mariana Subduction Zone, the Manus Trench, the New Guinea Trench, and the Ryukyu-Nankai Trench. Predicted wave amplitudes at the Municipalities of Saipan and Tinian would exceed 13 meters and would be greater than 7 meters along the Rota coastline should a M_w 9.0 earthquake occur in the Commonwealth of the Northern Mariana Islands.

2.8.1 TSUNAMI HAZARD DATA

Uslu et al., 2013, characterizes the potential threat for tsunamis along the coastlines of Saipan, Tinian, and Rota, considering 725 possible earthquake scenarios. These results were intended for warning and evacuation products for planning and education of local communities. Data consisted of grid files of flow depth and velocity grids for both local and distant scenarios for the Municipality of Saipan, and flow depth data alone for the Municipalities of Tinian and Rota.

Local and distant tsunami hazard data were provided in grid format for the Municipalities of Saipan, Tinian, and Rota; the data provided for the Municipalities of Tinian and Rota only included flow depth, while the data for the Municipality of Saipan included both flow depth and velocity. The local and distant grids for the Municipalities of Tinian and Rota are considered identical due to the lack of data for the distant event in these areas, as detailed in Table 2-22.

The hazard products supported a Hazus Level 2 assessment for Saipan and Level 1 for Rota and Tinian; please refer to Appendix C, Section C.6 for additional information.

Table 2-22: Commonwealth of the Northern Mariana Islands Hazard Data and Level of Hazus Analysis

Return Period	Hazus Data Input	Hazus Analysis
1,587 years	Flow Depth Grid and Velocity Grid using Energy Grade Line Equation for Rota and Tinian, Flow Depth Grid and Velocity Grid from numerical model for Saipan	Level 1 for Rota and Tinian, Level 2 for Saipan
2,200 years	1,587-year Flow Depth Grid and Velocity Grid using Energy Grade Line Equation for Rota and Tinian, Flow Depth and Velocity Grids including the maximum values between the 1,587-year and 2,200-year values for Saipan	Level 1 for Rota and Tinian, Level 2 for Saipan

Return periods were estimated using the same slip rate approach as Guam. However, because a larger magnitude (M_w 8.5) was used for the Commonwealth of the Northern Mariana Islands local scenario, a longer return period (1,587-year in the Commonwealth of the Northern Mariana Islands versus 500-year in Guam) is required to accumulate the additional strain (Table 2-23).

Table 2-23: NOAA Pacific Marine Environmental Laboratory Commonwealth of the Northern Mariana Islands Tsunami Hazard Data

Scenario	Tsunami Source	Return Period
Maximum Local Scenario M_w 9.0 Mariana Subduction Zone with 20m slip; Segment 54 (Uslu et al., 2013)	Mariana Subduction Zone - M_w 9.0	1,587 years
Maximum Distant Scenario M_w 9.0 RNSZ, Segment 12 (Uslu et al., 2013)	Ryukyu–Kyushu–Nankai Subduction Zone (RNSZ) – M_W 9.0	2,200 years

2.8.2 RETURN PERIOD DATA

Like the approach described for Guam, characteristic magnitude-frequency distributions for the Commonwealth of the Northern Mariana Islands were developed using the Kanamori (1977) slip-based scaling relationship together with slip rates and preferred coupling coefficients from Berryman et al. (2015), following Uslu et al. (2010, 2013) and Wood et al. (2019, 2023). Using convergence rates derived from the GEM active faults database (Berryman et al., 2015), Dr. Kwok Fai Cheung estimated return periods of approximately 1,587 years for the Maximum Local Scenario and 2,200 years for the Maximum Distant Scenario (Table 2-23).

2.8.3 AVERAGE ANNUALIZED BUILDING LOSS

Table 2-24: Top Three Counties and Total Territory-wide Average Annualized Building Loss and Exposure

Rank	County	Average Annualized Building Losses	Building Exposure to Tsunami	Building Loss Ratio (USD per $1 million)
1	Saipan	$141,862	3,313,303,743	$42.82
2	Tinian	$25,950	$120,381,649	$216.25
3	Rota	$17,678	$223,742,096	$79.27
	Territory Total	$185,490	$3,657,427,488	$50.72

Both the Commonwealth of the Northern Mariana Islands and Guam have similar overall building exposure to the tsunami hazard. However, building average annualized loss in the Commonwealth of the Northern Mariana Islands (Table 2-24) is generally lower than Guam since the local scenario for the Commonwealth of the Northern Mariana Islands has a longer return period (1,587-year in the Commonwealth of the Northern Mariana Islands versus 500-year in Guam).

2.8.4 AVERAGE ANNUALIZED RESIDENTIAL POPULATION LOSS

Residential population losses are based on modeled pedestrian evacuations (Wood and Peters 2025b) and population exposure (Wood et al., 2025a) for a local event scenario with a 1,587-year return period, resulting in an average annualized rate of 2.40 fatalities (Table 2-25). The largest potential fatality losses are in the Municipality of Saipan, where over 3,600 residents are exposed. Assuming a 10-minute delay in departure from the start of earthquake ground shaking, with wave-arrival times also estimated at 10 minutes, only about 2% of the residential population may reach safety. This finding highlights the influence of minimizing departure delays immediately following ground shaking. Given the proximity of high ground, potential fatalities decrease to just 3 with a 5-minute departure delay and to 0 with no departure delay (Wood et al. 2025a).

Table 2-25: Average Annualized Fatalities Based on Residential Population Unable to Evacuate Inundation Zone Using a 10 Minute Departure Delay

Rank	County	Average Annualized Fatalities	Scenario Fatalities	Exposed Population
1	Municipality of Saipan	2.24	3,554	4,989
2	Municipality of Rota	0.11	168	184
3	Municipality of Tinian	0.05	85	93
	Territory Total	2.40	3,807	5,266

2.8.5 STUDY LIMITATIONS

Hazard Data

In the Commonwealth of the Northern Mariana Islands, data quality and availability varied across the Municipalities of Rota, Tinian, and Saipan. Although two scenarios were used to produce average annualized losses, only the local scenario (1,587-year return period) had data for all three islands. Additionally, for the Riemann sums average annualized loss equation, it is optimal to have data for several return periods across a range of frequencies (see Appendix D). The limited availability of only two scenarios and two return periods in the Commonwealth of the Northern Mariana Islands creates a limitation. Uncertainty in the estimated return periods are also introduced using the scaling relationship and available slip rates for the Marianas Trench and Ryukyu–Kyushu–Nankai Subduction Zones.

Within the data for the local scenario, only the Municipality of Saipan had depth grid and velocity data, whereas the Municipalities of Rota and Tinian only had depth grids available. For the distant scenario (2,200-year return period), only the Municipality of Saipan had available data, so the maximum values were taken when combining the local scenario data and the distant scenario data for Municipality of Saipan. For the distant scenario in the Municipalities of Rota and Tinian, only values from the local scenario were used to supplement data due to its shorter return period. The

discrepancy in data quality and availability among the islands can cause variability in the loss results across islands.

Missing Hazard Data on Exposed Structures

The building inventory coverage analysis (Appendix F, Section F.3) indicates that all sections of the Commonwealth of the Northern Mariana Islands coast are covered by available hazard data.

Population Loss

Please refer to Section 4.4 for additional information regarding limitations across all study areas.

2.9. Oregon

The primary tsunami threat to the Oregon coast is associated with earthquakes generated within the Cascadia Subduction Zone, which can generate local events that strike the shore within minutes. Substantial evidence of paleotsunamis over the past 10,000 years has been found across Oregon, including marine turbidites in offshore channels and repeated significant tsunami deposits onshore. As introduced in Allan et al. (2020), at least 19 earthquakes of M_w 8.5 or greater have occurred in the last 10,000 years, with the most recent major event on January 26, 1700, approximately 325 years ago (Atwater et al., 2005). The conditional probability of an earthquake originating anywhere along the Cascadia Subduction Zone is estimated to be around 16% to 22% within the next 50 years, while the probability of a partial Cascadia Subduction Zone rupture that initiates along the southern Oregon coast is approximately 37% to 43% (Goldfinger et al., 2017).

Oregon is also exposed to distant tsunami threats around the Pacific Rim, including the Gulf of Alaska as demonstrated by the 5 Oregon fatalities caused by the 1964 Alaska earthquake (M 9.2).

In addition, there is risk to Oregon coastal communities because of local splay faults (i.e., the potential for smaller tsunamigenic earthquakes) and submarine landslide-generated tsunamis (Priest et al., 2001).

2.9.1 TSUNAMI HAZARD DATA

The Oregon Department of Geology and Mineral Industries (DOGAMI) provided runup grid data, depth grid data, and momentum flux grid data for five local Cascadia Subduction Zone scenarios ranging from M_w 8.7 to M_w 9.2, and two distant tsunami scenarios from the Gulf of Alaska (Witter et al., 2011; Priest et al., 2013) (Table 2-26). All Oregon hazard data were available in Hazus Level 3 ready formats.

Table 2-26: Oregon Department of Geology and Mineral Industries Tsunami Hazard Data

Scenario	Tsunami Source	Return Period
Cascadia Subduction Zone – M_w 8 .9 (M)	Local - Cascadia Subduction Zone	1,000 years

Scenario	Tsunami Source	Return Period
Cascadia Subduction Zone – M_w 8.7 (S)	Local - Cascadia Subduction Zone	2,000 years
Cascadia Subduction Zone – M_w 9.0 (L)	Local - Cascadia Subduction Zone	3,333 years
Cascadia Subduction Zone – M_w 9.1 (XL)	Local - Cascadia Subduction Zone	5,000 years
Cascadia Subduction Zone – M_w 9.1 (XXL)	Local - Cascadia Subduction Zone	10,000 years
1964 Alaska earthquake (M 9.2) - (AK64)	Distant - Alaska/Aleutian Subduction Zone	1,000 years
Alaska Maximum (AKMax)	Distant - Alaska/Aleutian Subduction Zone	1,000 years

2.9.2 RETURN PERIOD DATA

FEMA leveraged return periods for the Oregon Cascadia Subduction Zone events from DOGAMI Open-File Reports (Allan et al., 2020; Allan and O'Brien, 2023). According to Witter et al. (2013), the approximate relationships between the earthquake size classes correspond to approximate recurrence rates as follows: S, 1/2,000 year; M, 1/1,000 year; L, 1/3,333 year; and XL, <1/10,000 year. Although the recurrence for the XXL1 maximum considered event is not known, we used an estimate of 10,000 years for this study since it is the duration of the record (Table 2-26). The return period for the Alaska distant tsunami scenarios for Oregon (1,000 years) is higher than local scenarios in similar areas generated for Alaskan communities (e.g., 594 years for Chenega Bay and Tatitlek scenario) primarily due to differences in estimated scenario magnitudes (e.g., Mw 9.2 for the Oregon distant scenarios and Mw 9.0 for the Alaskan scenarios).

California and Washington have tsunami products based on Cascadia Subduction Zone earthquake scenarios that are different but comparable. In Washington, the one Cascadia Subduction Zone-related scenario is based on a Mw 9.0 earthquake with an estimated return period of 2,500 years, which is comparable to the Oregon "L" scenario. In California, the 2,475-year product is also comparable to the Oregon "L" scenario and the 975-year product is comparable to the Oregon "M" scenario.

2.9.3 AVERAGE ANNUALIZED BUILDING LOSS

Table 2-27: Top Five Counties and Total Statewide Average Annualized Building Loss and Exposure

Rank	County	Average Annualized Building Losses	Building Exposure to Tsunami	Building Loss Ratio (USD per $1 million)
1	Clatsop	$6,238,082	$15,733,886,200	$396.50

Rank	County	Average Annualized Building Losses	Building Exposure to Tsunami	Building Loss Ratio (USD per $1 million)
2	Lincoln	$2,499,598	$13,447,334,480	$185.89
3	Tillamook	$1,808,275	$7,382,810,981	$244.96
4	Curry	$1,339,995	$4,881,334,499	$274.53
5	Coos	$1,184,752	$12,233,437,625	$96.85
	State Total	$13,499,537	$57,877,623,046	$233.25

The losses are based on five return periods ranging from 1,000- to 10,000-year return period inundation, resulting in an estimated loss of about $13.5 million in buildings on an average annualized basis. Almost $60 billion in total building value is in the tsunami-affected census blocks (Table 2-27).

On a per capita level, Oregon's projected per capita loss based on the residential population exposed in all affected census blocks is about $126. The annualized building loss ratio is about $233 per $1 million in exposure.

2.9.4 AVERAGE ANNUALIZED RESIDENTIAL POPULATION LOSS

Residential population losses are based on annualizing DOGAMI modeled, pedestrian-evacuation results across all five local scenarios for Oregon (O'Brien and Allan, 2025). Population-exposure estimates based on the evacuation modeling (Wood et al., 2025a) results in an average annualized rate of 9.34 fatalities (Table 2-28) based on a 10-minute departure delay. The largest potential fatality losses are in Clatsop County, driven by the community of Seaside, with the second highest in Curry County, driven mostly by the community of Gold Beach. While Lincoln and Tillamook are near the top of the list for building losses (refer to Table 2-27), they rank slightly lower on population losses, possibly indicating that higher rates of the population can reach safety.

Table 2-28: Average Annualized Fatalities Based on Residential Population Unable to Evacuate Inundation Zone Using a 10 Minute Departure Delay

Rank	County	Average Annualized Fatalities	Scenario Fatalities*	Exposed Population*
1	Clatsop	6.77	9,267	20,491
2	Curry	1.10	3,098	6,962
3	Coos	0.74	2,778	11,061
4	Tillamook	0.48	901	7,063
5	Lincoln	0.24	445	11,447

Rank	County	Average Annualized Fatalities	Scenario Fatalities*	Exposed Population*
6	Lane	0.00	23	1,739
7	Douglas	0.00	1	1,976
	State Total	9.34	16,512	60,739

*Note: Residential population exposed is based on the sum of the population distributed to all inundated building points in tsunami hazard zones and fatalities represent the population unable to reach safety given a 10-minute departure delay (Wood et al., 2025a). The average annualized fatalities are across all available return periods (1,000-, 2,000-, 3,333-, 5,000- and 10,000-year).

2.9.5 OREGON TSUNAMI EVACUATION STUDIES

DOGAMI has completed several tsunami impact studies that have included assessment of both resident and temporary resident casualties based on enhanced datasets and methods for all Oregon high risk counties combined with earthquake impacts. These studies provide an opportunity to compare the results of this approach.

Although DOGAMI has completed studies for all high-risk counties, we selected Clatsop (Allan et al., 2020) and Curry counties (Allan et al., 2023) for comparison purposes because they have the most severe population losses. There are some slight differences in the approaches to distribute the residential populations based on Census data. Allan et al. (2020) used the American Community Survey (ACS) data products (2013–2017 census data for Clatsop County and 2014-2018 for Curry County) at the census block-group level whereas this study used the Census 2020 block-level population counts. Another difference is that the DOGAMI approach estimates the units for residential occupancies based on building area as outlined in Figure 2-2 of Allan et al. (2020), while the USGS leverages the unit counts in the National Structure Inventory data derived from LightBox (USACE, 2022). Allan et al. (2023) also provides additional comparisons using records from the Oregon Department of Motor Vehicles. Each are reasonable approaches based on data availability but can cause differences.

Table 2-29 compares the population scenarios for three of the return period scenarios for Clatsop and Curry Counties. Considering the known differences in the approach, the overall comparisons of population exposures are similar. Based on the comparison of Clatsop County results, the assumption that residents who are unable to reach safety are fatalities may overestimate population impacts. However, the FEMA results appear somewhat lower for two of the three scenarios for Curry.

This page intentionally left blank.

Table 2-29: Comparisons of Residential Exposures and Casualties by Return Period

County	Residents by Tsunami Zone						Potential Resident Casualties					
	1,000		3,333		10,000		1,000		3,333		10,000	
	DOGAMI	FEMA	DOGAMI	FEMA	DOGAMI	FEMA	DOGAMI	FEMA	DOGAMI	FEMA	DOGAMI	FEMA
Clatsop County	11,880	12,810	15,638	16,423	19,440	20,491	3,888	5,804	4,294	6,566	6,930	9,267
Curry County	1,974	1,734	3,451	3,164	6,940	6,960	257	335	1,150	1,109	3,776	3,139

Note: The FEMA methodology assumes all potential casualties are fatalities, whereas DOGAMI groups injuries and fatalities. FEMA does not assess temporary resident casualties.

Table 2-30 : DOGAMI Estimates of Potential Temporary Resident Casualties

County	Potential Temporary Resident Casualties		
	1,000	3,333	10,000
	DOGAMI	DOGAMI	DOGAMI
Clatsop County	7,681	8,129	14,588
Curry County	1,554	2,738	6,390

The largest difference in population loss results is the ability of DOGAMI to incorporate an approach for estimating temporary populations (Table 2-30). DOGAMI uses a peak summer weekend scenario to estimate this population to maximize the potential impact. This approach is critical for evacuation and other planning, including evaluating and siting vertical evacuation structures. However, including these data in this study would require the development of similar data across all states and territories. Currently, only Oregon and Washington would be able to produce these temporary population data.

This page intentionally left blank.

2.9.6 STUDY LIMITATIONS

Hazard Data

In Oregon, seven tsunami scenarios among five return periods were available, representing the Small (S), Medium (M), Large (L), X-Large (XL), and XX-Large (XXL) Cascadia Subduction Zone tsunamis, as well as the Alaska Maximum event and the 1964 Alaska earthquake (M 9.2). The latter two were modeled and originated in Alaska. These scenarios are deterministic, which can be a limitation because deterministic scenarios do not capture the complete range of possible tsunami scenarios that can occur. For more information about the hazard data limitations, please see the DOGAMI Special Paper 43 (Witter et al., 2011).

Missing Hazard Data on Exposed Structures

The building inventory coverage analysis (Appendix F, Section F.3) indicates that all sections of the coast in Oregon are covered by available hazard data.

Population Loss

Please refer to Section 4.4 for additional information regarding limitations across all study areas.

2.10. Puerto Rico

Significant tsunami events in 1867, 1868 and 1918 have affected the Puerto Rico coastal region. The 1867 and 1918 tsunamis were over 6 meters high (Reid and Taber, 1919), with the 1918 event resulting in 116 fatalities (Coffman et al., 1982). Although the source of the historical tsunamis has been local earthquakes, tsunamis affecting Puerto Rico can also be generated by regional and distant earthquakes, landslides, or volcanic activity.

2.10.1 TSUNAMI HAZARD DATA

Data were provided by the Puerto Rico Seismic Network, University of Puerto Rico at Mayaguez, Department of Geology. They consisted of 34 local tsunami scenarios among four main tsunami sources (Puerto Rico Trench, Muertos Trough, Mona Channel, and Anegada Passage) and ten return periods (Figure 2-1 and Table 2-31). Data were retrieved from an external hard disk that contained about 14 compressed terabytes (TB) of data. The data were in Network Common Data Form (NetCDF) format containing various resolutions with the highest resolution, 20 meters, used for this project. The data provided both flow depth and velocity and were considered a Level 2 analysis in Hazus.

The return periods are estimated using the Gutenberg-Richter law with parameters published for the GEM (Garcia-Pelaez et al., 2019).

Figure 2-1: Puerto Rico Scenario Sources

This map was generated with ArcPro, using World Imagery by Esri. Source: Esri, Maxar, GeoEye, Earthstar Geographics, CNES/Airbus, DS, USDA, AeroGRID, IGN, and the GIS User Community (Esri, 2025).

Table 2-31: University of Puerto Rico Tsunami Hazard Data

Scenario ID (Figure 2-1)	Tsunami Source	Return Period
ID_11_19N M_w - 7.6	Local - Puerto Rico Northern Zone	594 years
ID_2_19N M_w - 7.6	Local - Puerto Rico Northern Zone	594 years
ID_5_19N M_w - 7.6	Local - Puerto Rico Northern Zone	594 years
ID_6_19N M_w - 7.6	Local - Puerto Rico Northern Zone	594 years
ID_9_19N M_w - 7.6	Local - Puerto Rico Northern Zone	594 years
ID_17_Anegada_Passage M_w - 7.4	Local - Mona Rift Zone	717 years
ID_20_Anegada_Passage M_w - 7.4	Local - Mona Rift Zone	717 years
ID_4_FEMA - M_w 7.9	Local - Puerto Rico Northern Zone	1,026 years
ID_8_Anegada_Passage M_w - 7.6	Local - Mona Rift Zone	1,050 years
ID_15_Anegada_Passage M_w - 7.6	Local - Mona Rift Zone	1,050 years
ID_21_Anegada_Passage M_w - 7.6	Local - Mona Rift Zone	1,050 years
ID_25_Anegada_Passage M_w - 7.6	Local - Mona Rift Zone	1,050 years
ID_16_Mona Channel M_w - 7.6	Local - Mona Rift Zone	1,050 years
ID_12_Mona Channel M_w - 7.6	Local - Mona Rift Zone	1,050 years
ID_13_Mona Channel M_w - 7.6	Local - Mona Rift Zone	1,050 years
ID_182_Mona Channel M_w - 7.6	Local - Mona Rift Zone	1,050 years
ID_191_Mona Channel M_w - 7.6	Local - Mona Rift Zone	1,050 years
ID_9_Septentrional - M_w 7.8	Local - North Hispaniola Deformed Belt Zone	1,097 years
ID_10_Septentrional - M_w 7.8	Local - North Hispaniola Deformed Belt Zone	1,097 years
ID_1_FEMA - M_w 8.0	Local - Puerto Rico Northern Zone	1,231 years
ID_2_FEMA - M_w 8.0	Local - Puerto Rico Northern Zone	1,231 years
ID_14_Anegada_Passage M_w - 7.7	Local - Mona Rift Zone	1,271 years
ID_1_Puerto Rico Trench - M_w 8.0	Local - North Hispaniola Deformed Belt Zone	1,727 years
ID_8_Puerto Rico Trench - M_w 8.0	Local - North Hispaniola Deformed Belt Zone	1,727 years

Scenario ID (Figure 2-1)	Tsunami Source	Return Period
ID_11_Puerto Rico Trench - M_w 8.0	Local - North Hispaniola Deformed Belt Zone	1,727 years
ID_12_Puerto Rico Trench - M_w 8.0	Local - North Hispaniola Deformed Belt Zone	1,727 years
ID_16_Puerto Rico Trench - M_w 8.0	Local - North Hispaniola Deformed Belt Zone	1,727 years
ID_17_Puerto Rico Trench - M_w 8.0	Local - North Hispaniola Deformed Belt Zone	1,727 years
ID_19_Puerto Rico Trench - M_w 8.0	Local - North Hispaniola Deformed Belt Zone	1,727 years
ID_5_Puerto Rico Trench - M_w 8.0	Local - North Hispaniola Deformed Belt Zone	1,727 years
ID_3_FEMA - M_w 8.2	Local - Puerto Rico Northern Zone	1,773 years
ID_10_Muertos Trough M_w - 7.5	Local - Los Muertos Trough Zone (Shallow Seismicity)	6,584 years
ID_15_Muertos Trough M_w - 7.5	Local - Los Muertos Trough Zone (Shallow Seismicity)	6,584 years
ID_22_Muertos Trough M_w - 7.5	Local - Los Muertos Trough Zone (Shallow Seismicity)	6,584 years

2.10.2 RETURN PERIOD DATA

The estimated return periods for available scenarios in the Caribbean Territories used values from Caribbean GEM Report sources as outlined in Appendix G and summarized in Table 2-31. The locations of the tsunami scenarios were aligned with the Caribbean GEM source zones, and values from those sources along with the scenario magnitudes were used as inputs for the Gutenberg-Richter law to produce return period estimates. This method was chosen based on the recommendation of representatives of the Puerto Rico Seismic Network. Additional estimations beyond information from the Caribbean GEM Report were necessary because the tsunami scenarios that were modeled had higher magnitudes than the earthquakes in the report. Please see Appendix G for the Gutenberg-Richter law values for each Puerto Rico scenario.

Equation 2-2: Gutenberg-Richter law

$$\boldsymbol{logN = a - bm}$$

Where N is the annual rate of earthquakes with $M > m$, a is the total seismicity rate of the region, and where b is the relative distribution of earthquakes among magnitudes.

2.10.3 AVERAGE ANNUALIZED BUILDING LOSS

Average annualized losses are based on the return period scenarios above ranging from 594 to 6,584 years, where the ID_3_FEMA - M_w 8.2 scenario (see Table 2-31), with a 1,773-year return period, is the most impactful on the northern coast of Puerto Rico. Table 2-32 shows the total average annualized building losses for the top five municipios (county equivalents) in Puerto Rico, including the building value exposed in all affected census blocks in each municipio along with a building loss ratio expressed as the total average annualized loss in USD per $1 million in building exposure. Puerto Rico has about $42 billion in building exposure in tsunami-affected Census blocks resulting in about $2.5 million in average annualized building losses.

Table 2-32: Top Five Municipios and Total Territory-Wide Average Annualized Building Loss and Exposure

Rank	Municipio	Average Annualized Building Losses	Building Exposure to Tsunami	Building Loss Ratio (USD per $1 million)
1	San Juan	$628,675	$9,720,918,713	$64.68
2	Arecibo	$447,112	$2,821,603,435	$158.49
3	Hatillo	$347,927	$1,306,162,290	$266.41
4	Dorado	$288,215	$950,828,348	$303.38
5	Vega Baja	$153,995	$923,576,944	$166.84
	Territory Total	$2,544,236	$42,277,235,704	$60.18

The Municipio de San Juan contains the largest annualized building loss, while the Municipio de Dorado has the highest loss severity represented by the loss ratio.

2.10.4 AVERAGE ANNUALIZED RESIDENTIAL POPULATION LOSS

Residential population losses are based on the modeled scenarios in Table 2-31. Pedestrian evacuation modeling was done for certain segments of the Puerto Rico coastline (Peters and Wood, 2025) and then used to estimate exposed residential populations for each scenario (Wood et al., 2025a). The modeling coupled with the estimated return periods for each scenario results in an average annualized fatality rate of 17.94 for Puerto Rico (Table 2-33). This is the highest in the nation based on a 10-minute departure delay. Similar to building losses, potential population losses are highest for the FEMA M_w 8.2 Puerto Rico Trench scenario because it could affect the densely populated northern coast where almost 54,000 residents are in tsunami-hazard zones. In San Juan alone, this scenario could result in over 8,000 fatalities. Reducing departure delays may substantially reduce losses (Wood et al., 2025a).

Table 2-33: Top 10 Municipios Average Annualized Fatalities Based on Residential Population Unable to Evacuate Inundation Zone Using a 10-Minute Departure Delay

Rank	Municipio	Average Annualized Fatalities	Scenario Fatalities*	Exposed Population*
1	San Juan	4.72	8,256	18,813
2	Hatillo	4.05	3,921	2,075
3	Arecibo	2.21	2,937	3,913
4	Vega Baja	1.40	2,235	3,293
5	Dorado	0.86	1,497	1,889
6	Toa Baja	0.81	1,409	5,145
7	Camuy	0.67	653	829
8	Barceloneta	0.54	760	981
9	Carolina	0.52	905	5,204
10	Vega Alta	0.49	843	1,080
	Territory Total	**17.94**	**25,612**	**61,953**

*Note: Residential population exposed is based on the sum of the population distributed to all inundated building points in tsunami hazard zones and fatalities represent the population unable to reach safety given a 10-minute departure delay (Wood et al., 2025a).

2.10.5 STUDY LIMITATIONS

Hazard Data

With 34 scenarios analyzed from estimated return periods ranging from 594 to 6,584 years, a robust loss curve is expected. However, a Probabilistic Tsunami Hazard Analysis based on a decision tree approach and suite of return periods that include more distant sources may be beneficial for average annualized risk.

Additionally, inconsistencies in scenario modeling across the Caribbean Territories may result in varying outcomes even when using the same data sources. For example, in Puerto Rico, the modelling assumed that smaller segments of the Puerto Rico Trench ruptured, leading to lower magnitude events and shorter return periods. In contrast, the modeling for United States Virgin Islands assumed that the entire Puerto Rico Trench ruptured, resulting in higher magnitude events and longer return periods. Standardizing modeling approaches across states and territories may enhance the accuracy of nationwide tsunami risk assessments.

Missing Hazard Data on Exposed Structures

Appendix F, Section F.3.4 presents an analysis for Puerto Rico of the National Structure Inventory building points along the coast at elevations of less than 5 meters and less than 10 meters that are not included in current tsunami hazard coverage for Puerto Rico. The structures missing hazard data are located in the Municipio de Vega Alta. The analysis indicates a gap in coverage for 39 buildings with a combined valuation of nearly $17 million, situated along the coast at elevations of 10 meters or less. Given that the available hazard data covers $42 billion in building exposure (Table 2-32), this indicates that 99.9% of the building exposure in Puerto Rico is accounted for by the existing hazard data.

Population Loss

Puerto Rico's population loss assessment may benefit from incorporating visitor and non-residential populations, such as cruise ship passengers. In addition, there are known issues with Census data in Puerto Rico including an overall 9.8% error rate, 5.7% overestimate of population and an underestimate of vacant households (Heim and Hong, 2022). Please refer to Section 4.4 for additional information regarding limitations across all study areas.

2.11. United States Virgin Islands

United States Virgin Islands shares many of the same tsunami sources as Puerto Rico with several active tectonic sources capable of producing powerful tsunamis. The main difference is the proximity of tsunami sources. The largest recorded runup in the Caribbean region of 15.2 meters occurred on St. Thomas (Moore and Arcas, 2018, in press) on November 18, 1867. The tsunami originated from an estimated M 7.5 earthquake in the Anegada Passage located between St. Thomas Island and St. Croix Island (Zahibo et al., 2003). The 1867 earthquake produced a powerful series of waves that traveled to shore within 5 to 15 minutes. In Charlotte Amalie, reports indicated water rapidly receded from the shoreline by 10 meters followed by runups of 6 meters, killing 12. On St. Croix Island, waves of up to 9 meters were reported and in Christiansted, waves reached 91 meters inland. In total, this event resulted in 24 documented casualties (Lander et al., 2002b).

2.11.1 TSUNAMI HAZARD DATA

The NOAA PMEL provided runup, depth, and momentum flux data for thirteen scenarios from five sources (Anegada Passage, Puerto Rico Trench, Columbia/Venezuela Belt, Virgin Islands Trough, and Lesser Antilles Trench) across eight return periods listed in Table 2-34. Moore and Arcas (2018, in press) provide the parameters and technical descriptions for the sources in Table 2-34 except for the Anegada Passage sources. The Anegada Passage sources were incorporated during this study at the request of the Virgin Islands Territorial Emergency Management Agency (VITEMA), using source parameters provided by the University of Puerto Rico for Puerto Rico. These parameters will be included in an updated version of Moore and Arcas (2018, in press).

The hazard data provided support a Hazus Level 3 analysis. Please refer to Appendix C, Section C.9 for preprocessing steps.

Table 2-34: NOAA Pacific Marine Environmental Laboratory United States Virgin Islands Tsunami Hazard Data

Scenario	Tsunami Source	Return Period
ID_17_Anegada_Passage M_w - 7.4	Local - Mona Rift Zone	717 years
ID_20_Anegada_Passage M_w - 7.4	Local - Mona Rift Zone	717 years
ID_8_Anegada_Passage M_w - 7.6	Local - Mona Rift Zone	1,050 years
ID_15_Anegada_Passage M_w - 7.6	Local - Mona Rift Zone	1,050 years
ID_21_Anegada_Passage M_w - 7.6	Local - Mona Rift Zone	1,050 years
ID_25_Anegada_Passage M_w - 7.6	Local - Mona Rift Zone	1,050 years
ID_14_Anegada_Passage M_w - 7.7	Local - Mona Rift Zone	1,271 years
Puerto Rico Trench (PRT2) - M_w 8.7	Local - Puerto Rico Trench	4,414 years
Columbia/Venezuela Belt (FSCDB) - M_w 8.9	Local - Columbia/Venezuela Belt	8,496 years
Puerto Rico Trench (PRTG) - M_w 9.1	Local - Puerto Rico Trench	9,154 years
Virgin Islands Trough (1867) - M_w 7.8	Local - Virgin Islands Trough	14,008 years
Lesser Antilles Trench (LA2) - M_w 8.5	Local - Lesser Antilles Trench	141,182 years
Lesser Antilles Trench (LA) - M_w 8.5	Local - Lesser Antilles Trench	141,182 years

2.11.2 RETURN PERIOD DATA

Return periods for scenarios affecting United States Virgin Islands used the same Caribbean GEM sources and Gutenberg-Richter law approach as Puerto Rico. Please refer to Section 2.10.2 for an overview of the return period method used for the Caribbean Territories presented in Table 2-34. Please refer to Appendix G for the Gutenberg-Richter law return periods for the Caribbean Territory scenarios.

2.11.3 AVERAGE ANNUALIZED BUILDING LOSS

Table 2-35: Counties and Total Territory-wide Average Annualized Building Loss and Exposure

Rank	County	Average Annualized Building Losses	Building Exposure to Tsunami	Building Loss Ratio (USD per $1 million)
1	St. Thomas Island	$811,358	$6,926,847,761	$117.15
2	St. Croix Island	$309,070	$2,134,863,255	$144.83
3	St. John Island	$62,525	$1,050,635,449	$59.55
	Territory Total	$1,182,952	$10,112,346,465	$116.99

Based on the scenarios available, total building average annualized losses for United States Virgin Islands are about $1.2 million, with more than 69% occurring on St. Thomas Island and with almost $7 billion in building value exposed (Table 2-35). The loss ratio, indicating relative severity is highest on St. Croix Island, where about $2.1 billion in building value is exposed to potential tsunami impacts.

2.11.4 AVERAGE ANNUALIZED RESIDENTIAL POPULATION LOSS

Residential population losses are based on the modeled scenarios in Table 2-34, estimated return periods, pedestrian evacuation modeling for certain segments of the United States Virgin Islands coastline (Wood and Peters 2025c), and estimates of exposed residential populations for each scenario (Wood et al. 2025a). These data suggest an average annualized fatality rate of 2.01 for United States Virgin Islands (Table 2-36). The annualized risk to both the main counties, St. Thomas and St. Croix Islands, are very similar; however, St. Croix Island is affected by at least three Anegada Passage scenarios (ID_17, ID_21 and ID_25), while St. Thomas Island is affected only by ID_25 although more severely.

Evacuation modeling for all the non-Anegada Passage sources indicate sufficient time for most residents to evacuate in the three United States Virgin Islands counties (Wood and Peters 2025c; Wood et al. 2025a). This is primarily because much of the population exposure is non-residential occupancies and visitors, and high ground is generally accessible (Wood et al. 2025c). However, the FEMA study of average annualized losses does not include visitor or other non-residential populations or the seasonal and temporal population variability in the analysis.

Table 2-36: Average Annualized Fatalities Based on Residential Population Unable to Evacuate Inundation Zone Using a 10 Minute Departure Delay

Rank	County	Average Annualized Fatalities	Scenario Fatalities*	Exposed Population*
1	St. Thomas Island	1.16	1,218	3,078
2	St. Croix Island	0.85	819	769
3	St. John Island	-	-	342
	Territory Total	**2.01**	**2,037**	**4,189**

*Note: Residential population exposed is based on the sum of the population distributed to all inundated building points in tsunami hazard zones and fatalities represent the population unable to reach safety given a 10-minute departure delay (Wood et al., 2025a).

2.11.5 STUDY LIMITATIONS

Hazard Data

United States Virgin Islands has a significant range of scenarios and return periods to supplement the original worst-case scenario work of Moore and Arcas (2018, in press). However, accounting for distant sources may improve average annualized loss estimates as would a more robust Probabilistic Tsunami Hazard Analysis assessment.

Additionally, there were differences in how the scenarios were modeled between the Caribbean Territories which may affect results when looking at the same sources. For example, modelling in Puerto Rico was conducted based on the assumption that narrower segments of the Puerto Rico Trench could rupture, leading to lower-magnitude events with shorter return periods. In contrast, modeling for United States Virgin Islands assumed rupture of the entire Puerto Rico Trench, resulting in larger-magnitude events with much longer return periods. This approach in United States Virgin Islands yielded estimated return periods as high as 141,182 years. These larger-magnitude events would be catastrophic; however, due to their long return periods, they contribute minimally to average annualized losses. A Probabilistic Tsunami Hazard Analysis that combines both rare, catastrophic events and more frequent, lower-magnitude events could provide a more comprehensive risk profile for United States Virgin Islands, and standardizing modeling approaches across states and territories within a Probabilistic Tsunami Hazard Analysis framework could improve nationwide tsunami risk assessments.

Missing Hazard Data on Exposed Structures

The building inventory coverage analysis (Appendix F, Section F.3) indicates that all sections of the coast in United States Virgin Islands are covered by available hazard data.

Population Loss

The population loss assessment for United States Virgin Islands in this study is significantly limited by the exclusion of visitor and other non-residential populations (Wood et al. 2025c). Given the high number of employees and cruise-ship passengers in tsunami-hazard zones, their incorporation would likely increase potential population losses substantially. For example, the U.S. Virgin Islands Bureau of Economic Research (n.d.) reports over 2.5 million annual visitors, with more than 2 million arriving on cruise ships that dock at each island. Please refer to Section 4.4 for additional information regarding limitations across all study areas.

2.12. Washington

There are four main types of tsunami risk in Washington: distant earthquakes, landslides, an earthquake from the Cascadia Subduction Zone, and local crustal earthquakes (such as those along the Seattle fault zone or Tacoma fault). Each type affects different areas of the state and gives varying evacuation times, ranging from hours to just minutes. However, like the analyses for other states, only tsunamis generated by distant or local earthquakes are considered here.

2.12.1 TSUNAMI HAZARD DATA

The Washington Department of Natural Resources, Washington Geologic Survey (WGS) provided three deterministic scenarios, including one distant and two local, meeting the requirements for a Hazus Level 3 analysis (Table 2-37):

Alaska-Aleutian Subduction Zone: The mapped Alaska-Aleutian Subduction Zone distant tsunami scenario is a deterministic model that was developed by the NOAA Center for Tsunami Research at PMEL (Chamberlin et al., 2009) and is a hypothetical earthquake scenario with a similar magnitude to the 1964 Alaska earthquake (M 9.2). This scenario has uniform slip of 20 meters specified over a set of 20 “unit source" subfaults that correspond to the NOAA SIFT propagation database (Gica et al., 2008). A series of tsunami simulations with different combinations of unit sources led to the selection of this specific set of unit sources that produce the maximum tsunami impact to Washington’s waterways. The numerical modeling provided both flow depth and momentum flux, supporting a Hazus Level 3 analysis. Washington’s Alaskan scenario did not cover all exposed areas of the Washington coast, including the developed, low-lying areas of Grays Harbor and Pacific Counties. The Columbia River, which forms the border between Oregon and Washington, was modeled by DOGAMI (Allan and O’Brien, 2019); flow depth and velocity data for this area were incorporated as a Level 2 analysis in Hazus. The limitations section below discusses the effect of the incomplete data on the average annualized loss and how FEMA used an interim solution until the modelling is complete.

Cascadia Subduction Zone – M_w 9.0 (L1): This local scenario is published by Eungard et al. (2018) and simulates a M_w 9.0 earthquake event with a maximum slip of 27 meters producing over 18 meters of inundation in some areas. The L1 is intended to approximate the design requirements in the building code standard for critical facilities and is more conservative than previous tsunami scenario modeling.

Seattle Fault – M_w 7.3: This local scenario is based on the modeling described in Dolcimascolo et al. (2022). The mapped Seattle fault scenario is a geomorphic and deterministic model source selected to produce tsunami inundation in the locations with known Seattle fault zone tsunami deposits (e.g., West Point, Cultus Bay, Snohomish River delta). This agreement is seen as validation for using the observed vertical deformation data as the main constraint for a credible tsunami source model at the time of its development (Titov et al., 2003). The model was developed using the geomorphic constraints to not contradict the known paleoseismology, while also producing a surface deformation solution that would initiate a tsunami. Although the model is based on the Seattle fault zone rupture geometry of Koshimura et al. (2002), which uses the seismic reflection data of Pratt et al. (1997), the model is overly simplified and not geophysically constrained. For example, the Koshimura, et al. (2002) rupture model consists of 12 sub-faults (6 shallow and 6 deep) and the scenario selected for tsunami modeling includes only the six shallow sub-faults with tapered slip towards the shorelines, and on-land portions of the fault geometry are omitted altogether. Assumptions were made that the deeper sub-faults and onshore components of the fault system do not contribute significantly to tsunami generation. The lack of tsunami generation from these components is why tsunami risk in Lake Washington or Lake Sammamish east of Puget Sound is not included.

A fourth scenario for the Tacoma fault had also been previously modeled but not included in this study because changes in land development have occurred since the scenario was modeled, and thus the modeled scenario would not accurately represent potential impacts. The model results in this study do not include potential tsunamis from coseismic landslides, ruptures on nearby crustal faults or changes caused by liquefaction. The Washington Geological Survey also acknowledged that there are many other tsunami sources that threaten the State but have yet to be modeled.

Table 2-37: Washington Department of Natural Resources Tsunami Hazard Data

Scenario	Tsunami Source	Return Period
Alaska/Aleutian Subduction Zone – M_w 9.2	Regional - Alaska/Aleutian Subduction Zone	800 years
Cascadia Subduction Zone - M_w 9.0 (L1)	Local – Cascadia Subduction Zone	2,500 years
Seattle Fault – M_w 7.3	Local - Seattle fault zone	16,000 years

2.12.2 RETURN PERIOD DATA

The return periods for the three hazard scenarios (presented in Table 2-37) used in this study are estimated based on available literature considering the source parameters that were selected to model each tsunami scenario:

Alaska-Aleutian Subduction Zone – M_w 9.2: At this time, this scenario is Washington's "maximum considered" tsunami hazard for an earthquake generated along the Alaska-Aleutian Subduction Zone and is a close approximation of a 750-800-year return period. Chamberlin et al. (2009) suggest a mean return period of 750 years for the M_w 9.2 event. WGS also suggests, based on research of the Alaska Division of Geological & Geophysical Surveys (Nishenko et al., 2022), that larger earthquakes may be possible along the Alaska-Aleutian Subduction Zone (e.g., M_w 9.5); however, no peer-reviewed source models currently exist of those larger scenarios. The return period for the Alaska distant tsunami scenario for Washington (800 years) is higher than local scenarios in similar areas generated for Alaskan communities (e.g., 594 years for Chenega Bay and Tatitlek scenario) primarily due to differences in estimated scenario magnitudes (e.g., Mw 9.2 for the Washington distant scenario and Mw 9.0 for the Alaskan scenarios).

Cascadia Subduction Zone – M_w 9.0 (L1): The return period of 2,500 years is estimated for this scenario originally based on Eungard et al. (2018) to approximate the 2% probability of exceedance in 50 years. Witter et al. (2011) using the offshore turbidite history from Goldfinger et al. (2012) found evidence of four large scenarios including three of L1 size and one larger scenario during the Holocene (~10,000 years). Because Oregon provides a separate scenario and return period for the larger event, the comparable Oregon L1 scenario uses a 3,333-year return period based on three large events in ~10,000 years, while Washington uses 2,500-year based on four large events in ~10,000 years. In California, the 2,475-year product is comparable to the Washington Cascadia Subduction Zone scenario.

Seattle Fault Zone – M_w 7.3: Although a return period of 16,000-years is used for this study, the modeled Seattle fault zone earthquake scenario is not necessarily a ~16,000-year event. Rather, there has only been one tsunamigenic Seattle fault zone earthquake rupture that has been observed in the geologic record within the last ~16,000 years (A.D. 923), and the modeled scenario attempts to match the observed vertical deformation from that event (e.g., +7 meters at Restoration Point, +4 meters at Alki Point, -1 meter at West Point). Appendix A of Dolcimascolo et al. (2022) outlines additional difficulties in determining the tsunami return period of the Seattle fault zone scenario due to the lack of observations earlier than the A.D. 923 event.

2.12.3 AVERAGE ANNUALIZED BUILDING LOSS

Table 2-38 illustrates that over $95 billion in building value is exposed to potential tsunamis in Washington. Based on the three hazard scenarios described above, average annualized building loss is almost $12 million statewide.

Table 2-38: Top Five Counties and Total Statewide Average Annualized Loss Building and Exposure

Rank	County	Average Annualized Building Losses	Building Exposure to Tsunami	Building Loss Ratio (USD per $1 million)
1	Grays Harbor	$5,635,123	$15,804,453,296	$356.56
2	Pacific	$3,493,896	$7,279,525,681	$480.00
3	Clallam	$693,021	$2,707,787,746	$256.01
4	King	$590,042	$13,928,467,549	$42.36
5	Kitsap	$297,703	$11,867,639,256	$25.09
	State Total	$11,894,581	$95,338,844,573	$124.76

Grays Harbor and Pacific Counties account for 76% of the state's total average annualized building losses, despite coverage gaps in the 800-year distant scenario. King County's losses are largely driven by the Seattle fault scenario, which has a 16,000-year return period. Though only 3.8% of Washington's building stock are in census blocks at risk of tsunamis, a significant 57% of the building stock in Grays Harbor and 79% in Pacific Counties are exposed to potential tsunami impacts.

2.12.4 WASHINGTON POPULATION LOSS METHODOLOGY

Unlike Oregon and California, which have multiple Cascadia dominated scenarios, Washington has only one (Cascadia Subduction Zone L1 ~2,500-year) scenario to represent population loss due to a Cascadia Subduction Zone tsunamigenic event for the high-risk outer coast counties. Washington had the greatest number of potential fatalities from the Cascadia Subduction Zone scenario alone, but had the lowest average annualized loss since only one return period contributed. To help bridge this data gap, FEMA coordinated with tsunami subject matter experts from WGS, Washington Emergency Management Division (WEMD), CGS, California Governor's Office of Emergency Services (CalOES), and DOGAMI to produce a method that added a proxy 1,000-year Cascadia event. This was achieved by multiplying the losses from the Cascadia Subduction Zone L1 2,500-year scenario by 0.884, which was a ratio derived by the relationship between the Oregon M and L scenario losses in Seaside, Oregon, which was chosen as a comparable area to simulate (1) the risk that the outer coast of Washington faces due to the low-lying nature of the landscape, and (2) the evacuation difficulties that residents from both communities would face. The Seaside, Oregon, ratio was then applied to the 2,500-year Cascadia Subduction Zone L1 Census block-level population loss results to create the 1,000-year Cascadia Subduction Zone data which was added to the Riemann sums equation (Appendix D) to help provide a more complete picture of average annualized losses.

2.12.5 AVERAGE ANNUALIZED RESIDENTIAL POPULATION LOSS

Residential population losses are based on WGS evacuation modeling (Bauer, 2022) and population-exposure estimates (Wood et al., 2025a) for areas inundated by the Cascadia Subduction Zone and Seattle fault zone events and losses. The results are based on annualizing the residential population losses using estimated return periods of 2,500 and 16,000 years for the Cascadia Subduction Zone and Seattle fault zone events, respectively. The USGS also included bridge failure data provided by the State. The method described in Section 2.12.4 provided estimates of potential 1,000-year event population losses based on the loss ratio approach. The combination of losses from all three return periods results in an average annualized rate of 15.86 fatalities (Table 2-39).

Table 2-39 provides the totals for the state, as well as the top five counties based on average annualized loss. The scenario fatalities and exposed residential population in Table 2-39 is for the Cascadia Subduction Zone scenario only to allow comparisons and highlight the impacts for this catastrophic event. More than half of the average annualized loss is in Grays Harbor County alone, and Grays Harbor and Pacific Counties combine to represent 89% of the State's potential annualized fatalities. Despite being mostly rural, Clallam County has the 3rd highest risk of tsunami fatalities due to exposed populations mostly on the Makah and Quileute Indian Reservations.

Evacuation modeling summarized in Bauer (2022) and population-exposure estimates summarized in Wood et al. (2025a) for the distant source Alaska-Aleutian Subduction Zone tsunami indicates sufficient time to evacuate for the Washington counties. Statewide, the residential population exposed to the Cascadia Subduction Zone scenario is 65,587 and 10,716 are exposed to the Seattle fault scenario, with 6,870 exposed to both the scenarios according to Wood et al. (2025a).

Table 2-39: Average Annualized Fatalities Based on Residential Population Unable to Evacuate Inundation Zone Using a 10 Minute Departure Delay (Top Five Counties)

Rank	County	Average Annualized Fatalities	Scenario Fatalities*	Exposed Population*
1	Grays Harbor	8.35	8,651	32,303
2	Pacific	5.83	6,045	13,256
3	Clallam	0.69	715	3,040
4	King	0.41	1,769	897
5	Kitsap	0.28	1,226-	1,902
	State Total	15.86	15,583	69,820

*Residential population exposed is based on the sum of the population distributed to all inundated building points in tsunami hazard zones and fatalities represent the population unable to reach safety given a 10-minute departure delay (Wood et al., 2025a).

2.12.6 WASHINGTON TSUNAMI STUDIES

State of Washington agencies have modeled impacts and evacuation potential from tsunami scenarios. These studies provide an opportunity to compare the methods and data used to produce this national baseline of risk. This work included an advanced Hazus analysis, in which Washington developed its own detailed site-specific inventory data for buildings, known as User-Defined Facilities (UDF), potentially affected by the Cascadia Subduction Zone scenario (Bauer, 2022). This UDF dataset exposure can be compared to the baseline inventory dataset used for this study within the Cascadia Subduction Zone inundation area (Table 2-40). The UDF data development included improving the spatial locations based on satellite imagery, correcting areas of double coverage and incomplete coverage, and correcting incorrect attributes from the National Structure Inventory 2.0 dataset that were referenced (Bauer, 2022). This methodology was also used by Oregon DOGAMI for improving their datasets (Allan et al., 2020). The National Structure Inventory data were developed based on national parcel and footprint data (USACE, 2022) and have been improved by FEMA to update the valuations based on 2022 costs derived from RS Means, to address errors in the number of stories, and to assign seismic design levels and earthquake building types (FEMA, 2024c). The comparison shown in Table 2-40 indicates that the National Structure Inventory data produce slightly larger exposures and losses, although comparisons by communities and losses would provide additional findings.

Table 2-40: Comparisons of Washington UDF and National Structure Inventory (NSI)in the Cascadia Subduction Zone (CSZ) Inundation Area

Value	WA UDF (CSZ)	FEMA NSI (CSZ)	% Difference
Building Counts	39,429	43,754	9.9%
Building Value	$17,027,819,182	$19,716,188,653	13.6%
Content Value	$13,035,748,117	$15,967,311,303	18.4%
Cost Year	2021	2022	

The Washington population impact studies include both the residential and temporary population, whereas this population loss study is focused entirely on the residential population. This provides an opportunity to compare the population results from the two methods. Both Bauer (2022) and the USGS (refer to Section 2.2) distribute the Census block based residential population to residential occupancies based on unit counts; however, there are slight differences in the methods. One difference is that the Washington study estimates the units for residential occupancies based on building area as outlined in Figure 2-2 of Allan et al. (2020), while the USGS leverages the unit counts in the National Structure Inventory data derived from Lightbox (USACE, 2022). Both are reasonable approaches based on data availability. To evaluate the potential differences, the USGS provided population-exposure estimates using both the Washington UDF and National Structure Inventory data for residences (Table 2-41), which indicates that for the largest developed areas in tsunami-hazard zones, there are slightly larger residential exposures based on the FEMA inventory data, resulting in about 8% higher population losses. The Washington data produce small increases

in residential population exposure in the Cascadia Subduction Zone in the more rural Clallam and Jefferson Counties that may indicate gaps identifying exposed structures in rural areas using the National Structure Inventory data.

Table 2-41: Comparison of FEMA National Structure Inventory (NSI) and WA EMD Residential Population Impacts in Cascadia Subduction Zone Scenario High-Risk Counties

County	FEMA NSI Residential Population	WA EMD Residential Population	Difference *	FEMA NSI Residential Population Exposure	WA EMD Residential Population Exposure	Difference *
Clallam	4,463	3,446	1,017	692	819	(127)
Grays Harbor	35,396	30,355	5,041	8,428	7,718	710
Jefferson	4,572	1,405	3,167	2	6	(4)
Pacific	13,980	11,854	2,126	6,207	5,844	363
Wahkiakum	1,048	886	162	154	160	(6)

*Difference is National Structure Inventory minus UDF, () indicates WA EMD has larger values.

While the estimates in this study use 10-minute departure times, Washington's methodology also calculates fatality estimates using 15- and 20-minute departure times, which are not included in this study. These extended times account for factors such as ambulatory limitations, challenging nighttime evacuations (due to lack of lighting), tourists unfamiliar with evacuation routes, difficult terrain caused by secondary earthquake impacts and inadequate evacuation signage (Bauer, 2022).

The most significant differences between the approaches in this study and Washington's study is the incorporation of temporary populations in the Washington study. Using a nighttime summer scenario, the Washington study (Bauer, 2022) projects a temporary population of 95,012 visitors and 4,331 employees in overnight facilities, surpassing the residential population. This estimate does not include a daytime summer scenario, which would result in even higher temporary population figures. Additionally, the Washington study accounts for temporary populations outside of traditional buildings, including RVs, tents, yurts, liveaboards, and workers in facilities such as assisted living centers, emergency operation centers, prisons, and heavy industry factories, using methodologies established by Allan et al. (2020).

A thorough understanding of temporary populations is important for discussing the potential construction of vertical evacuation structures in areas lacking access to high ground. For example, Washington State's *Guide to Tsunami Vertical Evacuation Options on the Washington Coast* states the need for at least 58 vertical evacuation structures (Washington Emergency Management Division, 2021). However, because only Oregon and Washington are currently able to provide temporary population data, these data could not be included in this study.

2.12.7 STUDY LIMITATIONS

Hazard Data

Data availability in Washington varies across the tsunamigenic sources that threaten the coast. The State only has three earthquake-generated tsunami scenarios available (Cascadia L1, Alaska, Seattle fault), each are deterministic scenarios with estimated return periods. To most accurately represent the entire loss curve for a risk assessment, multiple return periods for each scenario and each tsunami source may be grouped in a Probabilistic Tsunami Hazard Analysis (Appendix D). Furthermore, not all the hazard data provided complete coverage of the coast for all scenarios. For example, the state did not have inundation-modeling data for portions of Grays Harbor and Pacific Counties on the Washington coast for the distant Alaska-Aleutian Subduction Zone scenario or inundation data based on current DEMs for the Tacoma fault. The state also does not have landslide-generated tsunami data available, which may help provide a more complete picture of tsunami risk and may be incorporated in future updates.

There were some slight differences observed in Washington's Alaska scenario momentum flux data that showed lower momentum flux values than expected. These discrepancies were due to the different numerical models and slightly different methods used to generate the tsunami hazard data. Two models were completed by WGS using GeoClaw for counties north of Grays Harbor County and PMEL (MOST) in Grays Harbor County and Pacific County. The PMEL dataset was post-processed to estimate momentum flux, using a scripting tool developed by WGS. Although previous National Tsunami Hazard Mitigation Program (NTHMP) benchmarking studies (Horrillo et al., 2014) have found that GeoClaw and MOST provide a good approximation of results, differences in the model software and the study area bounds led to inevitable slight discrepancies or edge effects in the datasets. These differences may be mitigated if adequate computational power were available to model the state seamlessly.

Missing Hazard Data on Exposed Structures

Appendix F, Section F.3.5 presents an analysis for Washington of the National Structure Inventory building points along the coast at elevations of less than 5 meters and less than 10 meters that are not included in current tsunami hazard coverage for all return periods. The structures missing 800-year return period hazard data are located in Pacific and Grays Harbor Counties. The provided data did not include inundation information for the 800-year return period in these counties. The analysis indicates a gap in coverage for 928 buildings, with a combined valuation of over $500 million, situated along the coast at elevations of 10 meters or less. Given that the available hazard data cover $95 billion in building exposure, this indicates that 99.9% of the building exposure in Washington is accounted for by the existing hazard data.

An additional building loss gap occurs because of the lack of Hazus 6.1 analysis coverage for several counties along the Columbia River (e.g., Clark, Cowlitz and Skamania) where Wood et al. (2025a) estimates a potential residential population exposure of 307 persons.

Population Loss

When estimating average annualized population losses, Washington is limited due to only having data for one return period per local source, with the Cascadia L1 affecting primarily the outer coast and the Seattle fault zone scenario affecting inner coast populations, compared to the five Cascadia return periods that the team was able to leverage for Oregon. Although Cascadia L1 population losses in Washington are larger, the average annualized population losses are disproportionately lower (refer to Section 4.4 for additional information on limitations). This gap has been addressed in part by using the loss ratio between the L (3,333-year return period) and M (1,000-year return period) Cascadia Scenarios from Seaside, Oregon. Please refer to Section 2.12.5 for additional information on the methodology used. Additional return period modelling work may better depict the entire loss curve for annualizing loss (Appendix D).

Please refer to Section 4.4 for additional information regarding population loss across all regions.

3. Results of the Study

3.1. Total Tsunami Average Annualized Loss

The study estimates over $1 billion in average annualized building and residential population losses from tsunamis in the 10 states and territories of the United States included in this study (Table 3-1 and Figure 3-1). The majority (79%) of the potential losses are from impacts to the residential population.

Table 3-1: Total Average Annualized Loss by State/Territory

Rank	State or Territory	Residential Population Losses	Building Losses	Total Average Annualized Loss
1	Puerto Rico	$224,305,720	$2,544,236	$226,849,956
2	Washington	$198,264,920	$11,894,581	$210,159,501
3	California	$129,923,119	$44,464,801	$174,387,920
4	Oregon	$116,780,112	$13,499,538	$130,279,650
5	Hawaii	$0	$91,771,117	$91,771,117
6	Alaska	$17,092,044	$27,974,573	$45,066,617
7	Guam	$35,896,211	$368,602	$36,264,813
8	American Samoa	$16,780,674	$14,989,682	$31,770,356
9	Commonwealth of the Northern Mariana Islands	$29,986,717	$185,490	$30,172,207
10	United States Virgin Islands	$25,087,151	$1,182,952	$26,270,103
	Total	**$794,116,668**	**$208,875,571**	**$1,002,992,240**

A few observations can be made from these results:

- Puerto Rico (Figure 3-1f) has the overall highest losses driven primarily by the large potential impacts on residential population. In the event of a large tsunami originating in the nearby Puerto Rico Trench, the 10-minute departure delay used in this report results in significant potential fatalities, as such an event could reach the densely populated northern coast within minutes. Reducing Puerto Rico's departure delay by just five minutes would lower the estimated losses to approximately 25% of the current estimate.

- Cascadia Subduction Zone-affected areas of California, Oregon, and Washington (Figure 3-1c) consistently produce the highest potential residential population losses even after departure

delays are reduced. This is a result of large populations in those States having longer travel times to safe areas.

- Hawaii (Figure 3-1d) has the highest potential average annualized building losses. However, because population losses to distant tsunamis are assumed to be addressed by warning systems, Hawaii's combined losses are reduced.
- The losses in Alaska (Figure 3-1a) and American Samoa (Figure 3-1e) result in the highest per capita losses in the Nation (Table 3-2).

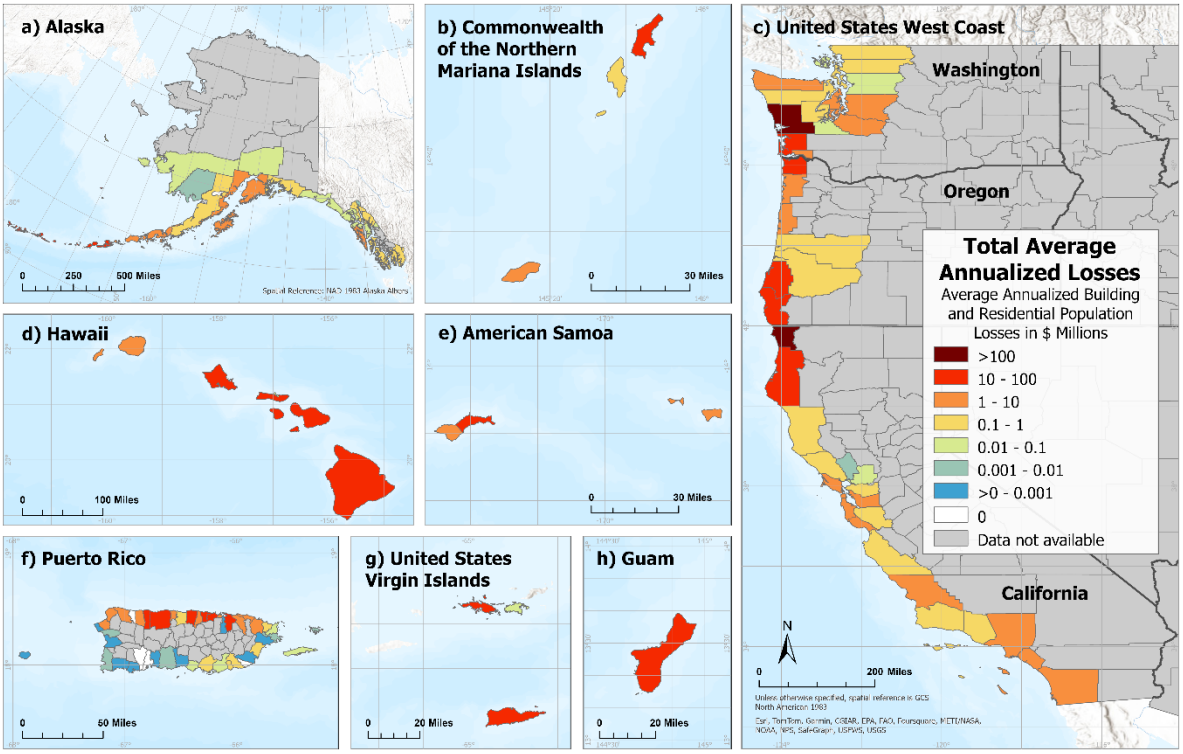

Figure 3-1: Total Average Annualized Losses by County or County Equivalent

3.2. Average Annualized Building Loss

Building losses are developed for each state based on the hazard data and methods described in Section 2. Table 3-2 ranks the building losses for each state and territory assessed in this study. Hawaii has nearly $92 million in building losses per year and almost $160 billion in building exposure to potential tsunami damage, while California has over $44 million in average annualized building loss and over $348 billion in exposure.

Table 3-2: Total Building Average Annualized Loss by State/Territory

Rank	State or Territory	Building Losses	Building Exposure (Based on Census Blocks with Losses)	Annualized Building Loss Ratio ($USD per $1 million exposure)
1	Hawaii	$91,771,117	$159,634,257,068	$575
2	California	$44,464,801	$348,610,274,427	$128
3	Alaska	$27,974,573	$26,530,081,448	$1,054
4	American Samoa	$14,989,682	$4,985,346,575	$3,007
5	Oregon	$13,499,537	$57,877,623,046	$233
6	Washington	$11,894,581	$95,338,844,573	$125
7	Puerto Rico	$2,544,236	$42,277,235,704	$60
8	United States Virgin Islands	$1,182,952	$10,112,346,465	$117
9	Guam	$368,602	$3,455,696,131	$107
10	Commonwealth of the Northern Mariana Islands	$185,490	$3,657,427,488	$51
	Total	**$208,875,571**	**$752,479,132,925**	

Figure 3-2 provides a thematic map of annualized building loss by county equivalent indicating several Hawaii (Figure 3-2d) and American Samoa (Figure 3-2e) counties that exceed $10 million annually. On the west coast, the highest building loss counties are along the coastal Bay Area of California, Grays Harbor County in Washington, and Clatsop County in Oregon (Figure 3-2c). Each of these areas have building losses that exceed $5 million annually. In Alaska (Figure 3-2a), each of the boroughs of Aleutians West, Kenai Peninsula and Kodiak Island exceed $5 million in annualized building loss.

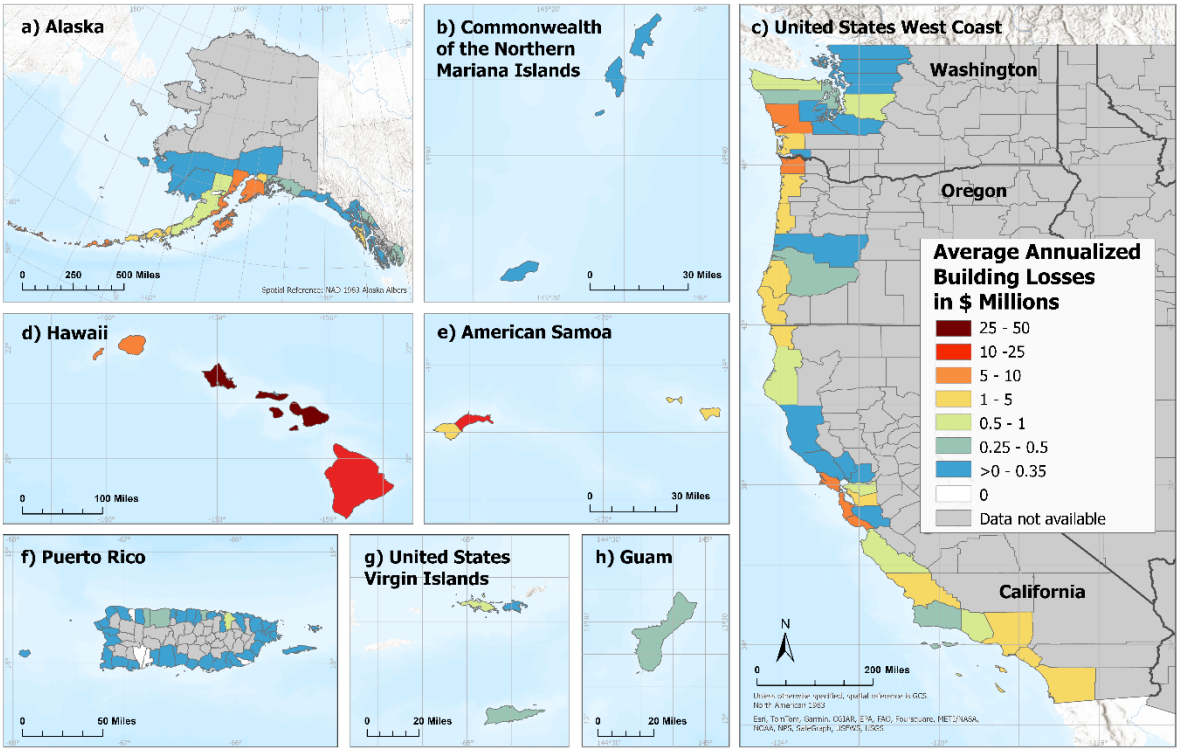

Figure 3-2: Building Losses (Capital Stock) by County or County Equivalent

Figure 3-3 provides a thematic map of the annualized building loss ratio by county equivalent based on the annualized loss in USD per $1 million in building exposure. Of the 10 county-level equivalents with the highest loss ratios exceeding $1,000 per million, six are in Alaska (Figure 3-3a). Additionally, all three county-level equivalents in American Samoa (Figure 3-3e) rank within the top 10, highlighting the substantial risk of these areas.

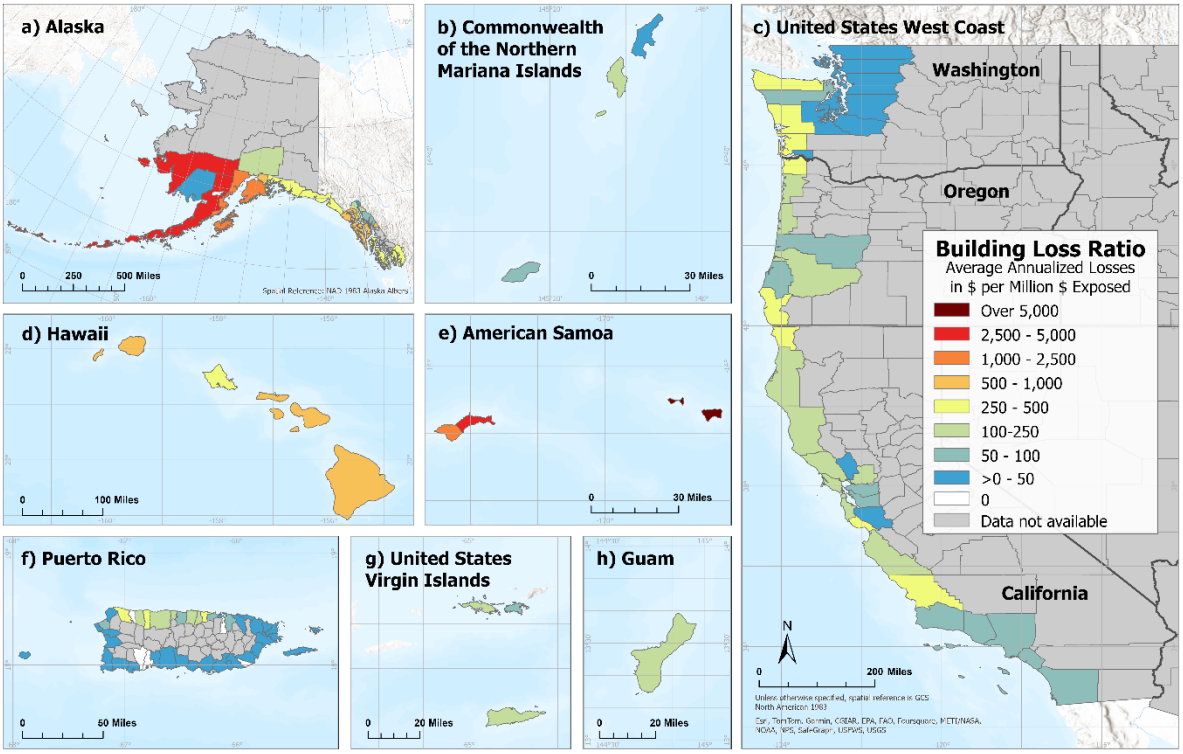

Figure 3-3: Building Loss Ratio by County or County Equivalent

3.3. Average Annualized Residential Population Loss

Table 3-3 provides the average annualized residential population losses based on population exposure and evacuation potential (Wood et al., 2025a) and VSL assuming a 10-minute uniform departure delay. A potential Cascadia Subduction Zone event drives the high residential population losses in California, Oregon, and Washington. Although estimated to have almost a 2,000-year recurrence, a M_w 8.2 scenario on the Puerto Rico Trench exposes a residential population of almost 54,000 persons along the northern shore of Puerto Rico to tsunami inundation and high losses (over 21,000 fatalities) when using a 10-minute departure delay. On a per capita basis the statewide losses are relatively low in California because much of the population is exposed to the threat of distant tsunamis and evacuation modeling suggests that there is sufficient time to evacuate (Wood et al., 2025a). The high per capita loss in Guam demonstrates that the arrival time is equal to or less than the 10-minute departure delay for much of the exposed residential population.

Table 3-3: Residential Population Average Annualized Loss (AAL) by State/Territory

Rank	State or Territory	AAL Fatalities	Population Loss Equivalence ($12.5 million VSL, 2022)	Residential Population Exposed *	Per Capita Residential Population Loss Equivalence
1	Puerto Rico	17.94	$224,305,720	61,953	$3,621
2	Washington	15.86	$198,264,920	69,820	$2,840
3	California	10.39	$129,923,119	486,209	$267
4	Oregon	9.34	$116,780,112	60,739	$1,923
5	Guam	2.87	$35,896,211	1,833	$19,583
6	Commonwealth of the Northern Mariana Islands	2.40	$29,986,717	5,266	$5,694
7	United States Virgin Islands	2.01	$25,087,151	4,189	$5,989
8	Alaska	1.37	$17,092,044	17,541	$974
9	American Samoa	1.34	$16,780,674	10,955	$1,532
10	Hawaii	0	$0	268,469	$0
	Total	63.53	$794,116,668	986,974	$805

*Residential population exposed is based on the sum of the population distributed to all inundated building points in tsunami hazard zones for each state (Wood et al. 2025a).

Average annualized residential population losses are shown in Figure 3-4. No fatalities are estimated for Hawaii (Figure 3-4d) and certain California counties (Figure 3-4c) because it is expected that the population exposed to distant tsunamis have time to reach safety, and insufficient hazard data are available to estimate fatalities for locally generated tsunamis in Hawaii. In Washington's Jefferson and Snohomish Counties (Figure 3-4c), evacuation modeling summarized in Bauer (2022) and population exposure summarized in Wood et al. (2025a) suggest zero fatalities, as the exposed residential population is expected to have sufficient time to evacuate with a 10-minute departure delay for local events. However, other local sources not currently modeled may still pose risks to populations in these counties. The Washington study (Bauer, 2022), which includes temporary populations and uses detailed, site-specific building inventory data, indicates that fatalities are possible in these counties. Refer to Section 2.12.6 for additional information.

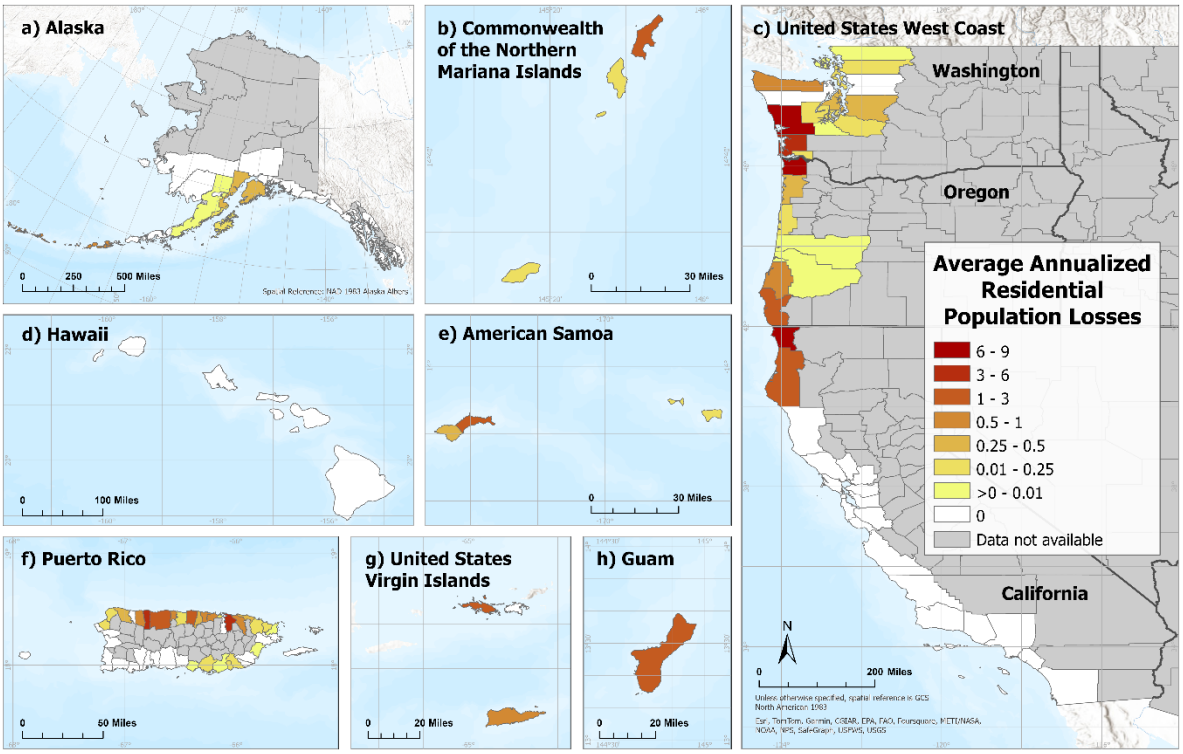

Figure 3-4: Average Annualized Residential Population Losses for Counties and County Equivalents

In Figure 3-4, zero values for California and Hawaii counties demonstrate the expectation of no residential population loss for distant tsunamis and also a lack of data for locally generated tsunamis.

3.4. Residential Population Average Annualized Loss by Departure Delay

This study uses the average annualized losses based on a uniform 10-minute departure delay. Additional analysis summarized in Wood et al. (2025a) demonstrates changes in evacuation potential based on reducing departure delays to 5 and 0 minutes for local tsunami scenarios (Table 3-4). No departure delay is unlikely due to strong ground motion, which in some cases may make evacuation unsafe, and in other cases, not realistic. However, especially in areas with nearby high ground, reducing departure delays may result in substantial reductions in potential losses. In Puerto Rico, a 5-minute improvement over the 10-minute departure delay may prevent 13.4 fatalities per year on an average annualized basis. Based on the $12.5 million VSL, this suggests an annual benefit exceeding $168 million.

While reductions in evacuation departure delays may reduce potential fatalities in some areas, additional measures may be warranted to further reduce the risk of significant fatalities in the local states affected by the Cascadia Subduction Zone. For Washington, with an assumed 0-minute departure delay and based on the residential population alone, the estimated average annualized

fatalities are 12.89 per year. If mitigated, this corresponds to an estimated annual potential benefit of over $161 million for Washington and $277 million nationally.

Table 3-4: Residential Population Average Annualized Loss (AAL) by Departure Delay

State or Territory	0- min AAL Fatalities	5- min AAL Fatalities	10-min AAL Fatalities
Puerto Rico	0.78	4.52	17.94
Washington	12.89	14.46	15.86
California	3.45	6.23	10.39
Oregon	4.51	6.72	9.34
Guam	0.29	0.76	2.87
Commonwealth of the Northern Mariana Islands	0	0.00	2.40
United States Virgin Islands	0.03	1.01	2.01
Alaska	0.14	0.70	1.37
American Samoa	0.08	0.12	1.34
Total	**22.17**	**34.51**	**63.53**

3.5. Historical Fatality Comparisons

Most of the potential fatalities caused by tsunamis in the U.S. are based on scenarios that have not happened in recent history (e.g., Cascadia Subduction Zone scenario). However, several states and territories with high rates of tsunami activity have had recent historical events that can be used for comparison purposes. Table 3-5 provides a summary by state and territory of recorded fatalities based on data extracted primarily from the NCEI (National Geophysical Data Center/World Data Service, n.d.). This table is intended for illustrative purposes only. Due to factors such as the age of primary data sources, gaps in historical recordkeeping, and challenges in distinguishing between direct and indirect tsunami-related fatalities, exact counts may vary. Significant events in Alaska (1788) and Washington (1820) may have resulted in over 100 fatalities each, but there is insufficient data to estimate losses, so these events are not included below (National Geophysical Data Center/World Data Service, n.d.).

As expected, based on population increases and the potential of future catastrophic events, the projected future average annualized fatalities (Table 3-4) are greater than the historical rates suggested in Table 3-5 of 784 fatalities across roughly 187 years (e.g., 4.2). The historical fatality rate from Table 3-5 for Alaska results is an average annualized fatality rate of 1.64 from both tectonic and landslide induced tsunamis and compares well with the 1.37 rate for Alaska based on the tectonic scenarios. This is also helpful in understanding that the potential gap caused by not

including landslide scenarios may be minimal. Because return periods for the Alaska landslide scenarios and comparable data do not exist for all states and territories, only tectonic tsunami sources are used.

Table 3-5: Documented Tsunami Fatalities

State/Territory	Documented Tsunami Fatalities	Tsunami Source Type	Distant/Local
Alaska	**293**		
1845	100	Landslide	Local
1853	64*	Landslide	Local
1883[1]	6*	Landslide	Local
1900	5	Earthquake and Landslide	Local
1917	1	Landslide	Local
1946	5	Earthquake and Landslide	Local
1958	5	Earthquake and Landslide	Local
1964	106	Earthquake and Landslide	Local
1994	1	Landslide	Local
American Samoa	**34**		
2009	34	Earthquake	Local
California	**18**		
1878	1	Landslide	Local
1930	1	Earthquake and Landslide	Local
1946	1	Earthquake and Landslide	Distant
1960[2]	1	Earthquake	Distant
1964	13	Earthquake and Landslide	Distant

State/Territory	Documented Tsunami Fatalities	Tsunami Source Type	Distant/Local
2011[3]	1	Earthquake	Distant
Guam	**1**		
1849	1	Earthquake	Local
Hawaii	**290**		
1837[2]	16	Earthquake	Distant
1868	47	Earthquake	Local
1877[2]	5	Earthquake	Distant
1923	1	Earthquake	Distant
1946	158	Earthquake	Distant
1960[2]	61	Earthquake	Distant
1975	2	Earthquake and Landslide	Local
Oregon	**5**		
1964	5	Earthquake and Landslide	Distant
Puerto Rico	**116**		
1918[4]	116*	Earthquake and Landslide	Local
United States Virgin Islands	**24**		
1867	24	Earthquake	Local
Washington	**3**		
1894	2	Landslide	Local
1965	1	Landslide	Local
Grand Total	**784**		

Note: The primary source for this table is NCEI (National Geophysical Data Center/World Data Service, n.d.) with additional updates from Lander[1] (1996), Lander et al.[2] (1989), Wilson et al.[3] (2013), and Coffman et al.[4] (1982).
*Due to the age of these events, there is some uncertainty regarding the true number of fatalities.

This page intentionally left blank.

4. Study Limitations

The average annualized loss estimates for buildings and populations provided by this study, though the first of their kind to exist at this scale, contain inherent uncertainties and gaps that affect the assessment of total risk and economic losses coastal communities face from tsunamis. Due to limitations in data availability and modeling capabilities, this study could not estimate losses for temporary and non-residential populations, non-seismic tsunami sources, or tsunami risk in the Great Lakes, East Coast and Gulf Coast regions.

Additionally, this study did not estimate potential damage to critical facilities or indirect economic losses sustained by communities and regions. Indirect economic losses may include those resulting from changes in product demand and supply, shifts in employment, and alterations in tax revenues. For instance, a tsunami affecting the ports of Los Angeles and Long Beach, California, could lead to over $1 billion in lost commerce for the U.S. for each day these ports are inoperable (Ross et al., 2013). While national assessments like this study provide a broad overview of tsunami impacts, they may not capture the detailed nuances of specific local geographies. As a result, state, territorial, or local-level impact data, when available, may be more suitable for decision-making in those areas.

Apart from the inherent limitations related to the scope of the study, constraints also arise from the quantity and quality of the data on exposure, hazards, and return periods, as well as from the methodologies employed for assessing losses. These limitations are detailed in the following sections, while state- and territory-specific limitations can be found in the study limitations section for each state or territory in Section 2.

4.1. Exposure Point Location Data

For the exposure point location data, the building and population average annualized loss studies use the non-randomized point-on-structure locations. In 2023, FEMA led an effort to improve earthquake building attributes in Hazus 6.1 and appended these data onto the National Structure Inventory database. At the structure level, attributes were enhanced using detailed building code adoption history, wall type and construction type data derived from parcel data, and more accurate building height data, including the number of stories. While the enhanced data provides updated location-specific building data, there are still limitations to using the data. These limitations include:

- The marine/harbor facilities and liveaboard structures are not explicitly captured in this data, therefore, no explicit losses for these structures or populations are captured. These facilities and structures are also affected by more frequent smaller tsunamis and may contribute significantly to average annualized losses.
- Incorrect locations for point-on-structure data exist within the dataset. For example, Alaska has some location-poor exposure points in areas such as St George Island, Alaska, where building points are mislocated in the ocean.
- Data limitations apply to this study. For more information on the limitations of the National Structure Inventory database, please refer to the National Structure Inventory Technical Documentation (USACE, 2022).

- Hazus General Building Stock (GBS) data limitations apply to this study. For more information on the limitations of the Hazus inventory data, please see the FEMA Hazus Inventory 6.1 Manual (FEMA, 2024c).

4.2. State/Territory Hazard Data

The tsunami hazard data availability was a limiting factor when conducting this study. For example, hazard data provided by the states and territories, except for California, were all deterministic or scenario-based data. For risk assessments involving average annualized loss estimates, probabilistic data are the standard for estimating economic losses because they account for the range of possible scenarios, including both rare, catastrophic scenarios and more frequent, lower-loss scenarios. In contrast, deterministic data are often focused on rare and catastrophic or maximum credible scenarios. Deterministic data may not account for uncertainty, whereas probabilistic data are created using methods that explicitly account for uncertainties in earthquake occurrence and tsunami generation processes.

In addition to the limitations presented by the data types provided by some states and territories, the availability of data also became a limitation. No states or territories had hazard data that represented all risks their communities face from tsunamis. Additionally, not all states and territories had the same quality or quantity of data; some states and territories were able to provide multiple deterministic scenarios for multiple return periods or probabilistic data for multiple return periods, while others only had one scenario for one return period. The discrepancy in data quality and data availability among the states and territories can complicate the ability to compare loss results across states and territories.

Further, tsunami hazard scenarios were not modeled with consistent source parameters across all states and territories. This is because much of these data were modeled separately by several different agencies and organizations across the country with a general intent to perform modeling for outreach and evacuation planning and to model the maximum probable scenarios, rather than to provide data for a nationally standardized risk assessment. A standardization of source parameters may help produce more consistent results across the nation for risk assessment. More information about the data limitations specific to each state and territory are listed in their respective sections in Section 2.

Finally, gaps in the hazard data provided to FEMA by states and territories have been observed along the coastlines in Alaska, California, Guam, Puerto Rico, and Washington. More information about gaps in the hazard data can be found in Appendix F, Section F.3. Additional modeling and research to fill these data gaps may benefit this study.

4.3. Building Loss Analysis Methodology

4.3.1 BUILDING EXPOSURE DATA

There are inherent uncertainties in computing losses using estimated building values and averaged building characteristics alongside modeled tsunami inundation, velocity, and momentum flux data. Please refer to the U.S. Army Corps of Engineers National Structure Inventory Technical Documentation for the limitations of the National Structure Inventory database (USACE, 2022) and the Hazus 6.1 Inventory Technical Manual (FEMA 2024b) for the limitations of the Hazus 6.1 GBS data.

4.3.2 HAZUS TSUNAMI MODEL

Please refer to the Hazus 6.1 Tsunami Technical Manual (FEMA, 2024b) for details on the Hazus Tsunami model and please refer to Appendix F, Section F.1 of this study for Hazus Tsunami model-related limitations based on analysis level.

4.4. Residential Population Loss Analysis Methodology

4.4.1 EVACUATION STUDY

The quality of data and methods used in the evacuation modeling summarized in Wood et al. (2025a) may result in additional uncertainties and gaps that can limit the accuracy of the results. Below are the assumptions that were made in the study along with the limitations that they may produce.

4.4.2 EXPOSURE DATA AND POPULATION METHODOLOGY

This study leveraged a site-specific version of the Hazus 6.1 National Structure Inventory data as the basis for locating residents and 2020 Census block counts of residents. Although this method provides uniformity, inherent uncertainties exist due to variations in accuracy of structure points, residential codes, and Census block-level population counts, as well as the assumption of uniform distribution of residents across multiple points in the same Census block.

4.4.3 LOCAL EVENT EVACUATION STUDY METHOD

To estimate the amount of time each resident may have to evacuate from a tsunami, the USGS and state partners have used geospatial, path-distance algorithms that integrate slope and landcover characteristics (Wood and Schmidtlein 2012; Jones 2024). However, a limitation of this method is the accuracy of the road network dataset and landcover used in the Pedestrian Evacuation Analyst tool. Road-network data do not include all available footpaths out of hazard zones, e.g., residents may cross parking lots or open fields to reach safety, and these individual-level decisions are not recognized in the modeling. Only American Samoa (Wood et al., 2019) and Guam (Wood et al., 2023) included non-road-based travel to estimate travel times to safety. Obstacles like fences and impermeable vegetation were considered in these studies through visual interpretation of imagery;

however, uncertainties may remain in evacuation routing. Site-specific validation of realistic evacuation routes was not possible at the scale required for this study.

To estimate the number of residents who may or may not have sufficient time to evacuate from a local tsunamigenic event, departure delays of 0, 5, and 10 minutes were assumed. These estimates assume that each resident will begin evacuation at those specific departure delay increments and will all evacuate with same base travel speed (modified by site-specific slope or landcover characteristics) for a given evacuation model (refer to Appendix H). In reality, at-risk individuals may not reach or be able to maintain consistent travel speeds during a tsunami evacuation. Additionally, using this method to compare evacuation across all the states and territories involved in this study does not incorporate the differences in the length or intensity of the ground shaking among these areas. The method also assumes that each resident will know that the ground shaking means evacuating to high ground and that each resident will know the optimal path to find high ground.

4.4.4 REGIONAL AND DISTANT EVENT EVACUATION STUDY METHOD

For regional and distant tsunami events, a similar logic was implemented to estimate the number of people who were able to evacuate in time by walking. Because regional and distant tsunamis used in this study have wave arrival times in the order of hours and residents would not be able to feel ground shaking from an earthquake occurring elsewhere, residents in hazard zones may not initiate evacuations until they receive official tsunami warnings to do so. NTHMP subject matter experts recommended using 65-, 75- and 90-minute departure delays after the start of the earthquake for distant tsunami scenarios. These longer departure delays were used to recognize that tsunami warning centers may need 60 minutes to issue a warning from the initiation of the tsunami, and evacuees may take an additional 5-, 15- and 30-minute delay from a warning being issued. Similar to the local tsunami event methods, this method assumes that each resident would begin evacuation at those specific departure delay increments and would all evacuate at the same walking speed (Appendix H). These assumptions may not be realistic because residents may decide to drive or decide to shelter in place. Traffic simulation models to estimate vehicle-based, tsunami evacuations (e.g., Henry and Wood 2017; Wood et al., 2020) may be a beneficial addition to this study to more accurately estimate the number of people who may evacuate from a regional or distant source tsunami.

4.4.5 FEMA STUDY FATALITY METHODOLOGY

In the Wood et al. (2025a) evacuation-modeling study, 0-, 5- and 10-minute departure delays following the start of ground shaking from a local event were chosen to estimate the number of residents who could not evacuate to safety prior to the wave arrival. For this study of average annualized losses, a 10-minute departure delay for local tsunami events was chosen for each state and territory to maintain a uniform approach. The 1.2 m/s walking speed was assumed based on the Federal Highway Administration (2023) Manual on Uniform Traffic Control Devices for Streets and Highways (MUTCD), with the assumption by FEMA that each person who cannot evacuate from the tsunami in time is a fatality, no matter the depth of inundation. These two assumptions do not account for the differences in how well an individual may or may not be prepared for tsunamis, the

duration or intensity of ground shaking among the states and territories involved in this study, or a host of other factors such as fitness, health, or human behaviors. As further research and methodologies explore these factors, more refined approaches can be developed to better estimate population losses for local events.

FEMA's Hazus tsunami model casualty estimation is described in the technical manual (FEMA, 2024b) and provides an alternative method to this study. The Hazus casualty model integrates the USGS pedestrian evacuation methodology (Jones, 2024) to estimate evacuation time based on either a road network or a land use landcover grid. In addition, the model applies a distribution function to estimate community reaction time as a median of a portion of the time available for evacuation and a standard deviation. The medians and standard deviations represent three potential levels of community preparedness and distribution of reaction times rather than a single reaction time. The default preparedness levels can be readily adjusted by the user based on local knowledge or additional data. The flow depth, with a threshold of 2 meters, is used to apply fatality rates of 99% where greater than 2 meters and 50% fatality 50% injury where less than 2 meters. This study implements a uniform approach to better allow the comparison of risk across jurisdictions.

4.4.6 PARAMETERS

Due to limitations in data availability, this average annualized loss study only incorporated residential populations. This study does not incorporate populations other than residents located at their homes, such as tourists, visitors, cruise ship passengers, liveaboards, campers, or employees. Please refer to the State Tsunami Evacuation Study sections in Section 2 for additional information on several state-conducted risk assessments that incorporate those data and allow comparisons. The potential population losses based on evacuation challenges or secondary fatalities (e.g., heart attacks, car crashes, etc.) are not included. Additional methodology development and study are required to accurately model fatalities from distant scenarios, including traffic evacuation modeling and behavior.

4.5. Return Period Estimation Methods

Annualizing tsunami loss provides an estimate of the long-term value of losses to buildings and population over a year's time. Section 2 provides a summary of how return periods were estimated for each state and territory. Average annualized loss is based on all potential future losses for a specific hazard type, averaged annually, and benefits from a comprehensive analysis of return intervals. Because some tsunami events can be rare but catastrophic, a range of return periods is required. Appendix D describes the method in detail and Appendix F (F-2) presents a study of the sensitivity to average annualized losses based on return period availability that is useful in characterizing the potential uncertainties incomplete return period data may cause.

Estimating the frequency at which a tsunami occurs is a challenge for the scientific community, but it is an essential part of generating data for a risk assessment because it serves as the approximation for annualized probability of the risk. Tsunamis do not occur at regular intervals and the return periods for large tsunamigenic earthquakes are often long, meaning it is common not to have

multiple events within the historical record to leverage for an estimate. Even when using the longer geologic record, uncertainties in the size and similarities of recorded events can make it difficult for subject matter experts to approximate tsunami frequencies. This task becomes increasingly difficult due to the limited availability of historical or technical data for each scenario. The historical record for tsunamis is incomplete in many areas, which, in part, affects how accurately tsunami scientists can estimate the occurrence of a specific tsunami event. Several methods to estimate return periods have been referenced throughout this study, including use of characteristic magnitude-frequency distributions, the Gutenberg-Richter law, and the use of paleoseismic, paleotsunami, and geodetic evidence. The use of this range of methods was intended to provide the best available data for estimates of return periods for each location. In some cases, such as Alaska, the lowest frequency return interval was selected to account for other uncertainties and gaps in the available data that are present.

5. Conclusion

This study translates complex information on tsunami sources and potential inundation into actionable information on potential population and economic impact. This approach enables planners and policymakers to make informed decisions to reduce potential impacts of tsunamis on communities. Annualizing estimated tsunami impacts allows for comparison across jurisdictions and with other natural hazards to aid decision makers in the prioritization of resources.

5.1. Study Findings

The total average annualized loss of over $1 billion per year in building and residential population losses indicates that while tsunami events are relatively rare, the impacts may be substantial. For example, the potential of a single statewide Aleutian source tsunami affecting Hawaii may impact almost one-third of the state's exposed built environment. The average annualized residential population loss in northern California, Oregon, and Washington, even with brief departure delays, indicate that estimated wave-arrival times are less than estimated travel times to safety for many residents to evacuate to naturally occurring high ground. The average annualized residential population losses based on different departure delays in U.S. territories demonstrate the importance of reducing departure delays to improve evacuation potential.

5.2. Next Steps

This report marks the first study of its kind to comprehensively estimate average annualized losses from tsunami in the United States across the Pacific Coast, Alaska, Hawaii, Pacific Territories and Caribbean Territories using state- or territory-provided tsunami hazard data. The findings and methodologies provide a national baseline for understanding the potential impacts of tsunamis; however, if a state- or territory-level tsunami risk assessment exists, those more localized results may be more appropriate for state or local planning. This study also identifies areas of potential research that may benefit future national assessments of the United States.

Numerous research opportunities remain that may improve FEMA's understanding of relative tsunami risk across different regions. Many of the limitations identified in this report may be addressed through improved data availability. As additional data become available across all tsunami-affected regions, incorporating these data may improve future risk assessments and related tsunami preparedness and response planning. Potential areas for further research include:

- Incorporating Great Lakes, East Coast, and Gulf Coast Tsunami Hazard Data: These regions may have risk from tsunamis generated by submarine landslides, meteotsunamis, and earthquakes. Adding these areas to future national assessments could provide greater geographic coverage.

- Incorporating Non-Earthquake Generated Tsunami Hazard Data: Portions of the U.S. coastline are threatened by tsunamis generated by non-earthquake sources. Developing hazard and return period data for tsunamis generated by submarine or subaerial landslides, volcanic eruptions, glacial calving, near-earth objects, and meteorological events could provide a more comprehensive understanding of tsunami risk across the U.S.

- Incorporation of Marine/Harbor Facilities and Liveaboards: Marine and harbor facilities are critical to both local economies and national infrastructure. In addition, liveaboards are particularly susceptible to tsunamis, including the more frequent and less catastrophic events (e.g., distant source tsunamis). Assessing the risk to these populations and maritime facilities could help in developing targeted mitigation measures to protect them from potential tsunami impacts.

- Population Loss Incorporating Non-Residential Populations: Non-residential populations, such as tourists, cruise ship passengers, and employees, can be substantial (Wood et al., 2025c), depending on the state or territory and time of day and year. A comprehensive understanding of these at-risk populations is especially important in local Cascadia Subduction Zone-affected states, where additional solutions, such as safe havens located above or outside of inundation zones, may be warranted to reduce potential loss of life. Including these populations may result in a more accurate assessment of potential human impacts and improve emergency preparedness plans.

- Incorporation of Critical Infrastructure: Infrastructure such as gas, water, and sewer pipelines, utility poles, transmission lines, roads, and bridges are vital for the functioning of communities. Their failure during a tsunami event could trigger indirect economic effects, including prolonged service outages, disruption of emergency response efforts, and impeded recovery operations.

- Regional and Distant Event Incorporation with Traffic Simulations: Incorporating traffic simulations into regional and distant scenarios may help in understanding evacuation logistics and improving emergency response plans.

- Additional Hazard Data to Fill in Gaps: Identifying and addressing gaps in current hazard data is essential for a more complete understanding of tsunami exposure. Collecting additional data may improve the accuracy of risk assessments and the effectiveness of mitigation strategies.

- Additional Hazard Data and Return Period Estimations: Gathering more data on the return periods of tsunamis could enhance predictive models and help in understanding the frequency of these events. Expanding hazard data to include various return periods could provide a more nuanced understanding of tsunami risk over different time frames. This could aid in developing robust, long-term strategies to mitigate the impact of tsunamis.

In conclusion, while this study provides a critical foundation for national tsunami risk assessment, ongoing research and data collection are imperative to fully understand and mitigate the risks posed by tsunamis. By addressing these next steps, we can enhance our preparedness, protect our communities, and reduce the potential effects of future tsunami events.

References

Alaska Science Center. (2024). The 1964 Great Alaska Earthquake and Tsunami. United States Geological Survey. https://www.usgs.gov/centers/alaska-science-center/science/1964-great-alaska-earthquake-and-tsunami.

Allan, J.C., O'Brien, F.E., Bauer, J.M., and Williams, M.C. (2020). Earthquake and Tsunami Impact Analysis for Coastal Clatsop County, Oregon, DOGAMI Open-File Report O-20-10, 69 pgs., https://pubs.oregon.gov/dogami/ofr/O-20-10/O-20-10_main-report-only.pdf.

Allan, J.C. and O'Brien, F.E., (2019). Columbia River simulated tsunami scenarios. Open-File Report O-19-03, Oregon Department of Geology and Mineral Industries, Portland, Oregon, 12 pp., https://pubs.oregon.gov/dogami/ofr/O-19-03/O-19-03_report.pdf

Allan, J.C. and O'Brien, F.E., (2023). Earthquake and tsunami impact analysis for coastal Curry County, Oregon. Open-File Report O-23-08, Oregon Department of Geology and Mineral Industries, Portland, Oregon, 93 pp., https://pubs.oregon.gov/dogami/ofr/O-23-08/O-23-08-report.pdf

Apatu, E. J., Gregg, C. E., Richards, K., Sorensen, B. V., & Wang, L. (2013). Factors affecting household adoption of an evacuation plan in American Samoa after the 2009 earthquake and tsunami. *Hawai'i Journal of Medicine & Public Health*, *72*(8), 267. https://pubmed.ncbi.nlm.nih.gov/24349889/

Apatu, E., Gregg, C., Wood, N., and Wang, L. (2016) Household evacuation characteristics in American Samoa during the 2009 Samoa Islands tsunami. Disasters 40(4):779–798.

Atwater, B.F., Musumi-Rokkaku, S., Satake, K., Tsuji, Y., Ueda, K. and Yamaguchi, D.K. (2005). The orphan tsunami of 1700—Japanese clues to a parent earthquake in North America: U.S. Geological Survey Professional Paper 1707, 144 p. https://doi.org/10.3133/pp1707.

Bai, Y., Yamazaki, Y., & Cheung, K. F. (2018). Amplification of drawdown and runup over Hawaii's insular shelves by tsunami N-waves from mega Aleutian earthquakes, Ocean Modelling, Volume 124, Pages 61-74, ISSN 1463-5003, https://doi.org/10.1016/j.ocemod.2018.02.006.

Bai, Y., Yamazaki, Y., & Cheung, K. F. (2023). Intercomparison of hydrostatic and nonhydrostatic modeling for tsunami inundation mapping. Physics of Fluids, 35(7), 077111. https://doi.org/10.1063/5.0152104

Bauer, J. (2022). Methods for Constructing Datasets for Use in the Washington State 2022 Cascadia Subduction Zone Earthquake-Tsunami Impact Study, for Washington Emergency Management Division, Camp Murray, Washington, dated June 30, 2022, 41 pgs.

Berryman K, Wallace L, Hayes G, Bird P, Wang K, Basili R, Lay T, Pagani M, Stein R, Sagiya T, Rubin C, Barreintos S, Kreemer C, Litchfield N, Stirling M, Gledhill K, Costa C (2015) The GEM Faulted Earth Subduction Interface Characterisation Project, GNS Science Miscellaneous Series 80. 34 p.. available at https://ndhadeliver.natlib.govt.nz/delivery/DeliveryManagerServlet?dps_pid=IE26233616 . Accessed 22 September 2025.

Briggs, R., Witter, R. C., Freymueller, J. T., Powers, P. M., Haeussler, P. J., Ross, S. L., Dura, T., Engelhart, S. E., Koehler, R. D., & Thio, H. K. (2024). An Alaska-Aleutian subduction zone interface earthquake recurrence model from geology and geodesy. *AGU Books, Chapter 10, pages 301-324. Tectonics and Seismic Structure of Alaska and Northwestern Canada: EarthScope and Beyond*. https://agupubs.onlinelibrary.wiley.com/doi/10.1002/9781394195947.ch10

Brocher, T.M., Filson, J.R., Fuis, G.S., Haeussler, P.J., Holzer, T.L., Plafker, G., and Blair, J.L. (2014). The 1964 Great Alaska Earthquake and tsunamis—A modern perspective and enduring legacies: U.S. Geological Survey Fact Sheet 2014–3018, 6 p., https://dx.doi.org/10.3133/fs20143018.

Butler, R., Burney, D., & Walsh, D. (2014). Paleotsunami evidence on Kauaʻi and numerical modeling of a great Aleutian tsunami. *Geophysical Research Letters, 41*(20), 6795–6802. https://doi.org/10.1002/2014GL061232

Chamberlin, C. D., Titov, V. V., & Arcas, D. (2009). Modeling tsunami inundation impacts on the Washington Coast from distant seismic sources. *Pacific Marine Environmental Laboratory*, 27.

California Geological Survey, (2025). Tsunami technical reports and data. https://www.conservation.ca.gov/cgs/tsunami/reports. Accessed 13 February 2025.

Coffman, J. L., von Hake, C. A., & Stover, C. W. (1982). Earthquake history of the United States (Revised edition through 1970, reprinted with 1971-1980 supplement; Publication No. 41-1). U.S. Department of Commerce, National Oceanic and Atmospheric Administration; U.S. Department of the Interior, Geological Survey. https://pubs.usgs.gov/publication/70114182

Cruise Lines International Association. (2025). CLIA Alaska Cruising in Alaska. https://cruising.org/en/alaska/cruising-in-alaska. Accessed 13 February 2025.

Department of Homeland Security (DHS). (2011). American Samoa 2009 earthquake and tsunami: After-action report (OIG-11-03). Department of Homeland Security Office of Inspector General. https://www.oig.dhs.gov/sites/default/files/assets/Mgmt/OIG_11-03_Oct10.pdf.

Dolcimascolo, A., Eungard, D. W., Allen, C., LeVeque, R. J., Adams, L. M., Arcas, D., Titov, V. V., González, F. I., & Moore, C. (2022). Tsunami inundation current speeds, and arrival times simulated from a large Seattle fault earthquake scenario for Puget Sound and other parts of the Salish Sea. *Washington Geological Survey, Map Series 2022-03*, 51.

Dominey-Howes, D., & Thaman, R. (2009). UNESCO-IOC International Tsunami Survey Team Samoa (ITST Samoa), interim report of field survey 14th-21st, October 2009.

Dudley, W. C., & Lee, M. (1998). *Tsunami!*. University of Hawai'i Press.

Earthquake Engineering Research Institute (EERI). (2010). Learning from earthquakes—Samoa earthquake and tsunami of September 29, 2009. EERI Special Report. Available at https ://www.eeri.org/site/image s/eeri_newsletter /2010_pdf/Samoa-Rpt.pdf . Accessed 29 Sept 2018.

Esri, 2025, Master Agreement Products and Services, revised February 14,2025, https://www.esri.com/content/dam/esrisites/en-us/media/legal/ma-full/ma-full.pdf. Accessed 2 June 2025.

Eungard, D. W., Forson, C., Walsh, T. J., Gica, E., & Arcas, D. (2018). Tsunami hazard maps of the Southwest Washington-model results from a ~2,500-year Cascadia subduction zone earthquake scenario. *Washington Geological Survey, Map Series 2018-01*, 11.

Federal Emergency Management Agency (FEMA). (2022). Hazus 6.0 Baseline Data Updates, Fact Sheet, https://www.fema.gov/sites/default/files/documents/fema_hazus-6-data-updates-factsheet.pdf.

Federal Emergency Management Agency (FEMA). (2023a). Hazus Estimated Annualized Earthquake Losses for the United States, FEMA P-366, April 2023, 98 pgs., https://www.fema.gov/sites/default/files/documents/fema_p-366-hazus-estimated-annualized-earthquake-losses-united-states.pdf.

Federal Emergency Management Agency (FEMA). (2023b). Benefit-Cost Analysis Sustainment and Enhancements, Standard Economic Value Methodology Report. Version 12.0, https://www.fema.gov/sites/default/files/documents/fema_standard-economic-values-methodology-report_2023.pdf

Federal Emergency Management Agency (FEMA). (2024a). *2024 Building code adoption tracking: FEMA Region 9*. Federal Emergency Management Agency. https://www.fema.gov/sites/default/files/documents/fema_fy24-bcat-region-9-report.pdf

Federal Emergency Management Agency (FEMA). (2024b). Hazus Tsunami Model Technical Manual, Hazus 6.1, July 2024, 165 pgs,https://www.fema.gov/sites/default/files/documents/Hazus_6.1_Tsunami_Model_Technical_Manual.pdf.

Federal Emergency Management Agency (FEMA). (2024c). Hazus Inventory Technical Manual, Hazus 6.1, August 2024, 251 pgs, https://www.fema.gov/sites/default/files/documents/fema_hazus-inventory-technical-manual-6.1.pdf

Federal Emergency Management Agency (FEMA). (2025a). USA Structures, FEMA Geospatial Resource Center, https://gis-fema.hub.arcgis.com/pages/usa-structures.

Federal Emergency Management Agency (FEMA). (2025b). Hazus Loss Library, Hazus Tsunami Scenario Study Regions and Results, https://hazards.fema.gov/hazus-loss-library/library. Federal Highway Administration. (2006). Pedestrian and bicyclist intersection safety indices: User guide (Publication No. FHWA-HRT-06-125). U.S. Department of Transportation.

Federal Highway Administration (2023) Pedestrian intervals and signal phases. Section 4I.06, Manual of Uniform Traffic Control Devices for Streets and Highways, 11th edition. pgs. 722 – 726.

Fisher, S., Goff, J., Cundy, A., Sear, D. (2023). A qualitative review of tsunamis in Hawai'i. *Natural Hazards*. *118* (3): 1797–1832. doi:10.1007/s11069-023-06076-w.

Garcia-Pelaez, R., Gee, R., Styron, V., & Poggi, V. (2019). PSHA input model documentation for Caribbean and Central America (CCA). https://hazard.openquake.org/gem/pdf/cca-report.pdf

Gica, E., Spillane, M. C., Titov, V. V., Chamberlin, C. D., & Newman, J. C. (2008). Development of the forecast propagation database for NOAA's Short-Term Inundation Forecast for Tsunamis (SIFT) (NOAA Technical Memorandum OAR PMEL-139). NOAA. https://repository.library.noaa.gov/view/noaa/11079

Goda, K., & De Risi, R. (2024). Time-dependent probabilistic tsunami risk assessment: Application to Tofino, British Columbia, Canada, subjected to Cascadia subduction earthquakes. *Natural Hazards, 1*(7). https://doi.org/10.1038/s44304-024-00006-x

Goldfinger, C., Nelson, C. H., Morey, A. E., Johnson, J. E., Patton, J. R., Karabanov, E., Gutiérrez-Pastor, J., Eriksson, A. T., Gràcia, E., Dunhill, G., Enkin, R. J., Dallimore, A., & Vallier, T. (2012). Turbidite event history—Methods and implications for Holocene paleoseismicity of the Cascadia subduction zone (U.S. Geological Survey Professional Paper 1661–F). U.S. Geological Survey. https://pubs.usgs.gov/pp/pp1661f/

Goldfinger, C., Galer, S., Beeson, J., Hamilton, T., Black, B., Romsos, C., Patton, J., Nelson, C.H., Hausmann, R., and Morey, A. (2017). The importance of site selection, sediment supply, and hydrodynamics: a case study of submarine paleoseismology on the Northern Cascadia margin, Washington USA: Marine Geology, v. 384, p. 4-46. https://doi.org/10.1016/j.margeo.2016.06.008.

González Vida, J.M., Castro, M.J., Ortega Acosta, S., Macías, J., and Millán, A. (2016). Performance Benchmarking of tsunami-HySEA for NTHMP Inundation Mapping Activities, Geophysical Research Abstracts Vol. 18, EGU2016-16169-2.

Hawaii Emergency Management Agency. (2021). Tsunami Incident Annex. https://dod.hawaii.gov/hiema/files/2021/09/FINAL-Tsunami-Incident-Annex-8.19.2021-part-1-signed.pdf

Hawai‘i Tourism Authority. (2024). Visitor statistics. Department of Business, Economic Development & Tourism. https://dbedt.hawaii.gov/visitor/

Heim, K., & Hong, J. (2022). *2020 Post-Enumeration Survey estimation report, PES20-G-04: Census coverage estimates for Puerto Rico*. U.S. Census Bureau. U.S. Government Publishing Office.

Henry, K. D., Wood, N. J., & Frazier, T. G. (2017). Influence of road network and population demand assumptions in evacuation modeling for distant tsunamis. *Natural Hazards: Journal of the International Society for the Prevention and Mitigation of Natural Hazards, 85*(3), 1665–1687

Homeland Infrastructure Foundation-Level Data (HIFLD). (2020), Open Data. https://hifld-geoplatform.opendata.arcgis.com/.

Horrillo, J., Grilli, S., Nicolsky, D., Roeber, V., and Zhang, J. (2014). Performance Benchmarking Tsunami Models for NTHMP's Inundation Mapping Activities. Pure and Applied Geophysics. 172. 10.1007/s00024-014-0891-y.

Jones J (2024) Pedestrian Evacuation Analyst software source code, v2.0.0, U.S. Geological Survey software release, https://doi.org/10.5066/P1WACACF

Jones J, Peters J, Wood N (2018b) Pedestrian tsunami evacuation results for two tsunami-evacuation zones (standard and extreme) and three travel speeds (impaired, slow, and fast walk) for O‘ahu, HI: U.S. Geological Survey data release, https://doi.org/10.5066/F7862FNT

Jones JL, Jones JM, Wood N (2018a) Pedestrian tsunami evacuation results for two tsunami-inundation zones (2009 and probable maximum tsunami (PMT)) and four travel speeds (slow walk, fast walk, slow run, and fast run) for American Samoa: U.S. Geological Survey data release, https://doi.org/10.5066/P9USLV20.

Kanamori H (1977) The energy release in great earthquake. Journal of Geophysical Research, 82(20): 2981–2987.

Koshimura, S., Mofjeld, H. O., González, F. I., and Moore, A. L. (2002). Modeling the 1100 bp paleotsunami in Puget Sound, Washington: Geophysical Research Letters, v. 29, no. 20, p 9-1–9-4, https://doi.org/10.1029/2002GL015170.

Lander, J. F. (1996). *Tsunamis affecting Alaska, 1737-1996.* Boulder, Colorado; U.S. Dept. of Commerce, NOAA, National Environmental Satellite, Data, and Information Service, National Geophysical Data Center.

Lander, J. F., Lockridge, P. A., & National Geophysical Data Center. (1989). *United States tsunamis (including United States possessions): 1690-1988*. U.S. Department of Commerce, National Oceanic and Atmospheric Administration, National Environmental Satellite, Data, and Information Service, National Geophysical Data Center.

Lander, J., Whiteside, L., and Hattori, P. (2002a). The Tsunami History of Guam: 1849-1993, v. 20, no. 3, Science of Tsunami Hazards, pg. 158-174.

Lander, J., Whiteside, L., and Lockridge, P.A. (2002b). A Brief History of Tsunamis in the Caribbean Sea, v. 20, no. 2, Science of Tsunami Hazards, pg. 57-94.

La Selle, S., Richmond, B. M., Jaffe, B. E., Nelson, A. R., Griswold, F. R., Arcos, M. E. M., Chagué, C., Bishop, J. M., Bellanova, P., Kane, H. H., Lunghino, B. D., & Gelfenbaum, G. (2020). Sedimentary evidence of prehistoric distant-source tsunamis in the Hawaiian Islands. *Sedimentology, 67*(6), 1249-1273. https://doi.org/10.1111/sed.12623

LightBox. (2020). Parcel Data, https://www.lightboxre.com/data/.

Lindell, M., Prater, C., Gregg, C., Apatu, E., Huang, S., and Wu, H. (2015) Households' immediate responses to the 2009 Samoa earthquake and tsunami. International Journal of Disaster Risk Reduction. 12: 328–340.

Ludwin, R.S., Dennis, R., Carver, D., McMillan, A.D., Losey, R., Clague, J., Jonientz-Trisler, C., Bowechop, J., Wray, J., and James, K., 2005, Dating the 1700 Cascadia Earthquake: Great Coastal Earthquakes in Native Stories. Seismological Research Letters; 76 (2): 140–148. https://doi.org/10.1785/gssrl.76.2.140

Lynett, P., McCann, M., Zhou, Z., et al. (2022). Diverse tsunamigenesis triggered by the Hunga Tonga-Hunga Ha'apai eruption. *Nature, 609*, 728–733. https://doi.org/10.1038/s41586-022-05170-6

McMurtry, G. M., Watts, P., Fryer, G. J., Smith, J. R., & Imamura, F. (2004). Giant landslides, mega-tsunamis, and paleo-sea level in the Hawaiian Islands. *Marine Geology, 203*(1-2), 219–233.

Microsoft, 2018, U.S. Building Footprints, https://github.com/microsoft/USBuildingFootprints.

Moore, C., and Arcas, D. (2018). Modeling tsunami inundation for hazard assessment of the U.S. Virgin Islands, NOAA Technical Memorandum, NOAA Center for Tsunami Research/Pacific Marine Environmental Laboratory (PMEL), Seattle, Washington, 37 pgs.

Moore, C. and Arcas, D. (in press) Modeling tsunami inundation for hazard assessment of the U.S. Virgin Islands. NOAA Technical Memorandum, Seattle, Washington.

National Geophysical Data Center/World Data Service. (n.d.). *NCEI/WDS Global Historical Tsunami Database*. NOAA National Centers for Environmental Information. https://doi.org/10.7289/V5PN93H7 [Accessed July 24, 2024]

National Tsunami Hazard Mitigation Program [NTHMP]. (2012). *Proceedings and results of the 2011 NTHMP model benchmarking workshop*. U.S. Department of Commerce/NOAA/NTHMP. (NOAA Special Report, 436 p.). Boulder, Colorado.

National Weather Service (2025). National Tsunami Hazard Mitigation Program. https://www.weather.gov/nthmp/. Accessed 3 February 2025.

Nishenko, S.P., Koehler, R.D., & Witter, R.C. (2022). Earthquake scenario catalog for the Alaska subduction zone. Alaska Division of Geological & Geophysical Surveys Miscellaneous Publication 168, 65 p. https://doi.org/10.14509/30897

O'Brien, F. and Allan, J. (2025). Path distance tsunami modeling for Oregon tsunami-hazard zones. Oregon Department of Geology and Mineral Industries, Open-File Report O-25-05, Portland Oregon, 4 p.

Okada, Y. (1985). Surface deformation due to shear and tensile faults in a half-space: Bulletin of the Seismological Society of America, v. 75, no. 4, p. 1135–1154, https://doi.org/10.1785/BSSA0750041135.

Peters, J. and Wood, N. (2025). Pedestrian evacuation time maps for Puerto Rico tsunami-hazard zones: U.S. Geological Survey data release, https://doi.org/10.5066/P13QYXUT.

Peters, J., Wood, N., Cheung, K.F., and Yamazaki, Y. (2023). Pedestrian evacuation time maps, flow depth time series, and population estimates for the island of Guam tsunami evacuation zone: U.S. Geological Survey data release, https://doi.org/10.5066/P93794E6.

Peters, J., Sherba, J.T., Henry, K.D., Wood, N.J., and Wilson, R. (2020). Pedestrian tsunami evacuation results for three California probabilistic tsunami hazard zones and four travel speeds (shapefiles) and impaired walk travel times for all zones by parcel land-use and flow depth class (tables): U.S. Geologic Survey data release, https://doi.org/10.5066/P95OPZ0D.

Pratt, T. L., Johnson, S., Potter, C., Stephenson, W., and Finn, C. (1997). Seismic reflection images beneath Puget Sound, western Washington State: The Puget Lowland thrust sheet hypothesis: Journal of Geophysical Research: Solid Earth, v. 102, no. B12, p. 27469–27489, https://doi.org/10.1029/97JB01830.

Priest, G. R., Baptista, A. M., Myers, E. P., and Kamphaus, R. A. (2001). Tsunami hazard assessment in Oregon. ITS 2001 Proceedings, NTHMP Review Session, Paper R-3. https://www.researchgate.net/profile/Antonio-Baptista-7/publication/228581151_Tsunami_hazard_assessment_in_Oregon/links/0deec523dd069ef93f000000/Tsunami-hazard-assessment-in-Oregon.pdf

Priest, G. R., Witter, R. C., Zhang, Y., Wang, K., Goldfinger, C., Stimely, L. L., English, J. T., Pickner, S. G., Hughes, K. L. B., Willie, T. E., & Smith, R. L. (2013). Tsunami inundation scenarios for Oregon (Open File Report O-13-19). Oregon Department of Geology and Mineral Industries.

Reid, H.F., Taber, S., (1919). The Porto Rico earthquakes of October-November, 1918. *Bull. Seismol. Soc. Am.* 9(4), 95–127, https://doi.org/10.1785/BSSA0090040095.

Robertson, I. (2023). Development of high-resolution probabilistic tsunami design zone maps compatible with ASCE 7-22 for higher-risk coastal areas of the Island of Maui, Phase II, and the Island of Kauai, State of Hawai'i. Prepared for State of Hawai'i, Office of Planning, Department of Business, Economic Development and Tourism.

Reese, S., Bradley, B., Bind, J., Smart, G., Power, W., and Sturman, J. (2011). Empirical building fragilities from observed damage in the 2009 South Pacific tsunami. Earth-Science Reviews 107:156–173

Ross, S. L., Jones, L. M., Miller, K. P., Wein, K. A., Wilson, R. I., Bahng, B., Barberopoulou, A., Borrero, J. C., Brosnan, D. M., Bwarie, J. T., Geist, E. L., Johnson, L. A., Kirby, S. H., Knight, W. R., Long, K., Lynett, P., Mortensen, C. E., Nicolsky, D. J., Perry, S. C., Plumlee, G. S., Real, C. R., Ryan, K., Suleimani, E., Thio, H., Titov, V. V., Whitmore, P. M., & Wood, N. J. (2013). SAFRR (Science Application for Risk Reduction) tsunami scenario—Executive summary and introduction (U.S. Geological Survey Open-File Report 2013–1170–A). In S. L. Ross & L. M. Jones (Eds.), The SAFRR (Science Application for Risk Reduction) tsunami scenario (U.S. Geological Survey Open-File Report 2013–1170, 17 p.). U.S. Geological Survey. http://pubs.usgs.gov/of/2013/1170/a/

Styron, R., & Pagani, M. (2020). The GEM Global Active Faults Database. *Earthquake Spectra, 36*(4), 875–918. https://doi.org/10.1177/8755293020944182

Suleimani, E. N., Salisbury, J. B., Nicolsky, D. J., & Koehler, R. D. (2019). Regional tsunami hazard assessment for the communities of Port Alexander, Craig, and Ketchikan, Southeast Alaska. *Report of Investigation 2019-7*. https://dggs.alaska.gov/webpubs/dggs/ri/text/ri2019_007.pdf

Suleimani, E. N., Salisbury, J. B., & Nicolsky, D. J. (2023). Tsunami inundation maps of Anchorage and upper Cook Inlet, Alaska. *Alaska Division of Geological & Geophysical Surveys Report of Investigation 2023-2*, 56. https://doi.org/10.14509/31018

Thio, H.K., Wei, Y., Chock, G.Y., & Li, W. (2017). Development of offshore probabilistic tsunami exceedance amplitudes for ASCE 7-16, proceedings of the .16th World Conference on Earthquake Engineering, 16WCEE 2017. https://www.wcee.nicee.org/wcee/article/16WCEE/WCEE2017-2004.pdf

Thio, H. K. (2019). Probabilistic tsunami hazard maps for the State of California (Phase 2). *State of California, Department of Conservation, California Geological Survey*, 168. https://filerequest.conservation.ca.gov/?q=AECOM-ProbabilisticTsunamiHazardMapsForCalifornia-Phase2.pdf

Titov, V. V., González, F. I., Mofjeld, H. O., and Venturato, A. J. (2003). NOAA TIME Seattle tsunami mapping project: Procedures, data sources, and products: NOAA Technical Memorandum OAR PMEL-124, https://www.pmel.noaa.gov/pubs/PDF/tito2572/tito2572.pdf.

Uslu, B., Titov, V., Eble, M. C., & Chamberlin, C. D. (2010). Tsunami hazard assessment for Guam. *Pacific Marine Environmental Laboratory, National Oceanic and Atmospheric Administration*. https://repository.library.noaa.gov/view/noaa/11107.

Uslu, B., Eble, M., Arcas, D., & Titov, V. (2013). Tsunami hazard assessment of the Commonwealth of the Northern Mariana Islands. *Tsunami Hazard Assessment Special Series: Vol. 3. Contribution No. 3949 from NOAA/Pacific Marine Environmental Laboratory*, 192. https://nctr.pmel.noaa.gov/hazard_assessment_reports/H03_CNMI_3949_lowres.pdf.

U.S. Army Corps of Engineers [USACE] (2022). NSI Technical References. Technical documentation. https://www.hec.usace.army.mil/confluence/nsi/technicalreferences/latest/technical-documentation.

U.S. Census Bureau (2020) Block-level decennial population and household data. Available at https://data.census.gov/. Last Accessed 27 September 2024

U.S. Census Bureau. (2023). *American Community Survey 5-year estimates, 2018-2022*. Retrieved from https://data.census.gov/

U.S. Geological Survey, 2024, National Digital Elevation Model, accessed March 2024 at URL https://www.usgs.gov/the-national-map-data-delivery

U.S. Virgin Islands Bureau of Economic Research. (n.d.). *U.S. Virgin Islands Bureau of Economic Research*. https://usviber.org/

Ward, P. J., Blauhut, V., Bloemendaal, N., Daniell, J. E., de Ruiter, M. C., Duncan, M. J., Emberson, R., Jenkins, S. F., Kirschbaum, D., Kunz, M., Mohr, S., Muis, S., Riddell, G. A., Schäfer, A., Stanley, T., Veldkamp, T. I. E., & Winsemius, H. C. (2020). Review article: Natural hazard risk assessments at the global scale. *Natural Hazards and Earth System Sciences, 20*(4), 1069–1096. https://doi.org/10.5194/nhess-20-1069-2020

Washington Emergency Management Division. (2021). A guide to tsunami vertical evacuation options on the Washington Coast. https://mil.wa.gov/tsunami#vertical

Wei, Y., Thio, H.K., Titov, V.V., Chock, G.Y., Zhou, H., Tang, L., & Moore, C.W. (2017). Inundation modeling to create 2,500-year return period tsunami design zone maps for the ASCE 7-16 standard, proceedings of the .16th World Conference on Earthquake Engineering, 16WCEE 2017. https://www.wcee.nicee.org/wcee/article/16WCEE/WCEE2017-450.pdf

Wilson, R. I., Admire, A. R., Borrero, J. C., Dengler L. A., Legg, M. R., Lynett, P., McCrink, T. P., Miller, K. M., Ritchie, A., Sterling, K. & Whitmore, P. M. (2013). Observations and impacts from the 2010 Chilean and 2011 Japanese tsunamis in California (USA). *Pure and Applied Geophysics, 170*(6-8), 1127–1147. https://doi.org/10.1007/s00024-012-0527-z

Witter, R. C., Zhang, Y.J., Wang, K., Priest, G. R., Goldfinger, C., Stimely, L. L.; English, J.T.; and Ferro, P. A. (2011) Simulating tsunami inundation at Bandon, Coos County, Oregon, using hypothetical Cascadia and Alaska earthquake scenarios: Oregon Department of Geology and Mineral Industries Special Paper 43, 57 p., http://www.oregongeology.org/pubs/sp/p-SP-43.htm.

Witter, R., Zhang, Y.J., Wang, K., Priest, G.R., Goldfinger, C., Stimely, L., English, J.T., and Ferro, P.A. (2013). Simulated tsunami inundation for a range of Cascadia megathrust earthquake scenarios at Bandon, Oregon, USA: Geosphere, v. 9, no. 6, p. 1783-1803, https://doi.org/10.1130/GES00899.1

Wood, N., Church, A., Frazier, T., & Yarnal, B. (2007). Variations in community exposure and sensitivity to tsunami hazards in the State of Hawai'i. *U.S. Geological Survey Scientific Investigation Report 2007-5208*, 42. https://doi.org/10.3133/sir20075208

Wood, N. J., & Schmidtlein, M. C. (2012). Anisotropic path modeling to assess pedestrian-evacuation potential from Cascadia-related tsunamis in the U.S. Pacific Northwest. *Natural Hazards, 62*(2), 275–300. https://doi.org/10.1007/s11069-011-9994-2

Wood, N., and Peters, J. (2025a). Pedestrian evacuation time maps for Alaska tsunami-hazard zones: U.S. Geological Survey data release, https://doi.org/10.5066/P149DSZZ.

Wood, N., and Peters, J. (2025b) Pedestrian evacuation time maps for the Commonwealth of the Northern Mariana Islands tsunami-hazard zones: U.S. Geological Survey data release, https://doi.org/10.5066/P13DVWKA.

Wood, N., and Peters, J. (2025c). Pedestrian evacuation time maps, population estimates, and cruise ship passenger estimates for USVI tsunami-hazard zones: U.S. Geological Survey data release. https://doi.org/10.5066/P13YX9AJ

Wood, N., Ratliff, J., Peters, J., and Shoaf, K. (2013). Population vulnerability and evacuation challenges in California for the SAFRR tsunami scenario, chap. I in Ross, S.L., and Jones, L.M., eds., The SAFRR (Science Application for Risk Reduction) Tsunami Scenario: U.S. Geological Survey Open-File Report 2013–1170, 50 p., http://pubs.usgs.gov/of/2013/1170/i/.

Wood, N., Jones, J., Peters, J., and Richards, K. (2018). Pedestrian evacuation modeling to reduce vehicle use for distant tsunami evacuations in Hawai'i, International Journal of Disaster Risk Reduction, Volume 28, Pages 271-283, ISSN 2212-4209, https://doi.org/10.1016/j.ijdrr.2018.03.009.

Wood, N., Jones, J.M., Yamazaki, Y., Cheung, K.F., Brown, J., Jones, J., and Abdollahian, N. (2019). Population vulnerability to tsunami hazards informed by previous and projected disasters: A case study of American Samoa, Natural Hazards 95, 505–528, https://doi.org/10.1007/s11069-018-3493-7.

Wood, N., Peters, J., Wilson, R., Sherba, J., and Henry, K. (2020). Variations in community evacuation potential related to average return periods in probabilistic tsunami hazard analysis: International Journal of Disaster Risk Reduction, v. 50, p. 101871, https://doi.org/10.1016/j.ijdrr.2020.101871.

Wood, N., Peters, J., Cheung, K. F., Yamazaki, Y., Calvo, D., & Guard, C. (2023). Modeling non-structural strategies to reduce pedestrian evacuation times for mitigating local tsunami threats in Guam. *International Journal of Disaster Risk Reduction, 95*, 103859. https://doi.org/10.1016/j.ijdrr.2023.103859

Wood, N., Peters, J., Sheehan, A., and Bausch, D. (2025a). National population exposure and evacuation potential in the United States to earthquake-generated tsunami threats. International Journal of Disaster Risk Reduction, 105511.

Wood, N.J., Peters, J., and Jones, J.L (2025b). Estimates of population exposure and evacuation potential for earthquake-related tsunami hazard zones in the United States: U.S. Geological Survey, https://doi.org/10.5066/P13GXERU.

Wood N, Peters J, and Moore C, (2025c) Population vulnerability of residents, employees, and cruise-ship passengers to tsunami hazards of islands in complex seismic regions: a case study of the U.S. Virgin Islands. International Journal of Disaster Risk Reduction. https://doi.org/10.1016/j.ijdrr.2025.105289

Sheehan A, Yeager C, Wood N, Bausch D, McDougall A, Johnson D, Peters J, and Zuzak C (2025) Data associated with the national assessment of potential average annualized losses from tsunamis in the United States, U.S. Geological Survey Data Release https://doi.org/10.5066/P1IAVNAE

Yang, H.L., Laverdiere, M., Hauser, T., Swan, B., Schmidt, E., Moehl, J., Reith, A., Adams, D., Morris, B., McKee, J., Whitehead, M., and Tuttle, M. (2024). A baseline structure inventory with critical attribution for the US and its territories. Sci Data 11, 502. https://doi.org/10.1038/s41597-024-03219-x Yamazaki, Y., Kowalik, Z., and Cheung, K. F. (2009). Depth-integrated, non-hydrostatic model for wave breaking and run-up. *International Journal for Numerical Methods in Fluids, 61*, 473–497. https://doi.org/10.1002/fld.1952

Yamazaki, Y., Cheung, K. F., and Kowalik, Z. (2011). Depth-integrated, non-hydrostatic model with grid nesting for tsunami generation, propagation, and run-up. *International Journal for Numerical Methods in Fluids, 67*, 2081–2107. https://doi.org/10.1002/fld.2485

Yun, N., and Hamada, M. (2012). Evacuation behaviors in the 2011 Great East Japan earthquake. Journal of Disaster Research 7(7): 458–467.

Zahibo, N., Pelinovsky, E., Yalciner, A., Kurkin, A., Koselkov, A., and Zaitsev, A. (2003). The 1867 Virgin Island tsunami: observations and modeling, Oceanologica Acta, Volume 26, Issues 5–6, Pages 609-621, ISSN 0399-1784, https://doi.org/10.1016/S0399-1784(03)00059-8.

Appendix

A. Glossary

Annual Return Period or Frequency – The reciprocal of a return period or recurrence interval.

Average Annualized Loss (AAL) – The estimated long-term value of losses in any given single year in a specified geographic area.

Average Annualized Building Loss – The estimated long-term value of building losses in any given single year in a specified geographic area.

Average Annualized Population Loss – The estimated long-term value of population losses in any given single year in a specified geographic area.

Capital Stock – Building structure, non-structural, content and inventory replacement value (2022 valuations).

Deterministic Scenario – Considers the impact of a single scenario with specific source parameters.

Digital Elevation Model – A data file that contains digital representations of cartographic information in raster form. DEMs consist of a sampled array of elevations from several ground positions at regularly spaced intervals.

Distant Tsunami – According to the International Tsunami Information Center, a distant tsunami originates from a source generally more than 1,000 km or more than 3 hours of tsunami travel time from its source. Refer to Pacific Ocean | Tsunami Programme UNESCO-IOC for more information.

Hazard – A source of potential danger or an adverse condition. For example, a hurricane occurrence is the source of high winds, rain, and coastal flooding, all of which can cause fatalities, injuries, property damage, infrastructure damage, interruption of business, or other types of harm or loss.

Hazard Identification – Hazard identification involves determining the physical characteristics of a particular hazard—magnitude, duration, frequency, probability, and extent—for a site or a community.

Hazus – FEMA's Hazus software provides standardized tools and data for estimating risk from earthquakes, floods, tsunamis, and hurricanes. Refer to Hazus | FEMA.gov or Appendix B for more information.

Local Tsunami – According to the International Tsunami Information Center, a local tsunami can be classified as such if it is from a nearby source with less than 1 hour tsunami travel time, or typically within about 200 km from its source. Refer to Pacific Ocean | Tsunami Programme UNESCO-IOC for more information.

Maximum Flow Depth – The maximum tsunami flow depth in feet above ground level.

Maximum Runup – The maximum tsunami runup elevation.

Mean Higher High Water (MHHW) – Mean Higher High Water is the average level of the highest tide for each day computed over a 19-year period.

National Structure Inventory (NSI) – The National Structure Inventory is a system of databases containing structure inventories of varying quality and spatial coverage. The purpose of the National Structure Inventory databases is to facilitate storage and sharing of point-based structure inventories used in the assessment and analysis of natural hazards. Flood risk is the primary usage, but sufficient data exists on each structure to compute damage and life safety risk due to other hazard types.

Regional Tsunami – According to the International Tsunami Information Center, a regional tsunami is classified when it is generally within 1,000 km or 1-3 hours tsunami travel time from its source. Refer to Pacific Ocean | Tsunami Programme UNESCO-IOC for more information.

Return Period or Recurrence Interval – The return period, or the recurrence interval, is the average time interval between occurrences of a specific event, such as a tsunami, at a particular location. It is often expressed in years. For example, a return period of 100 years means that, on average, a tsunami of a given size is expected to occur once every 100 years.

Risk – The likelihood of sustaining a loss from a hazard event defined in terms of expected probability and frequency, exposure, and consequences, such as death and injury, financial costs of repair and rebuilding, and loss of use.

Sea Level Rise (SLR) – Changes in mean global sea level, resulting from the transfer of fresh water from land to oceans (from land-based ice sheets and mountain glaciers) and from the thermal expansion of ocean water due to higher global temperatures.

Tsunami – A tsunami is a series of extremely long waves (multiple waves tens-to-hundreds of miles between crests) caused by a large and sudden displacement of the ocean. Tsunamis radiate outward in all directions from the point of origin and can move across entire ocean basins. When they reach the coast, they can cause dangerous coastal flooding and powerful currents that can last for several hours or days.

Wave Arrival Time – The time it takes for a tsunami to travel from its source to the first instance when a location on land experiences inundation.

B. Overview of Hazus

Hazus is a nationally standardized risk modeling methodology. It is distributed as free GIS-based desktop software with a collection of inventory databases for every U.S. state and territory. Hazus identifies areas with high risk for natural hazards and estimates physical, economic, and community impacts of earthquakes, hurricanes, floods, and tsunamis. The Hazus software, managed by FEMA's Natural Hazards Risk Assessment Program, partners with other federal agencies, research institutions, and regional planning authorities to ensure Hazus resources incorporate the latest scientific and technological approaches and meet the needs of the emergency management community.

Hazus is used for mitigation, recovery, preparedness, and response. Mitigation planners, GIS specialists, and emergency managers use Hazus to determine potential losses from disasters and to identify the most effective mitigation actions for minimizing those losses. Hazus supports the risk assessment requirement in the mitigation planning process. Response planners use Hazus to map potential impacts from catastrophic events and identify effective strategies for response and preparedness. Hazus is also used during real-time response efforts to estimate impacts from incoming storms or ongoing earthquake sequences.

The Hazus tsunami model has fewer capabilities than Hazus's other hazard models but can quantify and map risk information such as:

- Physical damage to residential and commercial buildings, as well as user-defined buildings.
- Economic loss to buildings, including lost jobs, business interruptions, and repair and reconstruction costs.
- Community impacts, including estimates of casualties based on an integrated USGS pedestrian evacuation model, estimated levels of community preparedness and flow depth.
- Cost-effectiveness of common mitigation strategies, such as enhancing community preparedness and warning, vertical evacuation structures, elevating or strengthening buildings in the inundation areas.

Full technical details regarding the loss estimation methodology in FEMA's Hazus tsunami model can be found in the Hazus Tsunami Technical Manual (FEMA, 2024b).

Hazus version 6.0 also included important baseline inventory dataset improvements to valuations, demographics, buildings, essential facilities, transportation, and utility systems. Highlights can be found in FEMA (2002) and this effort was followed by fixes to several attributes including the number of stories, updates to earthquake building types and seismic design levels in Hazus 6.1 (FEMA, 2024c) used for this study.

C. Tsunami Hazard Data Preprocessing

To generate the required inputs for Hazus 6.1 (refer to Section 2.1.1), the data outlined in Table 1-2 underwent preprocessing. While the numerical models used to produce the tsunami hazard data conform to NTHMP Mapping and Modelling Subcommittee benchmarking requirements as described in Macias et al., (2020) and NTHMP (2012), the outputs are provided in a broad variety of GIS outputs and units. Because Hazus losses are driven by overland flooding affecting buildings, negative flow depths and 0 values were removed. This section details the GIS methods applied on a state-by-state basis to convert the data from its original formats into the grid data necessary for Hazus ingestion.

C.1 ALASKA

Table C-1 below indicates which scenarios were utilized to develop tsunami hazard data for each community, as well as their corresponding segment of the Aleutian Arc and associated return period. Refer to Wood et al. (2025b) for more information on each scenario.

Table C-1. Alaska Division of Geological & Geophysical Surveys Tsunami Hazard Data

Community	Scenario	Tsunami Source(s) (Segment of Aleutian Arc)	Return Period
Adak	ri2019-1-max-flow-depth-adak	Andreanof	113
Akhiok	ri2021-6-max-flow-depth-akhiok	Kodiak, Kenai, Barren Islands	379
Akutan	ri2015-5-max-flow-depth-akutan	Andreanof, Fox Islands, Sanak	210
Anchor Point	ri2019_5_hazard_boundary_anchor_point	Kodiak, Barren Islands, Kenai, Prince William Sound	379
Anchorage	ri2023-2-scenario-09-upper-cook-inlet-flow-depth ri2023-2-scenario-16-upper-cook-inlet-flow-depth	Prince William Sound, Kenai, Kodiak	379
Atka	ri2019-1-max-flow-depth-atka	Andreanof	113

Community	Scenario	Tsunami Source(s) (Segment of Aleutian Arc)	Return Period
Chenega Bay	ri2014-3-max-flow-depth-scenarios-all_Chenega_Sawmill ri2014-3-max-flow-depth-scenarios-1-5_Chenega_Sawmill	Prince William Sound	594
Chignik	ri2016-8-max-inundation-line-chignik	Shumagin, Semidi	222
Chiniak	ri2021-6-max-flow-depth-chiniak	Kodiak, Kenai, Barren Islands	379
Cold Bay	ri2016-1-max-inundation-line-coldbay	Sanak, Shumagin	169
Cordova	ri2014-1b-max-inundation_Cordova	Prince William Sound, Kenai	441
Craig	ri2019_7_hazard_boundary_craig	Kodiak, Barren Islands, Kenai, Prince William Sound	379
Dillingham	ri2020_1_hazard_boundary_dillingham	Andreanof, Fox Islands, Sanak	210
Elfin Cove	ri2015-1-max-flow-depth-elfincove	Prince William Sound, Kenai	441
False Pass	ri2019-3-hazard-boundary-false-pass	Sanak, Shumagin	169
Gustavus	ri2015-1-max-flow-depth-gustavus	Prince William Sound, Kenai	441
Haines	ri2018-2-max-flow-depth-haines	Barren Islands, Kenai, Prince William Sound, Yakataga	441
Homer	ri2018-5v2-max-flow-depth-tectonic-homer ri2018-5v2-max-flow-depth-landslide-homer	Kodiak, Barren Islands, Kenai, Prince William Sound	379
Hoonah	ri2015-1-max-flow-depth-hoonah	Prince William Sound, Kenai	441

Community	Scenario	Tsunami Source(s) (Segment of Aleutian Arc)	Return Period
Hydaburg	ri2020-002a-hazard-boundary-hydaburg	Barren Islands, Kenai, Prince William Sound	441
Juneau	ri2017-9-tectonic-inundation-scenario-4-flow-depth_Juneau ri2017-9-composite-landslide-tectonic-flow-depth_Juneau ri2017-9-composite-landslide-flow-depth_Juneau	Barren Islands, Kenai, Prince William Sound, Yakataga	441
Karluk	ri2022-2-scenario-09-karluk-flow-depth ri2022-2-scenario-03-karluk-flow-depth	Kodiak, Semidi	169
Kasaan	ri2020_2_hazard_boundary_kasaan	Barren Islands, Kenai, Prince William Sound	441
Ketchikan	ri2019_7_hazard_boundary_ketchikan	Kodiak, Barren Islands, Kenai, Prince William Sound	379
King Cove	ri2016-1-max-inundation-line-kingcove	Sanak, Shumagin	169
Klawock	ri2020_2_hazard_boundary_klawock	Barren Islands, Kenai, Prince William Sound	441
Kodiak	ri2017-8-max-flow-depth-kodiak	Kodiak, Barren Islands	379
Larsen Bay	ri2022-2-scenario-09-larsen-bay-flow-depth ri2022-2-scenario-03-larsen-bay-flow-depth	Kodiak, Semidi	169
Metlakatla	ri2020_2_hazard_boundary_metlakatla	Barren Islands, Kenai, Prince William Sound	441
Nanwalek	ri2019_5_hazard_boundary_nanwalek	Kodiak, Barren Islands, Kenai, Prince William Sound	379
Nelson Lagoon	ri2020_1_hazard_boundary_nelson_lagoon	Andreanof, Fox Islands, Sanak	210

Community	Scenario	Tsunami Source(s) (Segment of Aleutian Arc)	Return Period
Nikolski	ri2016-7-max-inundation-line-nikolski	Fox Islands, Andreanof, Sanak	210
Old Harbor	ri2021-6-max-flow-depth-old-harbor	Kodiak, Kenai, Barren Islands	379
Ouzinkie	ri2021-6-max-flow-depth-ouzinkie	Kodiak, Kenai, Barren Islands	379
Pasagshak Bay	ri2019-6a-hazard-boundary-pasagshak	Kodiak, Semidi	169
Pelican	ri2020_2_hazard_boundary_pelican	Barren Islands, Kenai, Prince William Sound	441
Perryville	ri2019-3-hazard-boundary-perryville	Sanak, Shumagin	169
Platinum	ri2020_1_hazard_boundary_platinum	Andreanof, Fox Islands, Sanak	210
Point Baker	ri2020_2_hazard_boundary_point_baker	Barren Islands, Kenai, Prince William Sound	441
Port Alexander	ri2019_7_hazard_boundary_port_alexander	Kodiak, Barren Islands, Kenai, Prince William Sound	379
Port Graham	ri2019_5_hazard_boundary_port_graham	Kodiak, Barren Islands, Kenai, Prince William Sound	379
Port Lions	ri2021-6-max-flow-depth-port-lions	Kodiak, Kenai, Barren Islands	379
Port Protection	ri2020_2_hazard_boundary_port_protection	Barren Islands, Kenai, Prince William Sound	441
Saint George	ri2020_1_hazard_boundary_st_george	Andreanof, Fox Islands, Sanak	210
Saint Paul	ri2020_1_hazard_boundary_st_paul	Andreanof, Fox Islands, Sanak	210

Community	Scenario	Tsunami Source(s) (Segment of Aleutian Arc)	Return Period
Sand Point	ri2017-3-max-flow-depth-sand-point	Sanak, Shumagin, Semidi	169
Seldovia	ri2018-5a-max-flow-depth_Seldovia	Kodiak, Kenai	379
Seward	ri2022-3-seward-scenario-11-flow-depth ri2022-3-seward-scenario-10-flow-depth	Prince William Sound, Yakataga	594
Shemya	ri2019-4-hazard-boundary-shemya-all	Attu, Amchitka	295
Sitka	ri2013-3-hypothetical-composite-flow-depth_Sitka	Kodiak, Barren Islands, Kenai, Prince William Sound	379
Skagway	ri2018-2-max-flow-depth-skagway	Barren Islands, Kenai, Prince William Sound, Yakataga	441
Tatitlek	ri2014-1-max-flow-depth-tatitlek	Prince William Sound	594
Unalaska	ri2015-5-max-flow-depth-unalaska	Andreanof; Fox Islands; Sanak	210
Valdez	ri2013-1-hypothetical-composite-flow-depth_Valdez	Prince William Sound, Kenai	441
Whittier	ri2011-7-max-flow-depth_Whittier	Barren Islands, Kenai, Prince William Sound	441
Yakutat	ri2016_2_max_inundation_line_yakutat	Prince William Sound, Kenai	441

To produce runup grid data for both the vector and grid data, DEM coverage for all communities was needed. The DEM created used the best publicly available DEM data (USGS, 2024) and, where applicable, coseismic deformation was provided by the Geophysical Institute, University of Alaska Fairbanks. Refer to Appendix E, Section E.1 for DEM methodology.

Estimating Runup

The steps and geoprocessing tools associated with preprocessing vector data to create runup grid data are as follows. First, the "Feature Vertices to Points" tool was used to create point data along the evacuation zone polygon. Next, the "Extract Value to Points" tool was applied to extract grid values from the DEM at these points. An Inverse Distance Weighted (IDW) surface was then

generated from the elevation points where the DEM values exceeded 0 meters, with the resolution of the underlying DEM serving as the grid resolution. Finally, the "Extract by Mask" tool was used to clip the IDW surface to the extent of the original data, using the original inundated areas as the mask.

To create runup grid data from the grid data sources the "Raster Calculator" tool was used with the SetNull function to remove negative values from the maximum flow depth grids. Next, the deformed DEM was added to the maximum flow depth grids using the "Raster Calculator," resulting in the production of runup grid data for each area of interest.

Estimating Maximum Flow Depth

To estimate maximum flow depth in communities with vector data, the deformed DEM was subtracted from the runup grid data using “Raster Calculator”. In communities where maximum flow depth grids were provided by the Geophysical Institute, University of Alaska Fairbanks, no additional pre-processing was required.

Estimating Velocity

Maximum velocity was estimated for each area of interest using Equation 2-1 as outlined in Section 2.

Final Hazus Inputs

Final flow depth and velocity grids were developed for each return period using the ‘Mosaic to New Raster’ tool with the mosaic operator ‘maximum.’ These data were compiled into a single file geodatabase containing maximum flow depth and maximum velocity grids for the 113, 169, 210, 222, 295, 379, 441, and 594 return periods. The resultant grids are the final inputs required for Hazus Level 2 although the original hazard data for Alaska are considered Level 1 since they lacked velocity data from the original numerical model.

C.2 AMERICAN SAMOA

The KMZ files corresponding to each scenario were transformed into polygons using the KMZ to Layer tool. These polygons were subsequently projected to align with the coordinate system of the underlying DEM. A Triangulated Irregular Network (TIN) was generated from the polygons, employing the 'Hard Line' method. The resulting TIN was then converted into a grid format. To produce a runup grid, the DEM was added to the depth grid using the ‘Raster Calculator’ tool. Finally, the resulting runup grid was clipped to match the extent of the depth grid. The resultant grids are the final inputs for Hazus Level 1.

C.3 CALIFORNIA

Because the downloaded momentum flux and flow depth data were provided based on models run for 63 communities, it was necessary to mosaic this data at the state level for each return period. Using the 'Mosaic to New Raster' tool, the grids were combined into statewide datasets for

momentum flux and flow depth. During this process, the mosaic operator 'maximum' was applied to ensure that overlapping data retained the highest value. In total, 14 statewide grids were generated, representing momentum flux and flow depth at intervals of 72, 100, 200, 475, 975, 2,475 and 3,000 years.

To refine the quality of the data, unnecessary negative values were eliminated from the grids. Using the SetNull operation in the ‘Raster Calculator’ tool, negative values were removed from the analysis, nullifying any grid cell value <0. This operation was repeated across all grid datasets.

The maximum values for both momentum flux and flow depth were converted to median values and units were standardized for compatibility (refer to Table 2-3, Section 2).

Given the extensive length of California's coastline, the decision was made to split the state into two regions: Southern California (SoCal) and Northern California (NoCal), divided at the border of Monterey County to the north and San Luis Obispo County to the south. This division allowed for more targeted analysis and application of the data. Using the ‘Extract by Mask’ tool, the median momentum flux and median flow depth grids were clipped to the defined boundaries of NoCal and SoCal.

These processes resulted in the creation of final products necessary for 14 separate Level 3 Hazus analysis runs to cover both sections of the State for all seven return periods.

C.4 GUAM

During the initial analysis, it was observed that the NOAA runup grids contained a few anomalously high runup values considered artifacts, notably single grid cell anomalies with values as high as 35 meters for distant sources and 58 meters for local sources. Such anomalies, if intersecting with building points, may significantly distort the analysis results. To mitigate this issue, anomalies were identified as grid cells exhibiting runup values exceeding realistic thresholds. For local event scenarios, any grid cell with a runup value greater than 20 meters was considered anomalous, resulting in the removal of just 28 out of 3,213,596 cells. For distant source scenarios, grid cells with runup values exceeding 10 meters were considered anomalous, leading to the removal of just 98 out of 3,213,526 cells.

Grid cells with a 0 value were removed using a combination of GIS tools. Unnecessary negative values were eliminated from the grids using the SetNull operation in the ‘Raster Calculator’ tool, negative values were removed from the analysis, nullifying any grid cell value <0 where no inundation or losses are expected. The ‘Raster to Polygon’ tool with the 'do not simplify' option was employed to create a mask polygon feature class of the inundation area. The 'Extract by Mask' tool was used to extract the values within the inundation area from both local and distant grids, effectively eliminating the identified anomalies. This operation was repeated across all grid datasets.

To estimate runup values, University of Hawai‘i depth data were added to DEMs using the ‘Raster Calculator.’ The ‘Raster Analysis Environment Settings’ were modified to use the 'Minimum of Inputs’ for both local and distant scenarios. The 500-year runup grid was generated by mosaicking NOAA

and University of Hawai‘i local scenario (M_w 8.3 Mariana Subduction Zone source) runup grids using the maximum value. The 2,200-year runup grid was created by merging NOAA and University of Hawai‘i distant (East Philippines source) and local (500-year) grids, again using the maximum value.

Although there are no tsunami inundation products that cover the northern coast of Guam, as a result of high relief, there are few buildings exposed to tsunami inundation in the north. However, a small gap between the PMEL and University of Hawai‘i models along the southeastern coast appears to occur in an area where buildings may be exposed to potential tsunami impacts in low lying areas (Figure C-1) and are quantified in Appendix F, Section F.3.

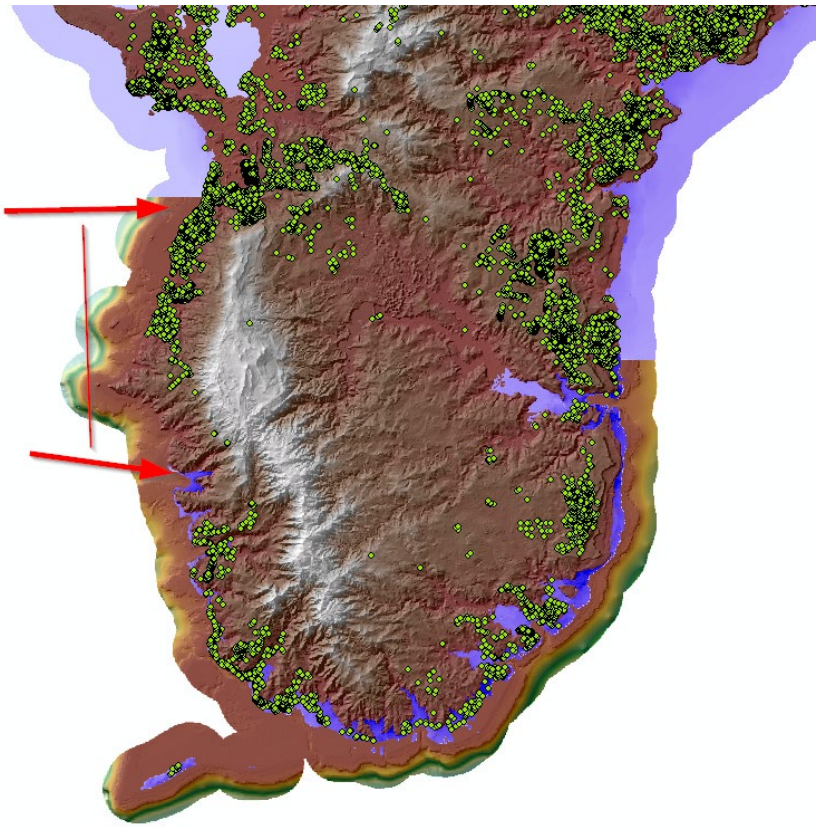

Figure C-1: Guam Tsunami Hazard Data Gaps

Figure C-1 Illustrates a stretch of the southeast coast without tsunami hazard data (blue) coverage and potential building exposure (green dots). It is noteworthy that for most areas, the runups for the local (500-year) scenarios are greater than those for the distant (2,200-year) scenarios, with the mosaiced 2,200-return period grids representing the maximum value across all scenarios.

C.5 HAWAII

400- and 1,500-Year Return Period Scenarios

The 400- and 1,500-year return period scenarios included only runup grid data, requiring the use of the Hazus Level 1 (runup only) approach (refer to Section 2.1.1), where the velocity is estimated using the empirical ASCE function (Equation 2-1).

1,500-Year Return Period Scenario

The high resolution ASCE 3,500-year data were provided by Robertson (2023) with a resolution of approximately 3 meters consisting of both maximum flow depth in feet above ground level and momentum flux.

To refine the quality of the data, unnecessary negative values were eliminated from the grids. Using the SetNull operation in the 'Raster Calculator' tool, negative values were removed from the analysis, nullifying any grid cell value <0. The maximum values for both momentum flux and flow depth were converted to median values and units were standardized for compatibility (refer to Table 2-3, Section 2).

C.6 COMMONWEALTH OF THE NORTHERN MARIANA ISLANDS

Tinian and Rota Islands

The local and distant grids for the Islands of Tinian and Rota were resampled to 1/3 arcsecond resolution using the 'Resample' geoprocessing tool to align with the DEM resolution. Using the SetNull operation in the 'Raster Calculator' tool, negative values were removed from the analysis, nullifying any grid cell value <0. Any erroneous areas disconnected from the coast were removed using the 'Extract by Mask' tool. The resultant grids provide the flow depth input for Hazus Level 1.

To estimate runup for the Islands of Tinian and Rota, the DEM (refer to Appendix E, Section E.2) was added to the flow depth grid data using Raster Calculator. Maximum velocity was estimated for each area of interest using the maximum flow depth grids, maximum runup values, and the empirical ASCE function (Equation 2- 1, Section 2). The maximum runup values were obtained by creating histograms of the runup grids; to reduce the influence of data anomalies, values with a cell count of <10 were not considered. The resultant grids provide the velocity input for Hazus Level 2 although the original hazard data are considered Level 1 because they lack velocity data provided by the numerical model.

Saipan Island

For both local and distant scenarios, unnecessary negative values were eliminated from the grids. Using the SetNull operation in the 'Raster Calculator' tool, negative values were removed from the analysis, nullifying any grid cell value <0. This operation was repeated across all grid datasets. Both flow depth and velocity data were provided, so this was the only step necessary to produce inputs for Hazus Level 2 because the velocity data were provided by the numerical model.

Given the influence of multiple data sources on the same locations, the data were mosaiced so that each return period included all shorter return periods. This approach ensured that the maximum values were applied at each location for every return period.

C.7 OREGON

To refine the quality of the data, unnecessary negative values were eliminated from the grids. Using the SetNull operation in the 'Raster Calculator' tool, negative values were removed from the analysis, nullifying any grid cell value <0. This operation was repeated across all grid datasets.

Next a mosaiced grid representing the 1,000-year return period was created. This was achieved using the 'Mosaic to New Raster' tool, which mosaiced the grid for the Cascadia Subduction Zone (M), AK64, and AKMax while retaining the maximum value for each pixel for the 1,000-year period. The creation of the 2,000-year grid was a unique situation because it approximates the small (S) Cascadia scenario while the medium (M) approximates the 1,000-year return period. As a result, the 2,000-year grid used to estimate losses was created by combining the 1,000- and 2,000-year grids, retaining the maximum value from either data source. It is important to note that the maximum values were primarily driven by the 1,000-year grid, leading to similar loss estimates for both time intervals.

The maximum values for both momentum flux and flow depth were converted to median values and units were standardized for compatibility (refer to Table 2-3, Section 2).

These data were compiled into a single file geodatabase containing median momentum flux and median flow depth grids for each of the five return periods as the final products necessary for a Level 3 Hazus analysis.

C.8 PUERTO RICO

The initial step in processing Puerto Rico data involved generating maximum momentum flux grids. This was accomplished using the batch "Make NetCDF Grid Layer" tool in ArcMap, with inputs from various NetCDF files, including all available segments of 19N, Anegada Passage, Mona Chanel, Muertos Trough, Puerto Rico Trench, Septentrional, and FEMA scenarios. The variable targeted for extraction was "max_mom_flux", however, this was determined to be the two-dimensional velocity in units of meters per second and needed to be post processed to estimate momentum flux. A similar NetCDF extraction approach was taken to create maximum height and deformed bathymetry grids, utilizing the same NetCDF data with the variable of interest being "max_height" and "deformed_bathy", respectively.

Depth grids were derived from runup grids by subtracting the deformed bathymetry from the runup grid using the batch 'Raster Calculator.' This subtraction produced maximum flow depth grids based on the deformed bathymetry.

The maximum values for velocity and flow depth were multiplied to estimate the maximum momentum flux and the converted to median values and units were standardized for compatibility (refer to Table 2-3).

Given the influence of multiple data sources on the same locations, the data were mosaiced so that each return period included all shorter return periods. This approach ensured that the maximum values were applied at each location for every return period.

These data were compiled into a single file geodatabase containing median momentum flux and median flow depth grids for each scenario as the final products necessary for Level 3 Hazus analysis although the original hazard data provide Level 2 Hazus data because momentum flux was not directly provided by the numerical model.

C.9 UNITED STATES VIRGIN ISLANDS

The initial step in processing United States Virgin Islands data involved generating maximum momentum flux grids. This was accomplished using the batch "Make NetCDF Grid Layer" tool in ArcMap (Esri, Redlands, California), with inputs from various NetCDF files, including Anegada Passage (ID 8-25), Puerto Rico Trench (PRTG), Puerto Rico Trench (PRT2), Virgin Islands Trough (1867), Lesser Antilles Trench (LA2), Lesser Antilles Trench (LA), and Columbia/Venezuela Belt (FSCDB). The variable targeted for extraction was "max_mom_flux." A similar approach was taken to create maximum height and deformed bathymetry grids, utilizing the same NetCDF data with the variable of interest being "max_height" and "deformed_bathy", respectively.

Depth grids were estimated from runup grids by subtracting the deformed bathymetry from the runup grid using the batch "Raster Calculator." This subtraction produced maximum flow depth grids.

To refine the quality of the data, unnecessary negative values were eliminated from the grids. Using the SetNull operation in the ‘Raster Calculator’ tool, negative values were removed from the analysis, nullifying any grid cell value <0. This operation was repeated across all grid datasets.

The maximum values for both momentum flux and flow depth were converted to median values and units were standardized for compatibility (refer to Table 2-3, Section 2).

Given the influence of multiple data sources on the same locations, the data were mosaiced so that each return period included all shorter return periods. This approach ensured that the maximum values were applied at each location for every return period.

These data were compiled into a single file geodatabase containing median momentum flux and median flow depth grids for each scenario because these are the final products necessary for Level 3 Hazus analysis.

C.10 WASHINGTON

To refine the quality of the data, unnecessary negative values were eliminated from the grids. Using the SetNull operation in the 'Raster Calculator' tool, negative values were removed from the analysis, nullifying any grid cell value <0. This operation was repeated across all grid datasets.

The maximum values for both momentum flux and flow depth were converted to median values and units were standardized for compatibility (refer to Table 2-3, Section 2).

Some modeling differences and edge effects were noted between the WGS GeoClaw model to the north and PMEL MOST model to the south, however, these appear to affect areas with limited building exposure.

Given the influence of multiple data sources on the same locations, the data were mosaiced so that each return period included all shorter return periods. This approach ensured that the maximum values were applied at each location for every return period.

These data were compiled into a single file geodatabase containing median momentum flux and median flow depth grids for each of the three return periods because these are the final products necessary for Level 3 Hazus analysis.

D. Average Annualized Loss Estimation Methodology

After the processing and analysis of hazard data, an internal analysis performed by the team transformed the losses from each scenario into average annualized losses. Table D-1 illustrates the Riemann sum method employed where the Hazus tsunami model computes annual losses for seven probabilistic return periods (RPs). The annual probability of the occurrence of the event is 1/RP. The differential probabilities are obtained by subtracting the annual occurrence probabilities. Next, the average loss is computed by averaging the annual losses associated with various return periods as shown in the column average losses. Once an average loss is computed, the average annualized loss is the summation of the product of the average loss and differential probability of experiencing this loss.

Table D-1: Average Annualized Losses Estimations

#	Return Period	Annualized Probabilities	Differential Probabilities		Return Period Losses	Average Losses	Differential Annualized Loss
			Formulas	Values			
1	3,000	0.000333	P3000	0.000333	L3000	L3000	P3000 x L3000
2	2,475	0.000404	P3000 – P2475	0.000070	L2475	(L3000+L2475)/2	(P3000 - P2475) x (L3000+L2475)/2
3	975	0.001026	P2475 – P975	0.000621	L975	(L2475+L975)/2	(P2475 – P975) x (L2475+L975)/2
4	475	0.002105	P975 – P475	0.001079	L475	(L975+L475)/2	(P975 – P475) x (L975+L475)/2
5	200	0.005000	P475 – P200	0.002894	L200	(L475+L200)/2	(P475 – P200) x (L475+L200)/2
6	100	0.010000	P200 – P100	0.005000	L100	(L200+L100)/2	(P200 – P100) x (L200+L100)/2
7	72	0.013888	P100 – P72	0.003888	L72	(L100+L72)/2	(P100 – P72) x (L100+L72)/2
						Total Average Annualized Loss	Σ ( )

Table D-2 shows the computation for average annualized loss based on building losses (structure, contents, and inventory) in California where the summation of the contribution for each return period is $44.5 million.

Table D-2: Average Annualized Building Loss Estimations

#	Return Period	Annualized Probabilities	Differential Probabilities	Return Period Losses (Thousands of $)	Average Losses (Thousands of $)	Differential Annualized Loss (Thousands of $)
1	3,000	0.000333	0.000333	$40,071,752	$40,071,752	$13,357
2	2,475	0.000404	0.000070	$32,923,282	$36,497,517	$2,580
3	975	0.001026	0.000621	$9,998,593	$21,460,937	$13,340
4	475	0.002105	0.001079	$2,508,010	$6,253,301	$6,751
5	200	0.005000	0.002894	$583,629	$1,545,819	$4,474
6	100	0.010000	0.005000	$418,804	$501,216	$2,506
7	72	0.013888	0.003888	$329,355	$374,080	$1,454
					Total	**$44,464**

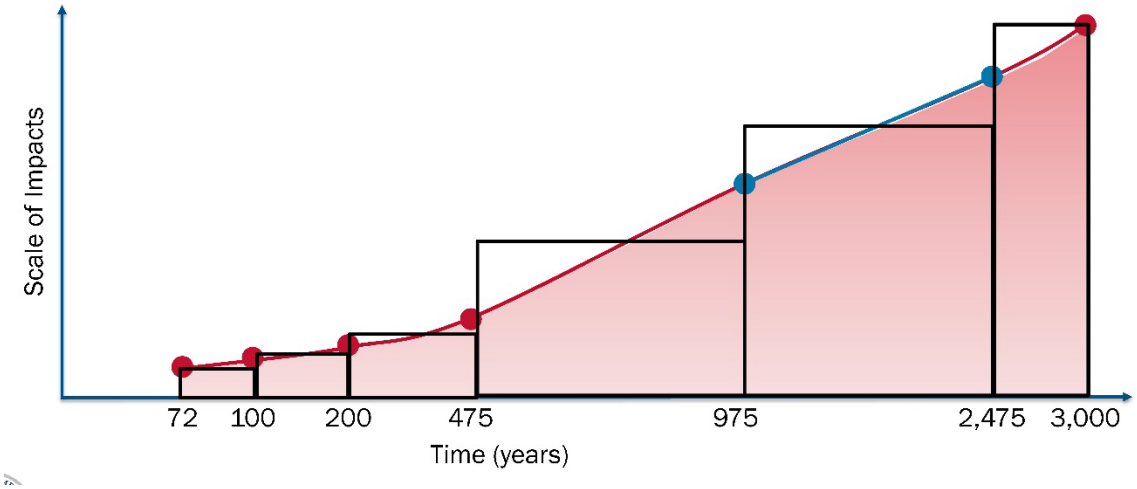

Figure D-1: Illustration of Estimating Area of Loss Curve Based on Input Return periods Using Riemann Sums Method

Figure D-1 illustrates schematically a Hazus 6.1 example of seven loss-numbers plotted against the exceedance probabilities for the ground motions used to estimate these losses. The team computed the average annualized loss by estimating the area under the loss probability curve as represented in Figure D-1. This area represents an approximation to the average annualized loss and is equivalent to taking the summation of the differential probabilities multiplied by the average loss for the corresponding increment of probability. In effect, the area under the curve is approximated by summing the area of rectangular slices.

The choice for the number of return periods is important for accurately evaluating average annualized losses because it ensures that a representative curve can be constructed through the data points. This, in turn, provides a reliable approximation of the area under the loss-exceedance probability curve. Appendix F.2 provides an evaluation of scenarios of return period availability based on the return periods available for California in comparison to other states.

E. Digital Elevation Model Methodology

Tsunami Hazard Analysis for Level 1 (Basic) provides a hazard loss estimation methodology that does not require the velocity data from the numerical model. The Level 1 methodology instead requires a flow depth grid and a DEM along with the maximum runup value combined with Equation 2-1 (Section 2) to estimate velocity and estimate losses. This section details the GIS methods utilized to create DEMs suitable for Hazus Level 1 inputs or estimating runup grids.

E.1 ALASKA

To produce runup grid data for both the vector and grid data, DEM coverage for all communities was needed. The DEM created used the best publicly available DEM data and, where applicable, coseismic deformation based on Okada (1985) was provided by the Geophysical Institute, University of Alaska Fairbanks. DEM availability can be found by community in Table E-1.

The best available DEM data were downloaded from the USGS National Map Viewer (USGS, 2024) where at least 1 arc-second resolution DEM data were available for all areas of interest and 1/3 arc-second DEM data were downloaded where available. The 1/3 arc-second data were resampled to a 1 arc-second resolution where needed to maintain consistency with the deformed bathymetry data. All DEM grids, including those originally at 1 arc-second resolution and those resampled from 1/3 arc-second to 1 arc-second, were then combined into a single mosaic grid, ensuring a unified elevation dataset.

To incorporate the deformed DEMs where available, the deformed grids were resampled to a 1 arc-second resolution for consistency with the underlying DEM produced from USGS data. Subsequently, the grids were re-projected to align with the spatial reference of the underlying DEM. To maintain uniformity, the deformation grids were converted to a 32-bit floating point format. Using the tool “Raster Calculator,” each deformation grid was added to the underlying DEM. Finally, the deformed DEMs and the original DEM were mosaiced using the 'minimum' mosaic operator, resulting in a single DEM that integrated the maximum coseismic deformation across the study area.

Table E-1: Alaska DEM Sources by Community

Community	Source DEM Resolution	Deformed Bathymetry Available	Return Period
Adak	1/3 arcsecond	No	113
Akhiok	1/3 arcsecond	Yes	379
Akutan	1/3 arcsecond	Yes	210
Anchor Point	1 arcsecond	Yes	379
Anchorage	1 arcsecond	Yes	379
Atka	1/3 arcsecond	No	113

Community	Source DEM Resolution	Deformed Bathymetry Available	Return Period
Chenega Bay	1 arcsecond	Yes	594
Chignik	1/3 arcsecond	Yes	222
Chiniak	1/3 arcsecond	Yes	379
Cold Bay	1/3 arcsecond	Yes	169
Cordova	1 arcsecond	Yes	441
Craig	1 arcsecond	No	379
Dillingham	1 arcsecond	Yes	210
Elfin Cove	1/3 arcsecond	Yes	441
False Pass	1/3 arcsecond	Yes	169
Gustavus	1/3 arcsecond	Yes	441
Haines	1 arcsecond	Yes	441
Homer	1 arcsecond	Yes	379
Hoonah	1/3 arcsecond	Yes	441
Hydaburg	1 arcsecond	No	441
Juneau	1 arcsecond	Yes	441
Karluk	1/3 arcsecond	Yes	169
Kasaan	1 arcsecond	No	441
Ketchikan	1 arcsecond	No	379
King Cove	1/3 arcsecond	Yes	169
Klawock	1 arcsecond	No	441
Kodiak	1/3 arcsecond	Yes	379
Larsen Bay	1/3 arcsecond	Yes	169
Metlakatla	1 arcsecond	No	441
Nanwalek	1 arcsecond	Yes	379
Nelson Lagoon	1/3 arcsecond	Yes	210
Nikolski	1/3 arcsecond	Yes	210

Community	Source DEM Resolution	Deformed Bathymetry Available	Return Period
Old Harbor	1/3 arcsecond	Yes	379
Ouzinkie	1/3 arcsecond	Yes	379
Pasagshak Bay	1 arcsecond	Yes	169
Pelican	1 arcsecond	Yes	441
Perryville	1/3 arcsecond	Yes	169
Platinum	1 arcsecond	Yes	210
Point Baker	1 arcsecond	No	441
Port Alexander	1 arcsecond	Yes	379
Port Graham	1 arcsecond	Yes	379
Port Lions	1/3 arcsecond	Yes	379
Port Protection	1 arcsecond	No	441
Saint George	1/3 arcsecond	Yes	210
Saint Paul	1/3 arcsecond	Yes	210
Sand Point	1/3 arcsecond	Yes	169
Seldovia	1 arcsecond	Yes	379
Seward	1 arcsecond	Yes	594
Shemya	1/3 arcsecond	No	295
Sitka	1 arcsecond	Yes	379
Skagway	1 arcsecond	Yes	441
Tatitlek	1 arcsecond	Yes	594
Unalaska	1 arcsecond	Yes	210
Valdez	1 arcsecond	Yes	441
Whittier	1 arcsecond	Yes	441
Yakutat	1/3 arcsecond	Yes	441

E.2 PACIFIC TERRITORIES

DEM data for American Samoa, Guam, and the Commonwealth of the Northern Mariana Islands were downloaded from the NOAA NCEI Continuously Updated Digital Elevation Model (CUDEM) – 1/9 Arc-Second Resolution Bathymetric-Topographic Tiles dataset (NOAA, 2024). The datasets from Guam and the Commonwealth of the Northern Mariana Islands used the NAD83 (MA11) datum and the UTM zone 55N projection, while the dataset for American Samoa used the NAD83 (HARN) datum and the UTM zone 2S projection.

To match the resolution of the runup grids, the grid datasets were resampled to 1/3rd arcsecond through bilinear interpolation. Each grid was masked using a 1 km buffer around the Hazus state boundaries feature class and mosaiced accordingly for each territory using the 32-bit depth setting.

F. Supplemental Studies Conducted

F.1 HAZUS LEVEL 1, LEVEL 2, AND LEVEL 3 COMPARISON ANALYSIS

This report examined the comparative analysis of Levels 1, 2 and 3 of tsunami hazard data for Crescent City, focusing on their methodologies, results, and implications for hazard assessment and planning. This comparison was essential for understanding the nuances of each analysis level and their applicability to hazard mitigation and response planning.

Methodologies

The California probabilistic data products are available for run-up amplitude, flow depth, velocity, and momentum flux (Thio, 2019), providing a unique opportunity to compare estimated loss across different levels of analysis within Hazus.

Level 1 Analysis

This analysis utilized the run-up amplitude and DEM, employing an empirical equation based on the ASCE-16 energy grade line equation. This equation, as described in Section 2, uses the maximum runup and DEM data to generate a velocity grid. The Hazus Technical Manual includes several comparisons between this empirical method and the velocities derived from the Short-term Inundation Forecasting for Tsunamis (SIFT) numerical model, showing good overall agreement. However, the empirical method does not accurately capture areas of high velocity that arise due to constrictions where flow depths are shallow, therefore, Level 1 is considered the least accurate of the analysis levels. The inputs for Level 1 analysis consisted of the CGS maximum amplitude grid and the CGS topography grid.

Level 2 Analysis

In the Level 2 Analysis, Hazus utilized the maximum velocity and flow depths provided by the CGS, ensuring that the velocity estimations were based on a detailed numerical modeling approach. However, this approach assumes that the maximum velocity and flow depth occur simultaneously and at the same location, which may not always be true. As a result, this assumption may lead to an estimation of losses that might exceed those predicted by the more comprehensive Level 3 approach. Despite this, the Level 2 method is designed to accommodate various formats and units, converting all end products to median flux and flow depths in feet. This standardization ensures that the outputs are compatible with the building fragility functions incorporated into the model.

Level 3 Analysis

In the Level 3 Analysis, Hazus assumes the user provides the data in the final format needed for Hazus loss estimation. This is median flux in cubic feet per second squared and median flow depth in feet. For this level of analysis, the CGS data were converted from maximums to medians, median flux values were converted from cubic meters per second to cubic feet per second, and median flow depth was converted from meters to feet. The data were adjusted to represent median values by

using the ‘Times’ tool in ArcGIS Pro, with a factor of approximately 0.6667 applied to all maximum momentum flux and maximum flow depth grids. The conversion for unit compatibility was executed using the ‘Times’ tool with specific factors of 35.3147 for momentum flux and 3.28084 for flow depth. This is considered the most accurate analysis from a hazard input data perspective and Hazus does not complete post processing of the input data.

Results

The analysis of return periods for Crescent City, California using Levels 1, 2, and 3 methodologies revealed varied implications for hazard assessment (Table F-1). The Level 1 approach, while robust, may underestimate high velocity zones where water depths are shallow. If buildings are exposed to those conditions, their damage may be underestimated. Level 2’s assumption that the max depth and velocity occur at the same time might overestimate losses. Level 3 provides the most accurate analysis for hazard input data and is based directly on the output of the numerical tsunami hazard model with the understanding that these models meet the NTHMP Mapping and Modeling Subcommittee (MMS) established benchmarking criteria (NTHMP, 2012).

This page intentionally left blank.

Table F-1: Average Annualized Loss (AAL) Comparison of Hazus Level 1, Level 2, and Level 3

AAL - Return Period - LEVEL 1	Annualized Probability	Differential Probability	Scenario Losses ($)	Average Loss Formula	Average Losses ($)	Average Annualized Losses ($)
3,000	0.00033333	0.00033333	$3,169,464,000	L3,000	$3,169,464,000	$1,056,488
2,475	0.00040404	0.00007071	$2,615,530,000	(L3,000+L2475)/2	$2,892,497,000	$204,520
975	0.00102564	0.00062160	$890,764,000	(L2,475+L975)/2	$1,753,147,000	$1,089,757
475	0.00210526	0.00107962	$435,318,000	(L975+L475)/2	$663,041,000	$715,834
200	0.00500000	0.00289474	$106,599,000	(L475+L200)/2	$270,958,500	$784,354
100	0.01000000	0.00500000	$14,290,000	(L200+L100)/2	$ 60,444,500	$302,223
					Total	**$4,153,175**
AAL - Return Period - LEVEL 2	**Annualized Probability**	**Differential Probability**	**Scenario Losses ($)**	**Average Loss Formula**	**Average Losses ($)**	**Average Annualized Losses ($)**
3,000	0.00033333	0.00033333	$4,934,015,000	L3,000	$4,934,015,000	$1,644,672
2,475	0.00040404	0.00007071	$3,541,090,000	(L3,000+L2,475)/2	$4,237,552,500	$299,625
975	0.00102564	0.00062160	$1,064,128,000	(L2,475+L975)/2	$2,302,609,000	$1,431,303
475	0.00210526	0.00107962	$343,624,000	(L975+L475)/2	$703,876,000	$759,920
200	0.00500000	0.00289474	$82,240,000	(L475+L200)/2	$212,932,000	$616,382
100	0.01000000	0.00500000	$7,013,000	(L200+L100)/2	$44,626,500	$223,133
					Total	**$4,975,034**
AAL - Return Period - LEVEL 3	**Annualized Probability**	**Differential Probability**	**Scenario Losses ($)**	**Average Loss Formula**	**Average Losses ($)**	**Average Annualized Losses ($)**
3,000	0.00033333	0.00033333	$4,609,796,000	L3,000	$ 4,609,796,000	$1,536,599
2,475	0.00040404	0.00007071	$3,020,690,000	(L3,000+L2,475)/2	$ 815,243,000	$269,765
975	0.00102564	0.00062160	$960,237,000	(L2,475+L975)/2	$ 1,990,463,500	$1,237,273
475	0.00210526	0.00107962	$268,420,000	(L975+L475)/2	$ 614,328,500	$ 663,243
200	0.00500000	0.00289474	$76,670,000	(L475+L200)/2	$ 172,545,000	$ 499,472
100	0.01000000	0.00500000	$6,947,000	(L200+L100)/2	$ 41,808,500	$ 209,043
					Total	**$4,415,394**

This page intentionally left blank.

Implications

- All levels of analysis produce reasonable results with Level 1 ~6% lower than Level 3 and Level 2 ~12% higher than Level 3.
- Level 1 is suited for rapid assessments but may require caution in areas known for high velocity flows with shallow depths.
- Level 2 might be preferable when a more cautious hazard assessment is needed, due to the potential for overestimation.
- Level 3 offers the greatest accuracy, recommended for detailed risk assessment, planning and mitigation strategies.

Following this pre-study analysis and the Tsunami Hazus Levels 1, 2, and 3 Comparison Analysis, it was determined that a Level 3 analysis may be the most appropriate approach when available; however, it increases confidence that other levels of analysis provide reasonable results and better understanding of the differences.

F.2 EVALUATION OF RETURN PERIOD SENSITIVITY

As outlined in Appendix D, providing a complete suite of return period losses improves the estimation of average annualized loss. This sensitivity analysis documents the methods, results, and implications of selecting various return period grids for accurately measuring average annualized loss based on probabilistic tsunami hazard data. The goal was to utilize California's high-quality multi-return period analysis, consisting of a suite of seven return periods, to determine the optimal number and range of return periods for regions with more limited data. This analysis evaluated the differences in average annualized loss when using two versus seven return periods and the impact of varying the spacing between return periods, helping to identify potential gaps in understanding total risk in data-scarce areas.

Methodologies

The CGS provided data for Probabilistic Tsunami Hazard Analysis for seven return periods (72, 100, 200, 475, 975, 2,475 and 3,000-years) (Thio, 2017). The CGS initially considered the 975- and 2,475-year return periods to be the most accurate from a modeling perspective given that these periods best represent the Cascadia Subduction Zone, which is crucial for tsunami modeling.

For this pre-study analysis, average annualized losses were estimated for all return periods for Crescent City, California, and compared with average annualized losses derived from using only the 975- and 2,475-year return periods, as well as other selected scenarios. This analysis was built on the results of the Tsunami Levels 1, 2, and 3 Comparison Analysis and incorporated manual average annualized loss estimations, as the Hazus tsunami model does not directly support average annualized loss estimation. The methodology used the Riemann sums midpoint method, commonly used in Hazus earthquake, flood, and hurricane models (Appendix D).

Evaluation

The average annualized loss for Crescent City were compared using the Hazus average annualized loss method for several scenarios. These were selected to demonstrate the relative percentage differences when using fewer scenarios and modifying the return period range. The selected scenarios were also intended to identify potential gaps in other tsunami-prone states based on their available return period data, including:

- Hawaii: 400, 1,500 and 3,500
- Oregon: 1,000, 2,000, 3,333, 5,000, and 10,000
- Washington: 800, 2,500, and 16,000

Table F-2 below summarizes the Level 3 results for Crescent City and the average annualized loss estimated for each return period scenario.

This page intentionally left blank.

Table F-2: Crescent City Average Annualized Loss (AAL) Estimation

AAL - Return Period - LEVEL 3	Annualized Probability	Differential Probability	Scenario Losses ($)	Average Loss Formula	Average Losses ($)	Average Annualized Losses ($)
3,000	0.00033333	0.00033333	$4,609,796,000	L3,000	$4,609,796,000	$1,536,599
2,475	0.00040404	0.00007071	$3,020,690,000	(L3,000+L2,475)/2	$3,815,243,000	$269,765
975	0.00102564	0.00062160	$960,237,000	(L2,475+L975)/2	$1,990,463,500	$1,237,273
475	0.00210526	0.00107962	$268,420,000	(L975+L475)/2	$614,328,500	$663,243
200	0.00500000	0.00289474	$76,670,000	(L475+L200)/2	$172,545,000	$499,472
100	0.01000000	0.00500000	$6,947,000	(L200+L100)/2	$41,808,500	$209,043
					Total	**$4,415,394**
100-, 200-, 475-, 975-, 2,475- and 3,000-years						
AAL - Return Period - LEVEL 3	**Annualized Probability**	**Differential Probability**	**Scenario Losses ($)**	**Average Loss Formula**	**Average Losses ($)**	**Average Annualized Losses ($)**
2,475	0.00040404	0.00040404	$3,020,690,000	L2,475	$3,020,690,000	$1,220,481
475	0.00210526	0.00170122	$268,420,000	(L2,475+L475)/2	$1,644,555,000	$2,797,754
					Total	**$4,018,235**
LEVEL 3: No 3,000 to emphasize 2,475						
2,475	0.00040404	0.00040404	$3,020,690,000	L2,475	$3,020,690,000	$1,220,481
975	0.00102564	0.00062160	$960,237,000	(L2475+L975)/2	$1,990,463,500	$1,237,273
475	0.00210526	0.00107962	$268,420,000	(L975+L475)/2	$614,328,500	$663,243
200	0.00500000	0.00289474	$76,670,000	(L475+L200)/2	$172,545,000	$499,472
100	0.01000000	0.00500000	$6,947,000	(L200+L100)/2	$41,808,500	$209,043
					Total	**$3,829,512**
100-, 200-, 475-, 975-, 2.475- and 3.000-years						
2,475	0.00040404	0.00040404	$3,020,690,000	L2,475	$3,020,690,000	$1,220,481
975	0.00102564	0.00062160	$960,237,000	(L2,475+L975)/2	$1,990,463,500	$1,237,273
					Total	**$2,457,754**

AAL - Return Period - LEVEL 3	Annualized Probability	Differential Probability	Scenario Losses ($)	Average Loss Formula	Average Losses ($)	Average Annualized Losses ($)
2,475	0.00040404	0.00040404	$3,020,690,000	L2,475	$3,020,690,000	$1,220,481
100	0.01000000	0.00959596	$6,947,000	(L2,475+L475)/2	$1,513,818,500	$14,526,541
					Total	**$15,747,022**
LEVEL 3: with 72-year						
3,000	0.00033333	0.00033333	$4,609,796,000	L3,000	$4,609,796,000	$1,536,599
2,475	0.00040404	0.00007071	$3,020,690,000	(L3,000+L2,475)/2	$ 815,243,000	$269,765
975	0.00102564	0.00062160	$960,237,000	(L2,475+L975)/2	$1,990,463,500	$1,237,273
475	0.00210526	0.00107962	$268,420,000	(L975+L475)/2	$ 614,328,500	$663,243
200	0.00500000	0.00289474	$76,670,000	(L475+L200)/2	$ 172,545,000	$499,472
100	0.01000000	0.00500000	$6,947,000	(L200+L100)/2	$ 41,808,500	$209,043
72	0.01388889	0.00388889	$824,000	(L100+L072)/2	$ 3,885,500	$15,110
					Total	**$4,430,504**
72-, 100-, 200-, 475-, 975-, 2,475- and 3,000-years						

The Average Annualized Loss results of each scenario combination above, are compared to the Average Annualized Loss using the entire suite in Table F-2.

This page intentionally left blank.

Table F-3: Average Annualized Loss (AAL) Relative to All Return Periods

Return Period Scenarios	Total AAL Economic Loss	% Relative to All Return Periods
100 through 3,000 (exclude 72)	$4,415,394	-0.34%
475 and 2,475 only	$4,018,235	-9.31%
Exclude 3,000 to emphasize 2,475	$3,829,512	-13.56%
975 and 2,475 only	$2,457,754	-44.53%
100 and 2,475 only	$15,747,022	255.42%
All Return Periods (7)	**$4,430,504**	**0.00%**

The results summarized in Table F-3 indicate that excluding the 72-year return period did not significantly affect the average annualized loss results. Furthermore, excluding the 72-year return period underscored the importance of selecting return periods that were neither too closely spaced nor too frequent (e.g., 100- or 72-year events) to avoid skewing the results. Specifically:

- **475- and 2,475-year events:** Provided average annualized losses within 10% of the complete suite of scenarios.
- **975- and 2,475-year events:** Significantly underrepresented the average annualized loss.
- **100- and 2,475-year events:** Significantly overrepresented the average annualized loss.

Based on the findings from Crescent City, California, the following conclusions were drawn for other states:

- Hawaii's available return periods would align well with the optimal distribution within 10% of the complete set despite limited data (e.g., 475- and 2,475-year events).
- Oregon lacks a shorter return interval because the 1,000-year event is the shortest; however, the availability of 5 return periods with a 9,000-year range can help mitigate the potential gap.
- Washington has a slightly shorter return period interval with the 800-year event versus the 975-year event, which is considered too long. However, because the 800-year event is relatively distant from the more optimal 475-year event, and the 800-year event data in Washington is not available for some of its highest-risk communities, The accuracy of Washington's average annualized losses may improve from both more return periods and higher-frequency scenarios.

F.3 DATA EXPOSURE ANALYSIS

Exposure analyses were conducted for all states and territories, and most were found to have complete hazard coverage for their entire coastlines. However, potential gaps in tsunami hazard data were observed in suspected areas of building exposure to inundation in Alaska, California,

Guam, Puerto Rico, and Washington. To identify potentially inundated structures, a 1-kilometer buffer was applied to the coastlines of the states and territories. Bounding polygons were generated from the hazard data from the sources summarized in Table 1-1, Section 1, and the extents of these polygons were removed from the analysis by erasing them from the 1-kilometer coastline buffer polygon. For points falling within the resultant polygon, the best available DEM data were used to extract elevation values to the building points. For the purposes of this sensitivity analysis, any selected building points with an elevation below 10 meters were classified as possibly exposed to tsunami hazards, with consideration given to points with an elevation below 5 meters. These elevation thresholds were intended to capture low-lying points near the coast that may be exposed to tsunamis because detailed tsunami modeling does not exist for these areas. Actual tsunami risk and tsunami modeling results may differ from the estimates provided in this section. It was assumed that points located inland from the hazard data were not exposed, regardless of the hazard data format, distance from the coastline, or elevation because coastal modeling exists for those areas. As a result, no gaps were identified in Oregon, Hawaii, American Samoa, the Commonwealth of the Northern Mariana Islands, or United States Virgin Islands.

F.3.1 ALASKA

A total of 6,050 structures in Alaska have been identified as lacking hazard data and may be exposed to tsunami hazards (Figure F-1 and Table F-4). Although the Nome Borough accounts for just under $2 billion in potential exposure—approximately 1/4 of the total possible exposure gap for Alaska, it is relatively distant from the Alaska-Aleutian Subduction Zone and likely lower risk. The high number of potentially threatened points in Alaska is attributable to the State's large geographic area, extensive coastline, and sparse population density, which may present challenges in terms of making the required investments in modeling the tsunami hazard.

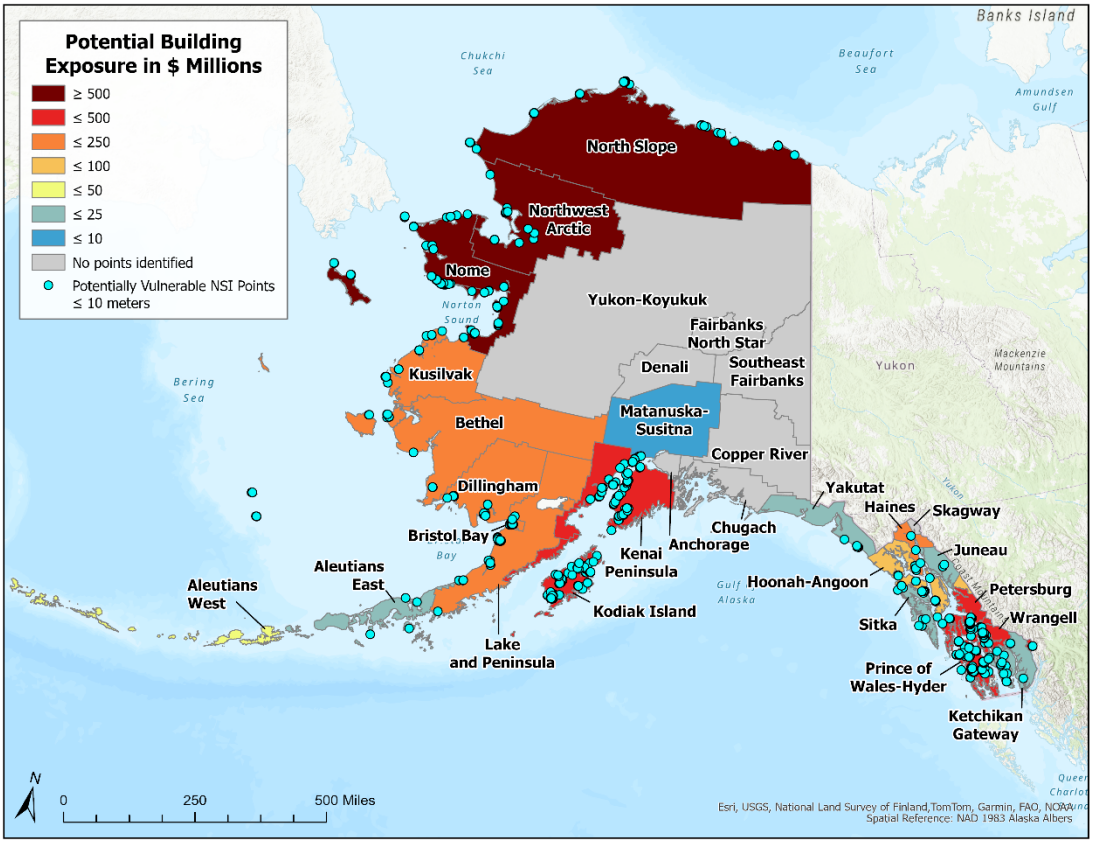

Figure F-1: Alaska National Structure Inventory Points without Tsunami Hazard Data Coverage

Table F-4: Alaska Potential Building Exposure for National Structure Inventory (NSI) Points Lacking Tsunami Hazard Coverage

Borough	Number of Structures < 5 meters	Potential Building Exposure < 5 meters	Number of Structures < 10 meters	Potential Building Exposure < 10 meters
Aleutians East	4	$5,222,429	11	$12,225,073
Aleutians West	27	$10,507,865	34	$27,413,543
Bethel	46	$19,291,696	134	$122,393,928
Bristol Bay	2	$42,241,625	74	$176,041,205
Dillingham	124	$97,092,455	221	$185,663,348
Haines	4	$9,534,018	64	$131,268,122
Hoonah-Angoon	37	$24,202,521	95	$60,373,184
Juneau	0	$0	3	$23,809,433
Kenai Peninsula	15	$13,288,385	187	$341,893,802
Ketchikan Gateway	2	$1,289,718	13	$11,957,886
Kodiak Island	52	$195,000,840	145	$489,078,486
Kusilvak	106	$58,466,605	229	$126,319,614
Lake and Peninsula	13	$34,870,167	114	$132,811,428

Borough	Number of Structures < 5 meters	Potential Building Exposure < 5 meters	Number of Structures < 10 meters	Potential Building Exposure < 10 meters
Matanuska-Susitna	5	$5,143,913	11	$6,108,149
Nome	628	$484,576,027	2,030	$1,868,662,831
North Slope*	163	$354,312,211	971	$1,539,083,740
Northwest Arctic*	767	$1,102,237,779	793	$1,127,519,651
Petersburg	7	$4,415,777	254	$263,362,083
Prince of Wales-Hyder	62	$60,075,702	338	$306,491,520
Sitka	0	$0	8	$20,833,252
Wrangell	26	$18,463,301	303	$334,948,149
Yakutat	2	$568,564	18	$12,709,165
Total	**2,092**	**$2,540,801,597**	**6,050**	**$7,320,967,593**

*Note: The coastal exposure in the North Slope and Northwest Arctic boroughs are removed from the gap analysis because the tsunami threat is minimal (refer to Section 2).

F.3.2 CALIFORNIA

A total of 1,696 structures in California have been identified as lacking hazard data and are potentially exposed to tsunami hazards. Of these, 650 structures are located in communities without tsunami hazard modeling such as Avalon on Catalina Island, while the remaining 1,046 are in areas with small gaps between the extents of tsunami hazard models in densely populated regions. Notably, a gap between models in San Mateo County accounts for over $1 billion in potential exposure—nearly half of the total exposure for structures in California without hazard data coverage. Refer to Figure F-2 for the locations of potentially exposed structures. Table F-4 provides a detailed breakdown of the number of these structures and their associated building values by county.

Figure F-2: California National Structure Inventory Points without Tsunami Hazard Data Coverage

Table F-5: California Potential Building Exposure for National Structure Inventory (NSI) Points Lacking Tsunami Hazard Coverage

County	Number of Structures < 5 meters	Potential Building Exposure < 5 meters	Number of Structures < 10 meters	Potential Building Exposure < 10 meters
Contra Costa	**0**	**$ 0**	**3**	**$ 52,680,629**
Gap in modeling extent	0	$ 0	3	$ 52,680,629
Humboldt	**0**	**$ 0**	**2**	**$ 560,187**
No tsunami hazard data	0	$ 0	2	$ 560,187
Los Angeles	**234**	**$ 233,106,758**	**646**	**$ 604,970,343**
Gap in modeling extent	66	$ 49,457,535	132	$ 118,086,620
No tsunami hazard data	168	$ 183,649,223	514	$ 486,883,723
Mendocino	**5**	**$ 20,449,779**	**10**	**$ 32,544,760**
No tsunami hazard data	5	$ 20,449,779	10	$ 32,544,760
Monterey	**40**	**$ 66,711,534**	**141**	**$ 124,873,896**
Gap in modeling extent	40	$ 66,711,534	139	$ 124,241,148
No tsunami hazard data	0	$ 0	2	$ 632,748
Orange	**3**	**$ 2,277,557**	**48**	**$ 142,980,007**
Gap in modeling extent	2	$ 1,316,485	47	$ 142,018,934
No tsunami hazard data	1	$ 961,073	1	$ 961,073
San Diego	**6**	**$ 3,707,969**	**70**	**$ 111,857,656**
Gap in modeling extent	0	$ 0	7	$ 5,863,819
No tsunami hazard data	6	$ 3,707,969	63	$ 105,993,837
San Luis Obispo	**1**	**$ 154,099**	**4**	**$ 3,035,243**
No tsunami hazard data	1	$ 154,099	4	$ 3,035,243
San Mateo	**649**	**$ 872,760,924**	**712**	**$ 1,015,777,565**
Gap in modeling extent	649	$ 872,760,924	712	$ 1,015,777,565
Santa Barbara	**7**	**$ 3,428,859**	**17**	**$ 21,917,709**
No tsunami hazard data	7	$ 3,428,859	17	$ 21,917,709
Santa Cruz	**0**	**$ 0**	**14**	**$ 29,553,761**
No tsunami hazard data	0	$ 0	14	$ 29,553,761
Sonoma	**2**	**$ 615,163**	**20**	**$ 6,868,043**
No tsunami hazard data	2	$ 615,163	20	$ 6,868,043
Ventura	**7**	**$ 5,817,574**	**9**	**$ 8,396,427**
Gap in modeling extent	6	$ 4,436,117	6	$ 4,436,117
No tsunami hazard data	1	$ 1,381,457	3	$ 3,960,309
Total	**954**	**$ 1,209,030,217**	**1,696**	**$ 2,156,016,224**

F.3.3 GUAM

A total of 500 structures in Guam have been identified as lacking hazard data and potentially exposed to tsunami hazards (Figure F-3 and Table F-6). During hazard data pre-processing, a small gap between the PMEL and University of Hawai‘i models along the southern coast was identified,

which results in 456 structures without tsunami hazard data coverage. The remaining 44 structures are located along the northern coast of Guam.

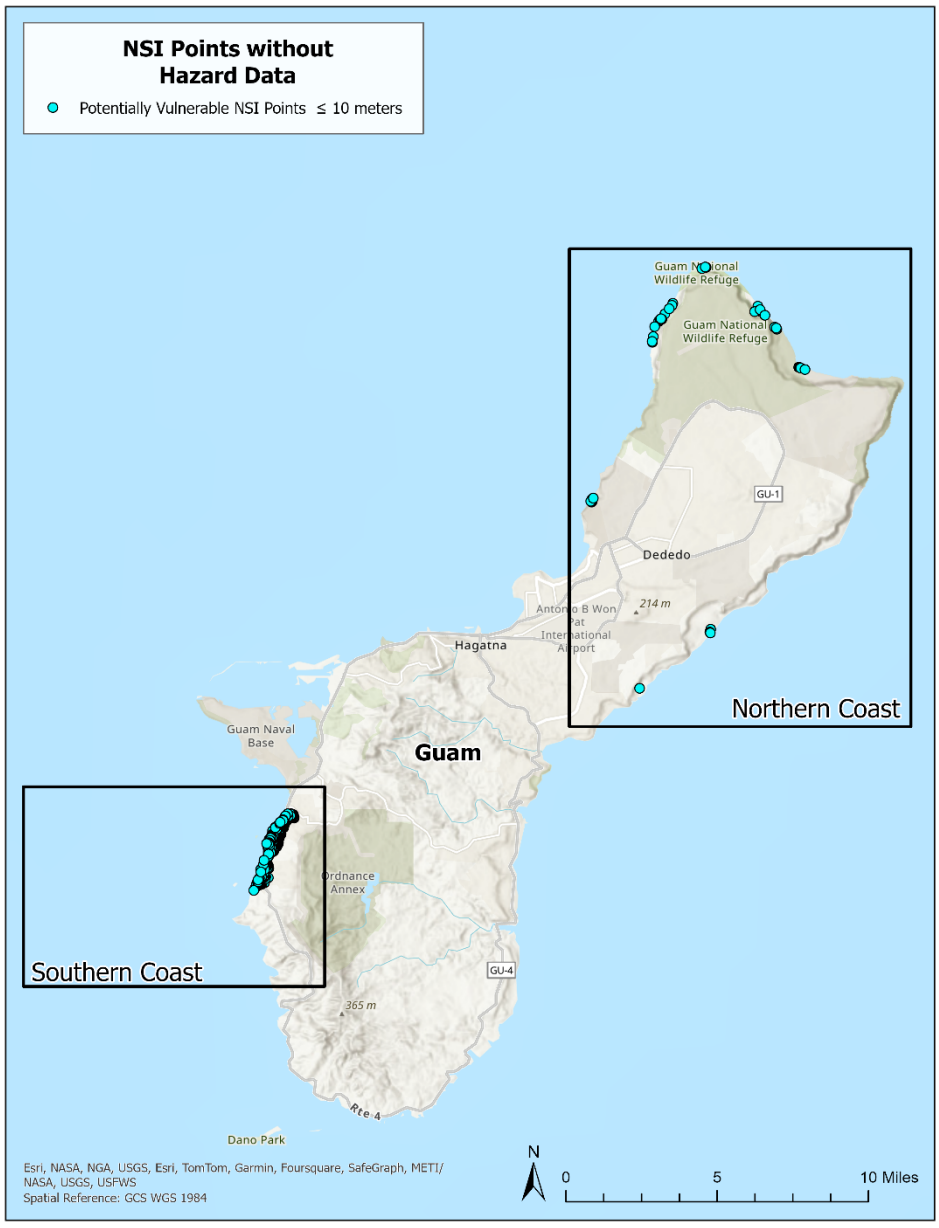

Figure F-3: Guam National Structure Inventory Points without Tsunami Hazard Data Coverage

Table F-6: Guam Potential Building Exposure for National Structure Inventory (NSI) Points Lacking Tsunami Hazard Coverage

Territory	Number of Structures < 5 meters	Potential Building Exposure < 5 meters	Number of Structures < 10 meters	Potential Building Exposure < 10 meters
Northern coast	7	$ 2,766,774	44	$ 44,169,283
Southern coast	301	$ 216,922,092	456	$ 340,668,261
Total	**308**	**$ 219,688,867**	**500**	**$ 384,837,544**

F.3.4 PUERTO RICO

A total of 39 structures in Puerto Rico have been identified as lacking hazard data and potentially exposed to tsunami hazards. The structures are located in the Municipio de Vega Alta and are a result of a small gap in tsunami hazard data coverage as shown in Figure F-4 and Table F-7.

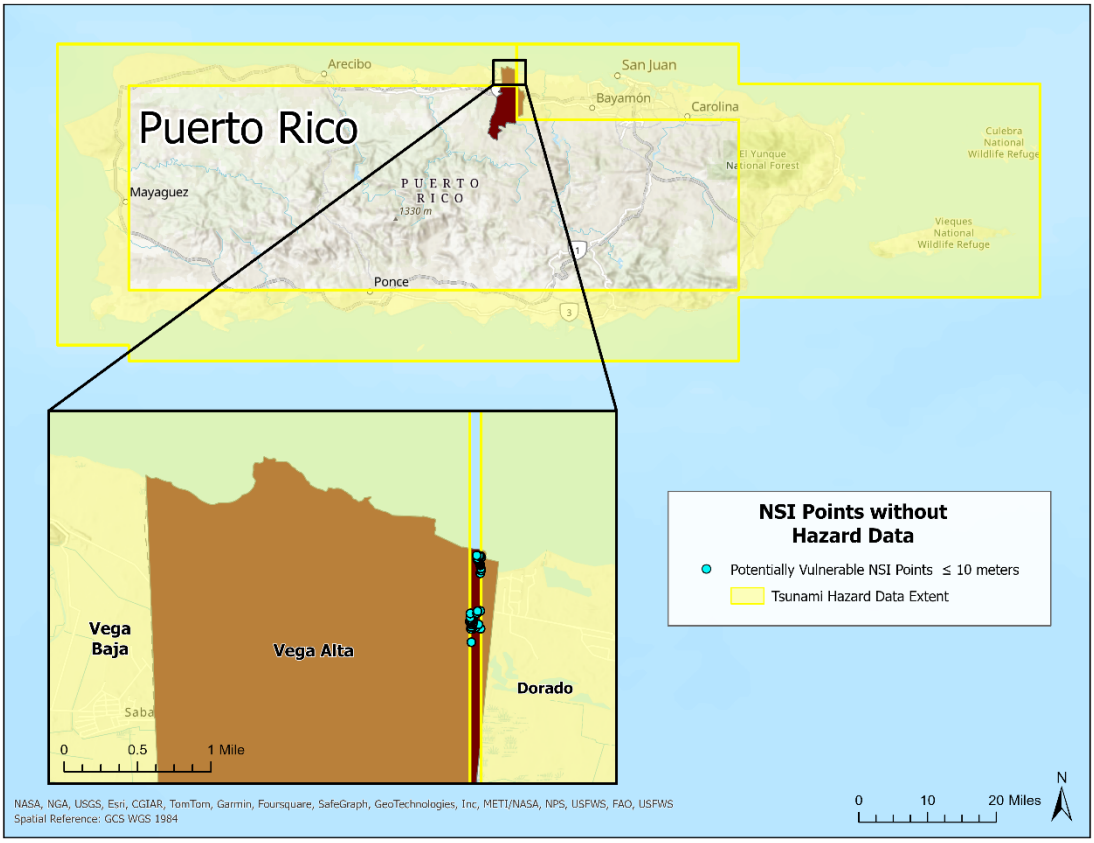

Figure F-4: Puerto Rico National Structure Inventory Points without Tsunami Hazard Data Coverage

Table F-7: Puerto Rico Potential Building Exposure for National Structure Inventory (NSI) Points Lacking Tsunami Hazard Coverage

Municipio	Number of Structures < 5 meters	Potential Building Exposure < 5 meters	Number of Structures < 10 meters	Potential Building Exposure < 10 meters
Vega Alta	7	$ 3,687,771	39	$ 16,775,636

F.3.5 WASHINGTON

A total of 928 structures in Washington have been identified as lacking complete hazard data and potentially exposed to tsunami hazards (Figure F-5 and Table F-8). While these structures are covered by the 2,500- and 16,000-year return period models, the 800-year return period model does not fully capture the extent of Grays Harbor and Pacific Counties. Grays Harbor County accounts for nearly $300 million in potential exposure—approximately half of the total possible exposure for structures in Washington without 800-year return period data.

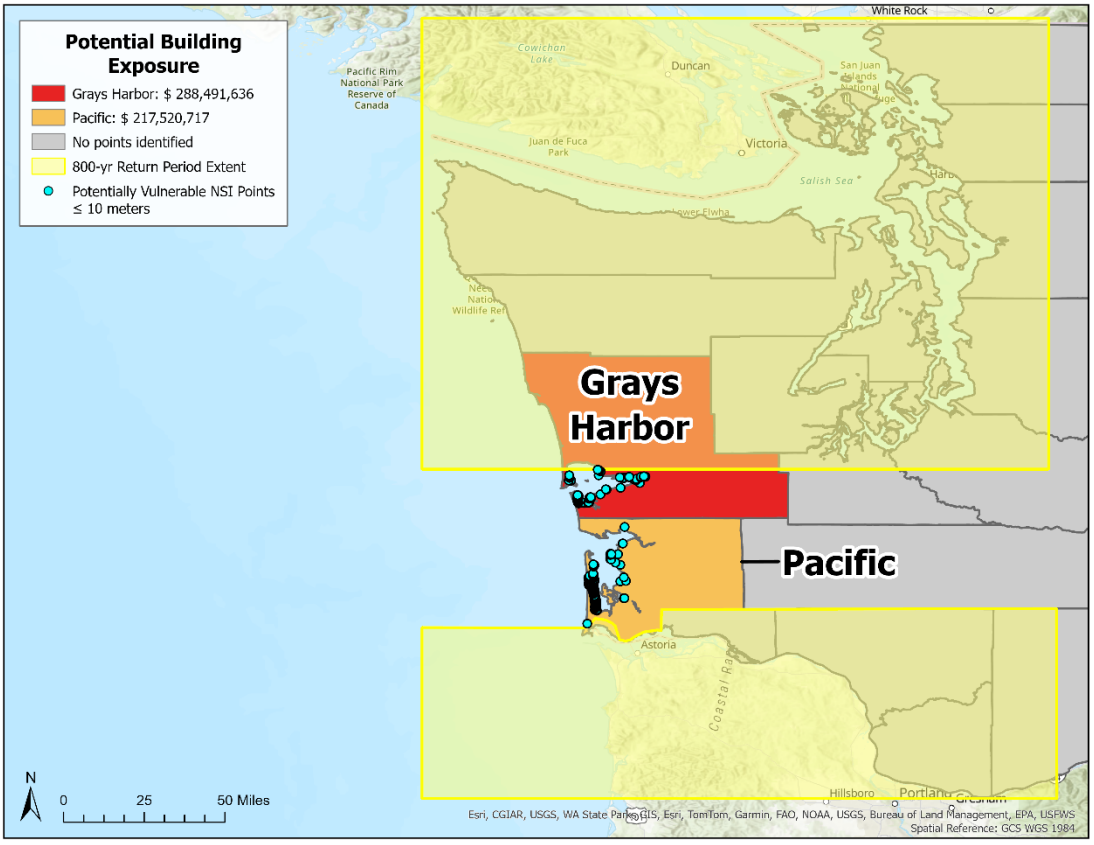

Figure F-5: Washington National Structure Inventory Points without Tsunami Hazard Data Coverage – 800-yr Return Period

Table F-8: Washington Potential Building Exposure for National Structure Inventory (NSI) Points Lacking Tsunami Hazard Coverage – 800-yr Return Period

County	Number of Structures < 5 meters	Potential Building Exposure < 5 meters	Number of Structures < 10 meters	Potential Building Exposure < 10 meters
Grays Harbor	28	$ 33,641,742	261	$ 288,491,636
Pacific	39	$ 13,358,601	667	$ 217,520,717
Total	**67**	**$ 47,000,343**	**928**	**$ 506,012,353**

G. Caribbean Territory Source Return Period Estimation

Return periods for Caribbean tsunami sources for both Puerto Rico and United States Virgin Islands are estimated using the GEM Caribbean and Central America model documentation of the source zones (Figure G-1) and Gutenberg-Richter distribution a and b values (Table G-1) from Garcia-Pelaez et al. (2019).

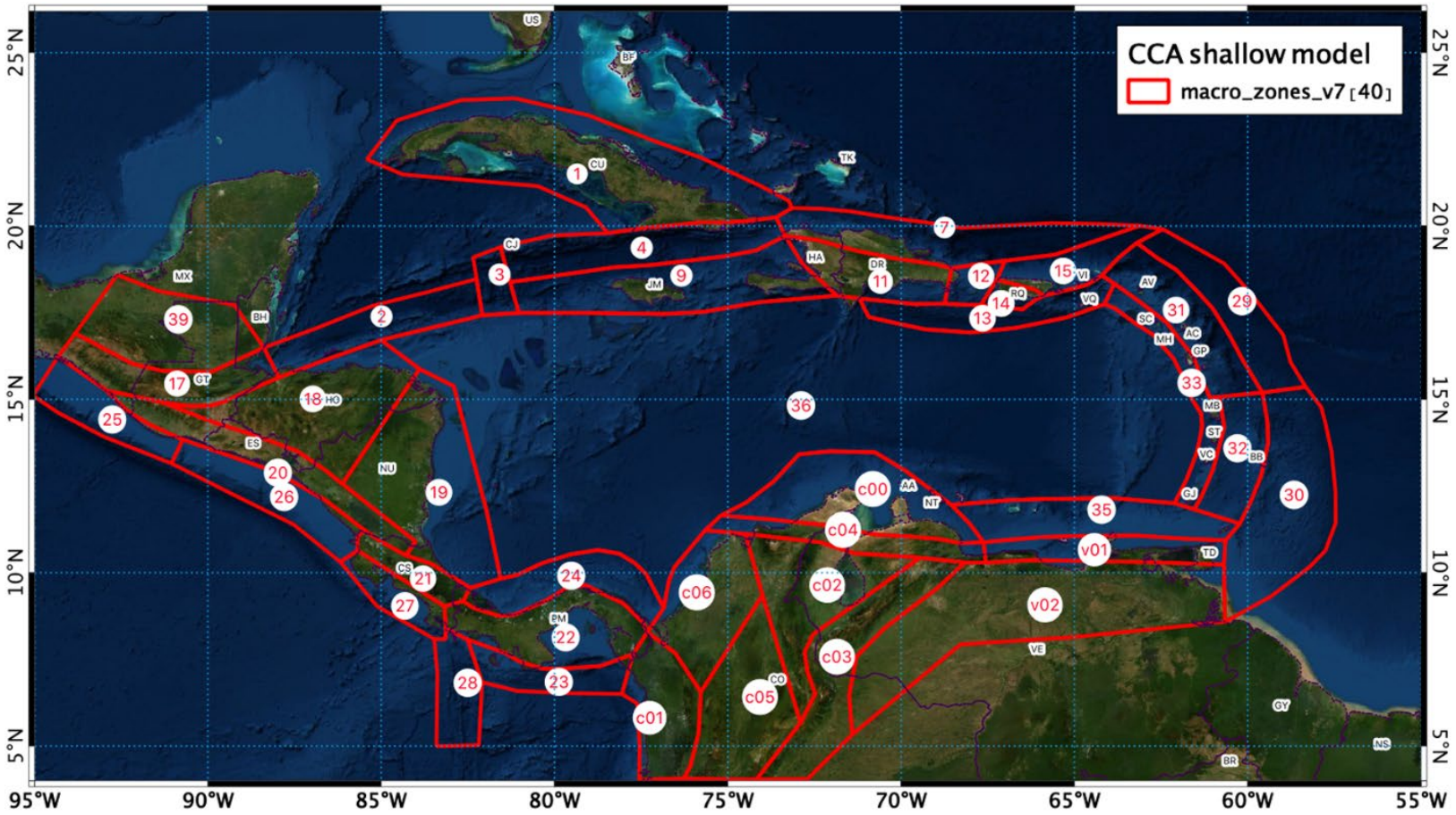

Figure G-1: Shallow source macro-zonation for the Central America and the Caribbean region (based on Figure 6, Garcia-Palaez et al., 2019).

Table G-1: Caribbean Scenarios with GEM Model Parameters and Estimated Recurrence

Scenario	Area	GEM Source Zone Name and Number (Figure G-1)	GEM a	GEM b	GEM Max M_w	Tsunami Scenario M_w	Estimated Rate (N) based on Scenario M_w	Recurrence (years)
ID_2_19N	Puerto Rico	Puerto Rico northern zone, #15	3.2456	0.792	6.57	7.6	0.0016842	594
ID_5_19N	Puerto Rico	Puerto Rico northern zone, #15	3.2456	0.792	6.57	7.6	0.0016842	594
ID_6_19N	Puerto Rico	Puerto Rico northern zone, #15	3.2456	0.792	6.57	7.6	0.0016842	594
ID_9_19N	Puerto Rico	Puerto Rico northern zone, #15	3.2456	0.792	6.57	7.6	0.0016842	594
ID_11_19N	Puerto Rico	Puerto Rico northern zone, #15	3.2456	0.792	6.57	7.6	0.0016842	594
ID_17_Anegada_Passage	Puerto Rico & United States Virgin Islands	Mona Rift Zone, #12	3.27162	0.828	6.4	7.4	0.0013945	717
ID_20_Anegada_Passage	Puerto Rico & United States Virgin Islands	Mona Rift Zone, #12	3.27162	0.828	6.4	7.4	0.0013945	717

Scenario	Area	GEM Source Zone Name and Number (Figure G-1)	GEM a	GEM b	GEM Max M_w	Tsunami Scenario M_w	Estimated Rate (N) based on Scenario M_w	Recurrence (years)
ID_4_FEMA	Puerto Rico	Puerto Rico northern zone, #15	3.2456	0.792	6.57	7.9	0.0009745	1,026
ID_8_Anegada_Passage	Puerto Rico & United States Virgin Islands	Mona Rift Zone, #12	3.27162	0.828	6.4	7.6	0.0009524	1,050
ID_15_Anegada_Passage	Puerto Rico & United States Virgin Islands	Mona Rift Zone, #12	3.27162	0.828	6.4	7.6	0.0009524	1,050
ID_21_Anegada_Passage	Puerto Rico & United States Virgin Islands	Mona Rift Zone, #12	3.27162	0.828	6.4	7.6	0.0009524	1,050
ID_25_Anegada_Passage	Puerto Rico & United States Virgin Islands	Mona Rift Zone, #12	3.27162	0.828	6.4	7.6	0.0009524	1,050
ID_16_Mona Channel	Puerto Rico	Mona Rift Zone, #12	3.27162	0.828	6.4	7.6	0.0009524	1,050

Scenario	Area	GEM Source Zone Name and Number (Figure G-1)	GEM a	GEM b	GEM Max M_w	Tsunami Scenario M_w	Estimated Rate (N) based on Scenario M_w	Recurrence (years)
ID_12_Mona Channel	Puerto Rico	Mona Rift Zone, #12	3.27162	0.828	6.4	7.6	0.0009524	1,050
ID_13_Mona Channel	Puerto Rico	Mona Rift Zone, #12	3.27162	0.828	6.4	7.6	0.0009524	1,050
ID_182_Mona Channel	Puerto Rico	Mona Rift Zone, #12	3.27162	0.828	6.4	7.6	0.0009524	1,050
ID_191_Mona Channel	Puerto Rico	Mona Rift Zone, #12	3.27162	0.828	6.4	7.6	0.0009524	1,050
ID_9_Septentrional	Puerto Rico	North Hispaniola deformed belt zone, #7	4.64272	0.985	7.7	7.8	0.0009114	1,097
ID_10_Septentrional	Puerto Rico	North Hispaniola deformed belt zone, #7	4.64272	0.985	7.7	7.8	0.0009114	1,097
ID_1_FEMA	Puerto Rico	Puerto Rico northern zone, #15	3.2456	0.792	6.57	8.0	0.0008121	1,231
ID_2_FEMA	Puerto Rico	Puerto Rico northern zone, #15	3.2456	0.792	6.57	8.0	0.0008121	1,231

Scenario	Area	GEM Source Zone Name and Number (Figure G-1)	GEM a	GEM b	GEM Max M_w	Tsunami Scenario M_w	Estimated Rate (N) based on Scenario M_w	Recurrence (years)
ID_14_Anegada_Passage	Puerto Rico & United States Virgin Islands	Mona Rift Zone, #12	3.27162	0.828	6.4	7.7	0.0007871	1,271
ID_1_Puerto Rico Trench	Puerto Rico	North Hispaniola deformed belt zone, #7	4.64272	0.985	7.7	8.0	0.0005791	1,727
ID_8_Puerto Rico Trench	Puerto Rico	North Hispaniola deformed belt zone, #7	4.64272	0.985	7.7	8.0	0.0005791	1,727
ID_11_Puerto Rico Trench	Puerto Rico	North Hispaniola deformed belt zone, #7	4.64272	0.985	7.7	8.0	0.0005791	1,727
ID_12_Puerto Rico Trench	Puerto Rico	North Hispaniola deformed belt zone, #7	4.64272	0.985	7.7	8.0	0.0005791	1,727
ID_16_Puerto Rico Trench	Puerto Rico	North Hispaniola deformed belt zone, #7	4.64272	0.985	7.7	8.0	0.0005791	1,727

Scenario	Area	GEM Source Zone Name and Number (Figure G-1)	GEM a	GEM b	GEM Max M_w	Tsunami Scenario M_w	Estimated Rate (N) based on Scenario M_w	Recurrence (years)
ID_17_Puerto Rico Trench	Puerto Rico	North Hispaniola deformed belt zone, #7	4.64272	0.985	7.7	8.0	0.0005791	1,727
ID_19_Puerto Rico Trench	Puerto Rico	North Hispaniola deformed belt zone, #7	4.64272	0.985	7.7	8.0	0.0005791	1,727
ID_5_Puerto Rico Trench	Puerto Rico	North Hispaniola deformed belt zone, #7	4.64272	0.985	7.7	8.0	0.0005791	1,727
ID_3_FEMA	Puerto Rico	Puerto Rico northern zone, #15	3.2456	0.792	6.57	8.2	0.0005639	1,773
Puerto Rico Trench (PRT2) - M_w 8.7	United States Virgin Islands	Puerto Rico northern zone, #15	3.2456	0.792	6.57	8.7	0.0002266	4,414
ID_10_Muertos Trough	Puerto Rico	Los Muertos trough zone (shallow seismicity), #13	4.37902	1.093	7.5	7.5	0.0001519	6,584

Scenario	Area	GEM Source Zone Name and Number (Figure G-1)	GEM a	GEM b	GEM Max M_w	Tsunami Scenario M_w	Estimated Rate (N) based on Scenario M_w	Recurrence (years)
ID_15_Muertos Trough	Puerto Rico	Los Muertos trough zone (shallow seismicity), #13	4.37902	1.093	7.5	7.5	0.0001519	6,584
ID_22_Muertos Trough	Puerto Rico	Los Muertos trough zone (shallow seismicity), #13	4.37902	1.093	7.5	7.5	0.0001519	6,584
Columbia/Venezuela Belt (FSCDB) - M_w 8.9	United States Virgin Islands	Guajira-Paraguana northern Colombia zone (Bonaire block), #c00	3.72478	0.86	6.35	8.9	0.0001177	8,496
Puerto Rico Trench (PRTG) - M_w 9.1	United States Virgin Islands	Puerto Rico northern zone, #15	3.2456	0.792	6.57	9.1	0.0001092	9,154
Virgin Islands Trough (1867) - M_w 7.8	United States Virgin Islands	Los Muertos trough zone (shallow seismicity), #13	4.37902	1.093	7.5	7.8	0.0000714	14,008

Scenario	Area	GEM Source Zone Name and Number (Figure G-1)	GEM a	GEM b	GEM Max M_w	Tsunami Scenario M_w	Estimated Rate (N) based on Scenario M_w	Recurrence (years)
Lesser Antilles Trench (LA2) - M_w 8.5	United States Virgin Islands	Northern Lesser Antilles volcanic arc zone, #31	5.39022	1.24	7.8	8.5	0.0000071	141,182
Lesser Antilles Trench (LA) - M_w 8.5	United States Virgin Islands	Northern Lesser Antilles volcanic arc zone, #31	5.39022	1.24	7.8	8.5	0.0000071	141,182

H. Evacuation Analysis Modeling Sources

Table H-1: Evacuation Modeling Sources by State/Territory

State or Territory	Tsunami Modeling Provider	Evacuation Modeling Source	Evacuation Modeling Citation
Alaska	University of Alaska Fairbanks	USGS Western Geographic Science Center (WGSC)	Wood and Peters (2025a)
American Samoa	University of Hawai‘i-Mānoa	USGS WGSC	Wood et al. (2019)
California	CGS	USGS WGSC	Wood et al. (2020); Peters et al. (2020)
Commonwealth of the Northern Mariana Islands	NOAA PMEL for Saipan; Robbie Greene for Rota and Tinian	USGS WGSC	Wood and Peters (2025b)
Guam	University of Hawai‘i-Mānoa	USGS WGSC	Wood et al. (2023); Peters et al. (2023)
Oregon	Oregon Department of Geology and Mineral Industries	DOGAMI	Allan and O'Brien (2023) Allan et al. (2020) O’Brien and Alllan (2025)
Puerto Rico	Puerto Rico Seismic Network	USGS WGSC	Peters and Wood (2025)
United States Virgin Islands	NOAA PMEL	USGS WGSC	Wood and Peters (2025c); Wood et al. (2025c)
Washington	WGS	WGS	Bauer (2022)

Table H-2: Evacuation Analysis Modeling Scenarios by State/Territory

State or Territory	Geography or Community	Scenario/PTHA Name	Source Name
Alaska	Adak, Alaska	Andreanof Islands_Mw88_S01 -- Scenario 1. Mw 8.8 earthquake in the Andreanof Islands region	Alaska-Aleutian Subduction Zone, Andreanof segment
Alaska	Anchor Point, Alaska	Mw 90_S03 -- Scenario 3. Mw 9.0 earthquake: maximum slip at 25–35 km (15–21 mi) depth	Alaska-Aleutian Subduction Zone, Kodiak segment
Alaska	Chignik, Alaska	Alaska Peninsula_Mw90_S05 -- Scenario 5: Mw 9.0 earthquake along the Alaska Peninsula, 13 km (8.1 mi) depth	Alaska-Aleutian Subduction Zone, Semidi segment
Alaska	Chiniak, Alaska	Kodiak Island_Mw93_S03bs -- Scenario 03-bs (#8): Inundation scenario files for Mw 9.3 earthquake in the area of Kodiak Island; 10-20 km depth with added splay fault in the backstop zone, dip angle 30 degrees	Alaska-Aleutian Subduction Zone, Kodiak segment
Alaska	Homer, Alaska	KI-KP region_mw93_S06 -- Scenario 6. Mw 9.3 earthquake in the KI-KP region: maximum slip at a depth of 15–35 km (9.3–21.7 mi) and uniform along-strike slip distribution	Alaska-Aleutian Subduction Zone, Kodiak segment
Alaska	Jakolof Bay, Alaska	Mw93_S06 -- Scenario 6. Mw 9.3 earthquake in the KI-KP region: maximum slip at a depth of 15–35 km (9.3–21.7 mi) and uniform along-strike slip distribution	Alaska-Aleutian Subduction Zone, Kodiak segment

State or Territory	Geography or Community	Scenario/PTHA Name	Source Name
Alaska	Kodiak, Alaska	Kodiak Island_Mw91_S06 -- Scenario 6: Mw 9.1 earthquake in the area of Kodiak Island, 15–25 km (9.3–15.5 mi) depth (Scenario 9 worst in southern areas)	Alaska-Aleutian Subduction Zone, Kodiak segment
Alaska	Nanwalek, Alaska	Mw 90_S03 -- Scenario 3. Mw 9.0 earthquake: maximum slip at 25–35 km (15–21 mi) depth	Alaska-Aleutian Subduction Zone, Kodiak segment
Alaska	Nikolski, Alaska	East Aleutian_Mw92_S07 -- Scenario 7. Mw 9.2 East Aleutian earthquake	Alaska-Aleutian Subduction Zone, Fox Islands segment
Alaska	Old Harbor, Alaska	Kodiak Island_Mw93_S03bs -- Scenario 03-bs (#8): Inundation scenario files for Mw 9.3 earthquake in the area of Kodiak Island; 10-20 km depth with added splay fault in the backstop zone, dip angle 30 degrees	Alaska-Aleutian Subduction Zone, Kodiak segment
Alaska	Ouzinkie, Alaska	Kodiak Island_Mw93_S06bs -- Scenario 6-bs: Mw 9.3 near Kodiak Island; 10 km (6.2 mi) depth, slip extending to the ocean bottom, with 30-degree dip	Alaska-Aleutian Subduction Zone, Kodiak segment
Alaska	Pasagshak Bay, Alaska	Kodiak Island_Mw93_S03 -- scenario-03: Inundation scenario files for Mw 9.3 earthquake in the area of Kodiak Island; 10-20 km depth	Alaska-Aleutian Subduction Zone, Kodiak segment

State or Territory	Geography or Community	Scenario/PTHA Name	Source Name
Alaska	Perryville, Alaska	Mw90_S03 -- Scenario 3 - Mw 9.0 earthquake: Maximum slip at 25–35 km (15.5–21.7 mi) depth	Alaska-Aleutian Subduction Zone, Shumagin segment
Alaska	Port Graham, Alaska	Mw 90_S03 -- Scenario 3. Mw 9.0 earthquake: maximum slip at 25–35 km (15–21 mi) depth	Alaska-Aleutian Subduction Zone, Kodiak segment
Alaska	Port Lions, Alaska	Kodiak Island_Mw93_S06bs -- Scenario 6-bs: Mw 9.3 near Kodiak Island; 10 km (6.2 mi) depth, slip extending to the ocean bottom, with 30-degree dip	Alaska-Aleutian Subduction Zone, Kodiak segment
Alaska	Seldovia Village, Alaska	Mw93_S06 -- Scenario 6. Mw 9.3 earthquake in the KI-KP region: maximum slip at a depth of 15–35 km (9.3–21.7 mi) and uniform along-strike slip distribution	Alaska-Aleutian Subduction Zone, Kodiak segment
Alaska	Seldovia, Alaska	Mw93_S06 -- Scenario 6. Mw 9.3 earthquake in the KI-KP region: maximum slip at a depth of 15–35 km (9.3–21.7 mi) and uniform along-strike slip distribution	Alaska-Aleutian Subduction Zone, Kodiak segment
Alaska	Seward, Alaska	Alaska_Aleutian_Mw90_S10 -- Scenario 10: Mw 9.0 earthquake with 50 m (164 ft) of maximum slip in the shallow part of the rupture	Alaska-Aleutian Subduction Zone, Prince William Sound segment

State or Territory	Geography or Community	Scenario/PTHA Name	Source Name
Alaska	Shemya, Alaska	Mw90_S02 -- Scenario 2. Mw 9.0 earthquake: Maximum slip at 15–25 km (9–15 mi) depth	Alaska-Aleutian Subduction Zone, Attu segment
Alaska	Valdez, Alaska	Gulf of Alaska_Mw88_S14 -- Scenario 14. Mw8.8 earthquake in the Gulf of Alaska region: 13-28 km (8.1-17.4 mi), variable slip along strike;	Alaska-Aleutian Subduction Zone, Prince William Sound segment
American Samoa	American Samoa	Mw 9.05 probable maximum tsunami, high tide and 25-year SLR	Tonga Trench Subduction Zone
American Samoa	American Samoa	2009 Mw 8.1	Tonga Trench Subduction Zone
California	California	Probabilistic Tsunami Hazard Analysis - ARP 975 year	Probabilistic
California	California	Probabilistic Tsunami Hazard Analysis - ARP 2,475 year	Probabilistic
Commonwealth of the Northern Mariana Islands	Saipan, Rota, Tinian	Local - Mw 9.0 Mariana Subduction Zone with 20m slip; Segment 54	Mariana Subduction Zone
Guam	Guam	Local preferred maximum (Mw 8.3 Mariana Subduction Zone)	Mariana Subduction Zone
Oregon	Oregon	Cascadia Subduction Zone: S	Cascadia Subduction Zone
Oregon	Oregon	Cascadia Subduction Zone: M	Cascadia Subduction Zone
Oregon	Oregon	Cascadia Subduction Zone: L	Cascadia Subduction Zone
Oregon	Oregon	Cascadia Subduction Zone: XL	Cascadia Subduction Zone

State or Territory	Geography or Community	Scenario/PTHA Name	Source Name
Oregon	Oregon	Cascadia Subduction Zone: XXL	Cascadia Subduction Zone
Puerto Rico	Puerto Rico	19N, Segment 2, Mw 7.6	Puerto Rico northern zone
Puerto Rico	Puerto Rico	Anegada Passage, Segment 15, Mw 7.6	Anegada Passage, Mona Rift Zone
Puerto Rico	Puerto Rico	Anegada Passage, Segment 21, Mw 7.6	Anegada Passage, Mona Rift Zone
Puerto Rico	Puerto Rico	Mona Channel, Segment 16, Mw 7.6	Mona Channel, Mona Rift Zone
Puerto Rico	Puerto Rico	Mona Channel, Segment 12, Mw 7.6	Mona Channel, Mona Rift Zone
Puerto Rico	Puerto Rico	Mona Channel, Segment 13, Mw 7.6	Mona Channel, Mona Rift Zone
Puerto Rico	Puerto Rico	Mona Channel, Segment 182, Mw 7.6	Mona Channel, Mona Rift Zone
Puerto Rico	Puerto Rico	Mona Channel, Segment 191, Mw 7.6	Mona Channel, Mona Rift Zone
Puerto Rico	Puerto Rico	Muertos Trough, Segment 15, Mw 7.5	Muertos Trough
Puerto Rico	Puerto Rico	Puerto Rico Trench, Segment 11, Mw 8.0	Puerto Rico Trench, North Hispaniola deformed belt zone
Puerto Rico	Puerto Rico	Puerto Rico Trench, Segment 12, Mw 8.0	Puerto Rico Trench, North Hispaniola deformed belt zone
Puerto Rico	Puerto Rico	Puerto Rico Trench, Segment 16, Mw 8.0	Puerto Rico Trench, North Hispaniola deformed belt zone

State or Territory	Geography or Community	Scenario/PTHA Name	Source Name
Puerto Rico	Puerto Rico	Puerto Rico Trench, Segment 19, Mw 8.0	Puerto Rico Trench, North Hispaniola deformed belt zone
Puerto Rico	Puerto Rico	FEMA, Segment 2, Mw 8.0	Puerto Rico northern zone
Puerto Rico	Puerto Rico	FEMA, Segment 3, Mw 8.2	Puerto Rico northern zone
Puerto Rico	Puerto Rico	FEMA, Segment 4, Mw 7.9	Puerto Rico northern zone
United States Virgin Islands	St. Thomas, St. John, and St. Croix	Puerto Rico Trench (PRTG) - Mw 9.1	Puerto Rico Trench, North Hispaniola deformed belt zone
United States Virgin Islands	St. Thomas, St. John, and St. Croix	ID_15 - Anegada Passage, Segment 15, Mw 7.6	Anegada Passage, Mona Rift Zone
United States Virgin Islands	St. Thomas, St. John, and St. Croix	ID_17 - Anegada Passage, Segment 17, Mw 7.4	Anegada Passage, Mona Rift Zone
United States Virgin Islands	St. Thomas, St. John, and St. Croix	ID_21 - Anegada Passage, Segment 21, Mw 7.6	Anegada Passage, Mona Rift Zone
United States Virgin Islands	St. Thomas, St. John, and St. Croix	ID_25 - Anegada Passage, Segment 25, Mw 7.6	Anegada Passage, Mona Rift Zone
Washington	Washington	Cascadia L1	Cascadia Subduction Zone
Washington	Washington	Seattle fault Mw 7.3+	Seattle fault zone